

Deforming the Double-Scaled SYK & Reaching the Stretched Horizon From Finite Cutoff Holography

Sergio E. Aguilar-Gutierrez  ^a

^a *Qubits and Spacetime Unit, Okinawa Institute of Science and Technology Graduate University, Onna, Okinawa 904 0495, Japan*

E-mail: sergio.ernesto.aguilar@gmail.com

ABSTRACT: We study the properties of the double-scaled SYK (DSSYK) model under chord Hamiltonian deformations based on finite cutoff holography for general dilaton gravity theories with Dirichlet boundaries. The formalism immediately incorporates a lower-dimensional analog of $T\bar{T}(+\Lambda_2)$ deformations, denoted $T^2(+\Lambda_1)$, as special cases. In general, the deformation mixes the chord basis of the Hilbert space in the seed theory, which we order through a modification of the Lanczos algorithm. The resulting chord number in the ordered basis represents a wormhole length at a finite cutoff in the bulk. We study the thermodynamic properties of the deformed theory; the evolution of n -point correlation functions with matter chords; the growth of complexity of the Hartle-Hawking state; and the entanglement entropy between the double-scaled algebras for a given chord state. The latter, in the triple-scaling limit, manifests as the minimal codimension-two area in the bulk following the Ryu-Takayanagi formula. By performing a sequence of T^2 and $T^2 + \Lambda_1$ deformations in the upper tail of the energy spectrum in the deformed DSSYK, we concretely realize the cosmological stretched horizon proposal in de Sitter holography by Susskind [1]. We discuss other extensions with sine dilaton gravity, end-of-the-world branes, and the Almheiri-Goel-Hu model.

Contents

1	Introduction	1
2	Dilaton Gravity at Finite Cutoff and its Boundary Dual	6
2.1	Hamiltonian Deformations from Finite Cutoff Holography	7
2.2	Solutions to the Flow Equation	10
2.3	Thermodynamics	11
3	Deforming the DSSYK Model: Chord Basis, Bulk Length & Complexity	16
3.1	Review of the DSSYK model	17
3.2	Chord Basis and Hamiltonian Representations	20
3.3	Path Integral Formulation of the Deformed DSSYK	21
3.4	State Complexity	23
3.5	IR/UV Triple-Scaling Limits and $T^2(+\Lambda_1)$ Deformations	27
4	Correlation Functions	29
4.1	n-Point Correlation Functions	31
4.2	Semiclassical Evaluation	32
4.3	Triple-Scaling Limit of Crossed Four-Point Functions	37
5	Holographic Entanglement Entropy from Double-Scaled Algebra	39
5.1	Double-Scaled Algebra & Entanglement Entropy	39
5.2	Boundary Perspective: Entropy from Chord Number State	41
5.3	Bulk Perspective: RT Formula	43
6	Stretched Horizon Holography From the Deformed DSSYK Model	45
6.1	UV Limit of the DSSYK Model vs dS Space at Finite Cutoff	46
6.2	Hyperfast State Complexity Growth	48
6.3	Hyperfast Scrambling From OTOCs	49
6.4	Holographic Entanglement Entropy and dS Space	50
7	Discussion	52
7.1	Outlook	53
A	Notation	60
B	Evaluation of Time/Space-like Geodesics in (3.50)	63
C	Sine Dilaton Gravity at Finite Cutoff	64

D Deformations with End-Of-The-World Branes and Wormholes	69
D.1 Matter Chords as ETW Branes from Deformed DSSYK Model	69
D.2 Deformed ETW Brane theory	71
D.3 Euclidean Wormholes from the DSSYK Model	72
E Almheiri-Goel-Hu Model	75
F First Law of Thermodynamics at Finite Cutoff	82

1 Introduction

T \bar{T} Deformations and Their Bulk Interpretation Explicit examples of holography outside the anti-de Sitter (AdS)/ conformal field theory (CFT) correspondence [2] remains, arguably, not well understood and perplexing in comparison with those in conventional AdS/CFT. However, there are different approaches to bridge the gap. Some of the best studied examples have been developed through a class of tractable irrelevant deformations in the boundary theory for CFT_2 introduced in $T\bar{T}$ deformations in [3] with several appealing properties [3–12] (reviewed in [13–15]). Single-trace $T\bar{T}$ -deformations (e.g. [16, 17]) modify the bulk’s background metric, while double-trace $T\bar{T}$ -deformations break the conformal symmetry in the dual quantum field theory (QFT). Depending on the sign of the deformation, the latter case can be interpreted in the bulk as a finite cutoff in AdS [18]; or gluing an auxiliary AdS path connected to the original asymptotic boundary [19, 20] or introducing mixed boundary conditions in the asymptotic boundary [21]; among others. Given that the deformation parameter introduces a length scale, it serves to regularize the deformed theory. This has motivated studying higher [10, 22–26] and lower dimensional analogs/extensions [27–37], and we collectively refer to them as T^2 deformations¹, as well as other multitrace deformations [38–44] under active scrutiny. T^2 deformations have several exciting features, and they deserve further development in an explicitly solvable ultraviolet (UV)-finite setting, which is our aim in this work.

The DSSYK Model and its Holograms Another prominent approach, lower dimensional quantum gravity offers the possibility of developing non-AdS holography from first principles in an analytically tractable manner.

In particular, the Sachdev-Ye-Kitaev (SYK) model [45–48] in the double-scaling limit [49, 50], called the DSSYK model [51, 52], is a remarkable testbed to develop concepts and techniques to study lower-dimensional quantum gravity from a concrete and solvable (through chord diagram methods [51, 52]) boundary theory relevant for holography beyond AdS/CFT, which might carry some relevant lessons in higher dimensional holography. Key insights to

¹Also referred to as 1D $T\bar{T}$ deformations in the lower-dimensional case in [27, 28].

understand the DSSYK model and its bulk dual have been recognized from the double-scaled [53–55] and chord [56] von Neumann algebras of the DSSYK model, as well as its quantum group structure [57–62]; from Krylov complexity [54, 63–79] for operators [80] and states [81] (see recent reviews in [74, 82, 83]) in connection to bulk geodesic lengths [37, 53, 56, 84–89] as an explicit realization of the volume=complexity (CV) conjecture [90], and holographic entanglement entropy [91, 92] in terms of a Ryu-Takayanagi (RT) [93, 94] formula (see e.g. [95–98] for reviews, and [99–101] for extensions). However, there has been active debate about the specific bulk dual to the DSSYK model. The most-discussed bulk dual proposals include sine dilaton gravity [61, 85, 87, 102–107], and de Sitter (dS) space through different approaches, including Schwarzschild-dS₃ space [76, 88, 89, 105, 108–110], and dS₂ space as a s-wave reduction of dS₃ space, where the DSSYK model is conjectured to live in the **stretched cosmological horizon** (illustrated in Fig. 1 (d)) which is defined as a timelike codimension-one surface with Dirichlet boundary conditions somewhere in the static patch very close to the cosmological horizon, possibly a few Planck’s lengths away [1, 110–120]. Other interesting approaches can be found in e.g. [92, 109, 121–126].

At a first glance, it might seem the diversity of bulk dual proposals for the same boundary theory means that at least some of them might be incorrect. However, they are not necessarily incompatible with one another [34, 69, 92, 105]. For instance, concrete connections between dS₃ space holography with sine dilaton gravity as its world-sheet theory and complex Liouville string [127–132] and the SYK model as a collective field theory was recently investigated in [105]. To fully understand the DSSYK model, the relationship between these different proposals needs to be closely studied.

Addressing Susskind’s Conjectures A prominent member in this family of proposals, initiated by the work of Susskind [1] seemingly has very different features from the others [115]. Whether it fits with sine dilaton gravity and other dS₃ proposals, or if it is incompatible with the other proposals is not well-understood. According to [1], there are specific properties expected in dS holography that are realized by the DSSYK model at infinite (Boltzmann) temperature. Namely, [1] postulates the following conjectures:

- (i) There is a RT formula in dS space that takes the same form as in AdS space when the asymptotic boundary is replaced by the stretched horizon.
- (ii) The scrambling time as measured by the operator size [133] of Majorana fermions (which is linearly related to the out-of-time-ordered correlators (OTOCs) of the same fermionic operators [133]) is of the order of the dS length scale.
- (iii) There is a similar (hyper)fast growth of (some notion of) complexity associated to the exponential growth of the dS scaling factor.
- (iv) The DSSYK model at infinite (Boltzmann) temperature satisfies these properties.

The stretched horizon conjectures are seemingly *in tension* with the DSSYK model being located at the asymptotic boundaries of an effective AdS₂ black hole in sine dilaton gravity [85] (as well as some entropic considerations [115]). Nevertheless, there is a specific regime in sine dilaton gravity where the theory reduces Jackiw-Teitelboim (JT) [134, 135] gravity and

to dS JT gravity [77, 102]. This limit in the bulk corresponds to zooming in the UV regime in the energy spectrum of the DSSYK model. However, the boundary theory would be located at \mathcal{I}^\pm when taking the appropriate limit [77, 102]. In contrast, the boundary theory would be located at the stretched horizon in Susskind’s proposal. The tension between them is closely related to dS_2/CFT_1 and static patch holography in dS_2 space.

To move the asymptotic boundary from \mathcal{I}^\pm to inside the static patch, we cannot restrict ourselves to T^2 deformations, since they lead to a complex energy spectrum once the theory reaches a Killing horizon [18]. However, it was recently realized by [136] that by applying a two-step process the boundaries can pass behind the horizon of AdS_3 black holes through $T\bar{T}$ and $T\bar{T} + \Lambda_2$ deformations (which have been recently updated to $T^2 + \Lambda_3$ deformations [137]). In this process, the corresponding boundaries move from the asymptotic region to the black hole horizon through a $T\bar{T}$ deformation, and then from the horizon towards the singularity through a $T^2 + \Lambda_2$ deformation. This procedure was recently applied in dS_3 holography by [138]; albeit without a concrete boundary theory in dS_3/CFT_2 .

Thus, a natural way to resolve this tension is based on finite cutoff holography, by T^2 deforming the DSSYK model in the UV limit of its energy spectrum and implementing a lower dimensional version of $T\bar{T} + \Lambda_2$ deformations [139–143] to place the boundary theory near the cosmological horizon of dS_2 space.² Due to the finite cutoff distance where the DSSYK model is located, this corresponds to an infinite Tolman temperature [12, 145–147], which is the temperature experienced by an observer at a finite distance in a gravitational spacetime. Since the inverse temperature in the bulk naturally controls the time scales in the boundary theory, applying a deformation in the DSSYK model would lead to the hyperfast properties conjectured by [1]. The infinite temperature limit of the boundary theory is indeed the primary reasoning behind the hyperfast conjectures in [1].

Aims of This Work We study chord Hamiltonian deformations in the DSSYK model.³ We focus on the boundary description with guidance from finite cutoff holography for general dilaton gravity theories; particularly the infrared (IR) and UV triple-scaling limits in the DSSYK model, which are associated to JT and dS JT gravity respectively. The main goals of our evaluations are:

- To investigate the thermodynamic properties and dynamical observables, such as state complexity of the deformed chord theory associated to a finite cutoff in the bulk dual of the DSSYK model, while allowing general counterterms in the bulk to study its relevance in the holographic dictionary.

²Note that dS_3 space with Dirichlet boundaries is thermodynamically unstable, and thus also its s-wave sector; while in the $dS_{d+1 \geq 4}$ case, it does not lead to a well-posed initial value problem [144].

³In the lower-dimensional context, this seems to be a natural choice given that the ensemble-averaged description of the SYK model is the one with a clearer bulk theory dual at the disk topology level. One could first perform the T^2 deformation in the physical SYK model, work out its double-scaling limit and take ensemble averaging at the end, to study the differences with respect to our approach. However, this procedure might not have a chord Hamiltonian description, or it would be non-trivially modified. This might also lead to a different holographic dual, if any. We discuss more details about this in the outlook, Sec. 7.1.

- To deduce the natural chord basis and the corresponding representation of the chord operators under a Hamiltonian deformation, as well as the entanglement entropy between the double-scaled algebras in the deformed theory.
- To realize Susskind’s stretched horizon proposal from the UV triple-scaling limit [92] of the DSSYK model from finite cutoff holography by combining the previous results.⁴

Results First, we present a more complete derivation of the flow equation for the energy spectrum of the deformed boundary theory following up our companion work [34] based on finite cutoff holography for dilaton gravity theories in [27–29]. For that, we consider the Hamilton-Jacobi (HJ) equation in a generic dilaton-gravity theory and we derive the flow equation encoding the energy spectrum of the dual. In contrast to the previous literature [27–29, 32, 37], we allow the counterterm in the bulk action to be modified when the boundary radial cutoff is finite. This results in more general Hamiltonian deformations in the boundary dual, including as special cases one-dimensional T^2 deformations and a lower dimensional analog of $T\bar{T} + \Lambda_2$, which we refer to as $T^2 + \Lambda_1$ deformations. This construction extends the holographic dictionary between the DSSYK model and a generic dilaton-gravity theory dual at finite cutoff.⁵ We analyze the thermodynamic properties of the deformed model from its partition function (including the density of states, microcanonical temperature, and heat capacity) and its n -point correlation functions. Next, we find that in the semiclassical limit, they have the same functional dependence as the seed theory, but the parameters involving the “fake” temperature [85] (also called “tomperature” [1], which is associated to the decay rate of correlation functions) contain a redshift factor, associated to a Tolman temperature with respect to an observer at a finite distance in the bulk; as expected from finite cutoff holography [18, 164]. A summary of the thermodynamics and correlation functions of the deformed model is shown in Fig. 2.

Since the chord Hamiltonian is deformed, the chord number basis used to tridiagonalize the seed Hamiltonian does not do the same in the deformed theory. We will also derive the chord basis that is associated to the length of an Einstein-Rosen bridge in the dual AdS_2 black hole (which we refer to as a “wormhole length”) at a finite cutoff, and we study the representation of operators in the chord algebra, and we find a map to the original basis. We use these results to propose a natural definition of state complexity in the seed theory reproducing the wormhole length in the bulk at finite cutoff, which is expected to reproduce Krylov spread complexity in the deformed chord theory. Lastly, we evaluate the von Neumann entropy with respect to a density matrix associated to the chord number of the DSSYK model. The algebraic entanglement entropy is holographic, it matches the dilaton in JT gravity and dS JT gravity at a finite cutoff when we restrict to the IR and UV triple-scaling limits in the chord theory.

⁴See [63, 73, 75, 76, 148–158], and [1, 159–163] for studies on quantum complexity and entanglement entropy (through bilayer vs monolayer proposals [161–163]) in connection to the dS stretched horizon conjecture in [1].

⁵The evaluations in this work are at the non-perturbative level in the deformation parameter, unless explicitly stated.

Conjecture	Confirmation in Deformed DSSYK	Details
Hyperfast complexity growth (iii+iv)	✓	Sec. 6.2
Hyperfast scrambling (ii+iv)	✓	Sec. 6.3
Validity of RT formula using the stretched horizon (i+iv)	✗	Sec. 6.4

Table 1. Comparison between the (i-iv) conjectures in [1], which were explained above, and the explicit realization of the cosmological stretched horizon from the $T^2 + \Lambda_1$ deformation of the UV limit of the DSSYK model, corresponding to the assumption (iv). Two out of the three remaining conjectures are satisfied in this model. Further details can be found in the respective sections.

In particular, when applying our results in the UV limit of the DSSYK model, we realize Susskind’s proposal for stretched horizon holography [1], by implementing the T^2 and $T^2 + \Lambda_1$ deformations, and taking a limit in deformation parameter such that the boundary is placed inside the static and close to the cosmological horizon. The thermodynamic properties of the model match those in dS₂ JT gravity at a finite cutoff. Due to the fake temperature being infinite, the rate of growth of OTOCs and state complexity are enhanced; the scrambling time is order one in units with respect to the dS length scale, instead of order $\log N$ expected for a fast scrambler [1], with N being the number of Majorana fermions ($\rightarrow \infty$ in the DSSYK model). Our notion of state complexity reproduces the minimal length between the finite Dirichlet boundaries in dS₂, and it reaches a maximum value at a time order one expected for hyperfast complexity growth [149]. Meanwhile, the algebraic entanglement entropy for the chord number state agrees with the RT formula for dS₂ JT gravity if the boundaries are in the Milne patch of dS₂ (Fig. 1 (c)). The cosmological horizon limit reproduces the Gibbons-Hawking (GH) entropy of dS₃ space. However, if the boundaries are located in the static patch the RT formula in dS₂ does not apply, the dilaton at the minimal extremal surface becomes trivial (see Sec. 6.4). However, in higher dimensions there are more possible entangling surfaces where Susskind’s conjecture might apply; our study takes the dS₂ geometric perspective instead of a dS₃ embedding, whose precise connection with the DSSYK model is actively debated [105, 108, 115].

A summary comparing our results and the conjectures in [1] is displayed in Tab. 1.

In addition, we provide other generalizations and analysis of the results in the appendices. In particular, we study the consequences of interpreting the results in terms of *sine dilaton gravity* in finite cutoff holography. The energy spectrum generically becomes complex-valued since the bulk metric and dilaton at the cutoff location are complex-valued. In those cases, there is no Lorentzian evolution, rather than the deformed theory being non-unitary, so the DSSYK Hamiltonian is not isometrically dual to a canonically quantized Arnowitt–Deser–Misner [165–171] (ADM) Hamiltonian in the bulk, which is the generator of

time translations. We adopt a similar prescription as in Cauchy slice holography [172–175], where the stress tensor is allowed to be complex-valued. However, in contrast to previous literature, the T^2 deformation parameter is generically a complex number, and it can take both positive or negative values (without an auxiliary geometric extension [19, 20]). Later, we T^2 deform the Almheiri-Goel-Hu (AGH) model [176], which is a simplification of the DSSYK model in the $q \rightarrow 1$ described by the Heisenberg-Weyl algebra. This integrable analog of the DSSYK model allows for analytic evaluations of correlation functions beyond the semiclassical limit.

Outline The paper is organized as follows. In Sec. 2, we introduce Hamiltonian deformations in holographic quantum mechanics based on moving the HJ equation of the dual dilaton graviton theory with Dirichlet boundary conditions and we study its thermodynamic properties. In Sec. 3 we specialize the results in the DSSYK model to deduce a chord basis associated to a bulk geodesic in finite cutoff holography, and the representation of the chord operators after the deformation. We also propose a notion of state complexity. In Sec. 4 we evaluate correlation functions, including its semiclassical and its triple-scaling limits. In Sec. 5, we investigate the entanglement entropy between the double-scaled algebras in the deformed DSSYK model, and their holographic interpretation. In Sec. 6 we apply our previous results to realize the stretched horizon proposal of Susskind. We then conclude in Sec. 7 with a summary of our findings, and some relevant future directions.

In addition, App. A contains a summary of the notation used in the manuscript. In App. B we provide more details about the derivation of spacelike and timelike extremal geodesic lengths connecting the asymptotic boundaries of an effective AdS_2 black hole. App. C discusses reality conditions in sine dilaton gravity at a finite cutoff. In App. D we explore chord Hamiltonian deformations in the presence of ETW branes and Euclidean wormholes in the bulk. In App. E we T^2 -deform the AGH model to study its thermodynamics and correlation functions. At last, in App. F we discuss the first law of thermodynamics in the deformed DSSYK.

2 Dilaton Gravity at Finite Cutoff and its Boundary Dual

Before specializing to the DSSYK model, we generalize previous studies of T^2 deformations for holographic (0+1)-dimensional models [27, 28, 177] assuming a dual dilaton gravity model with Dirichlet boundary conditions. In this section, we are particularly interested in deriving the energy flow equation in holographic quantum mechanics with a Hamiltonian deformation, and to study its semiclassical thermodynamics. In particular, one recovers a lower dimensional analog of $T\bar{T}$ and $T\bar{T} + \Lambda_2$ deformations as special cases. In addition, the reader is referred to App. C for details on the reality conditions to implement the chord Hamiltonian deformations from sine dilaton gravity at a finite cutoff.

Outline In Sec. 2.1, we study HJ equation in dilaton gravity theories and the associated flow equation. In Sec. 2.2 we study its solutions, including one-dimensional T^2 deformations

and we propose a “ $T^2 + \Lambda_1$ ” deformation in the DSSYK model, which can be interpreted as pushing the finite cutoff inside the black hole horizon/ outside the cosmological horizon. In Sec. 2.3 we study the thermodynamic properties of the deformed theories, specializing to the DSSYK model for concreteness.

2.1 Hamiltonian Deformations from Finite Cutoff Holography

Our first goal is to derive the flow equation controlling the evolution of the energy spectrum of a (0+1)-dimensional system dual to a generic dilaton gravity theory of the form

$$I_E \equiv -\frac{\Phi_0}{2\kappa^2} \left(\int_{\mathcal{M}} d^2x \sqrt{g} \mathcal{R} + 2 \int_{\partial\mathcal{M}} dx \sqrt{h} K \right) - \frac{1}{2\kappa^2} \left(\int_{\mathcal{M}} d^2x \sqrt{g} (\Phi \mathcal{R} + U(\Phi)) + 2 \int_{\partial\mathcal{M}} dx \sqrt{h} \left(\Phi_B K - \sqrt{G(\Phi_B)} \right) \right), \quad (2.1)$$

where the first line is a topological term, $U(\Phi)$ and $G(\Phi_B)$ are generic C^∞ functions. This is a generalization of the flow equation in [27] for dilaton-gravity theories without AdS boundary conditions, which are motivated by the proposed duality between sine dilaton gravity and the DSSYK model [61]. While we will derive the flow for theories of the general form (2.1). One should note that a canonical choice of the counterterm is

$$G(\Phi_B)^{(\text{others})} = \int^{\Phi_B} d\Phi U(\Phi), \quad (2.2)$$

which guarantees the on-shell action to be finite when $\Phi_B \gg 1$; however, we will not make this restriction in deriving the flow equation below, since we investigate cases where Φ_B is a finite cutoff, instead of a radial regulator of the asymptotic boundary.⁶ Also, note that in the following one may allow $g_{\mu\nu}$ and $\Phi \in \mathbb{C}$; which is the case of interest for sine dilaton gravity at finite cutoff. We will discuss this case in detail in App. C.

The strategy proposed in [22] is to recover the T^2 flow equation from the HJ equation controlling radial evolution along the flow.⁷ For this reason, we will consider the dilaton-gravity theory as the input for defining the deformed DSSYK model.⁸ However, we will recover a larger class of deformations than the T^2 case.

⁶If one were to follow (2.2), the Φ_B variation of the boundary action leads to the on-shell mean-curvature at the radial boundary

$$K = \frac{U(\Phi_B)}{2\sqrt{G(\Phi_B)}}. \quad (2.3)$$

⁷A different but related approach is taken in [29], who instead study the radial quantization of the Wheeler-DeWitt (WDW) [178, 179] equation (at the reduced phase space level), and the path integral dilaton gravity of the form (2.1); without a counterterm, (see e.g. (2.20) [29]). After properly introducing the corresponding counter term, one can then recover a relation equivalent to [27], which agrees with results (see (2.15)) after rescaling.

⁸An alternative way to define it would be to keep the asymptotic boundary in the same location but modify the boundary conditions instead of using Dirichlet [21]. This type of procedure was considered by [27] in JT gravity. We reserve future directions to study if such modifications can be adapted to this context (see more comments in Sec. 7.1).

We begin considering the general variation of an action of the form (2.1), given by

$$\delta I_E = -\frac{1}{2} \int_{\mathcal{M}} d^2x \sqrt{g} [\mathcal{E}^{\mu\nu} \delta g_{\mu\nu} + \mathcal{E}_\Phi \delta \Phi] + \int_{\partial\mathcal{M}} d\tau \sqrt{h} \left[\frac{1}{2} \tilde{T}^{ab} \delta h_{ab} + \mathcal{O}_{\Phi_B} \delta \Phi_B \right], \quad (2.4)$$

where

$$\mathcal{E}_{\mu\nu} \equiv \nabla_\mu \nabla_\nu \Phi - g_{\mu\nu} \nabla^2 \Phi + \frac{1}{2} g_{\mu\nu} U(\Phi), \quad (2.5)$$

$$\mathcal{E}_\Phi \equiv \mathcal{R} + \partial_\Phi U(\Phi). \quad (2.6)$$

Here we have introduced the Brown-York (BY) [180] stress tensor and the scalar operator conjugate to Φ , which we denote respectively as:

$$\tilde{T}^{ab} \equiv \frac{2}{\sqrt{h}} \frac{\delta I_E}{\delta h_{ab}} = \frac{2}{\sqrt{h}} \left(\pi^{ab} + \frac{\sqrt{h}}{4\kappa^2} \sqrt{G(\Phi_B)} h^{ab} \right), \quad (2.7a)$$

$$\mathcal{O}_{\Phi_B} \equiv \frac{1}{\sqrt{h}} \frac{\delta I_E}{\delta \Phi_B} = \frac{1}{\sqrt{h}} \left(\pi_{\Phi_B} + \frac{\sqrt{h}}{4\kappa^2 \sqrt{G(\Phi_B)}} G'(\Phi_B) \right), \quad (2.7b)$$

where $G'(\Phi_B) \equiv \frac{dG(\Phi_B)}{d\Phi_B}$; and π_{Φ_B} and π^{ab} are the canonical momenta of h_{ab} and Φ_B , defined as

$$\pi^{ab} \equiv -\frac{\sqrt{h}}{4\kappa^2} h^{ab} n^c \nabla_c \Phi_B, \quad \pi_{\Phi_B} \equiv -\frac{\sqrt{h}}{2\kappa^2} K. \quad (2.8)$$

We can now study the HJ equation controlling the radial equation of on-shell solutions. Using the general variation (2.4) evaluated onshell (i.e. $\mathcal{E}_{\mu\nu} = 0$, $\mathcal{E}_\Phi = 0$), we recover

$$\partial_{\Phi_B} I_E^{(\text{on})} = \int_{\partial\mathcal{M}} d\tau \sqrt{h} \left[\frac{1}{2} \tilde{T}^{ab} \partial_{\Phi_B} h_{ab} + \mathcal{O}_{\Phi_B} \right], \quad (2.9)$$

and we have to implement the ADM Hamiltonian constraint \mathcal{H} for general dilaton gravity theories (2.1), which we evaluate at the cutoff location and it is given by [181]

$$\mathcal{H} \equiv 4\kappa^2 \pi_{\Phi_B} \pi^{\tau\tau} - \frac{1}{4\kappa^2} U(\Phi_B) = 0. \quad (2.10)$$

This constraint leads to the following relation for the dilaton source in (2.7b):

$$\mathcal{O}_{\Phi_B} = \frac{U(\Phi_B) + \left(\frac{2\kappa^2}{G(\Phi_B)} \tilde{T}_\tau^\tau - 1 \right) G'(\Phi_B)}{4\kappa^2 \sqrt{G(\Phi_B)} \left(\frac{2\kappa^2}{G(\Phi_B)^2} \tilde{T}_\tau^\tau - 1 \right)}. \quad (2.11)$$

Following the procedure of [28], we need to identify the scaling of the different terms in (2.9) with respect to r_B . Similar to [22, 27], we recognize that at the finite boundary, Φ_B , we should have the following scaling for the metric and the stress tensor given the counterterm (2.1),

$$\sqrt{h} = \sqrt{G(\Phi_B)} \sqrt{\gamma}, \quad \tilde{T}_{\tau\tau} = \sqrt{G(\Phi_B)} T_{\tau\tau}, \quad (2.12)$$

which is a choice of normalization to match the boundary metric in the bulk to the metric of the boundary theory.⁹ Moreover, in 1D we can express the following relation [27],

$$I_E = \int d\tau \sqrt{\gamma} T_\tau^\tau = \int d\tau \sqrt{\gamma} E_y , \quad (2.13)$$

where γ_{ij} is the background metric of the 1D quantum mechanical theory, and T_{ij} the corresponding boundary stress tensor, and in the last equality we use the fact that in (0+1)-dimensions, $T_\tau^\tau \equiv E_y$ which denotes the energy spectrum of the deformed theory, y denotes a deformation parameter, which we define below. This allows us to express the HJ equation (2.10) as

$$\partial_{\Phi_B} \int_{\partial\mathcal{M}} d\tau \sqrt{\gamma} T_\tau^\tau = \int_{\partial\mathcal{M}} d\tau \sqrt{\gamma} \frac{G'(\Phi_B) \left(\left(\frac{2\kappa^2}{G(\Phi_B)} T_\tau^\tau \right)^2 - 1 \right) + U(\Phi_B)}{2 \left(\frac{2\kappa^2}{G(\Phi_B)} T_\tau^\tau - 1 \right)} . \quad (2.14)$$

Using the relation (2.13), we identify that (2.14) can then be expressed as a flow equation for the spectrum of the boundary theory

$$\partial_y E_y = \frac{(E_y)^2 + (\eta - 1)/y^2}{2(1 - yE_y)} ,$$

(2.15)

where we have defined the parameters

$$y \equiv 2\kappa^2/G(\Phi_B) , \quad \eta \equiv U(\Phi_B)/G'(\Phi_B) . \quad (2.16)$$

Note that while E_y depends on both y and η , where the latter is not completely determined by y . The functional dependence on the parameter η will be implicit in all expressions involving y to lighten the notation.

The above relation can be interpreted as a flow equation (2.15) for the energy spectrum of the boundary dual to the dilaton gravity theory at finite cutoff. Indeed, (2.15) takes the same form as other places in the literature (see e.g. [28, 29]) which are restricted to $\eta = U(\Phi_B)/G'(\Phi_B) = 1$. The latter choice of counterterm $G'(\Phi_B) = U(\Phi_B)$ leads to a finite on-shell action in general dilaton-gravity theories with asymptotic Dirichlet boundaries [181]. Meanwhile, the case $\eta = -1$ ($U(\Phi) \rightarrow -U(\Phi)$ with $G(\Phi_B)$ fixed) can be used when the cutoff surface is located at some finite r_B , so there is no issue with the renormalization of the on-shell action, while keeping the same holographic identification for the deformation parameter (2.16). We remark that the deformation parameter (2.16) and the flow equation (2.15) generalize the results in [28] which are a special case of this formulation, corresponding to a class of asymptotically AdS dilaton gravity theories.¹⁰

⁹I thank Simon Lin for comments about this.

¹⁰We reported some of these findings in a companion work [34], here we provide more details about the derivation. Note that [37] finds the same results as us in [34] from a different method.

Deformed Boundary Hamiltonian We promote (2.15) to an operator relation in the quantum theory as

$$\partial_y \hat{H}_y = \hat{\Theta}(\hat{H}_y, y) , \quad \hat{\Theta} = \frac{1}{2} \left(\hat{H}_y^2 + y^{-2}(\eta - 1) \right) \left(1 - y \hat{H}_y \right)^{-1} \quad (2.17)$$

where $\hat{\Theta}(\hat{H}_y, y)$ is the $T\bar{T}$ deformation operator [182], and \hat{H}_y is the Hamiltonian deformation of the boundary theory.

2.2 Solutions to the Flow Equation

First, notice from (2.16) that $\eta = \eta(y)$ generically. As mentioned in the introductions, when we deformed the boundary theory starting at the asymptotic boundary in the bulk, we need to set $G(\Phi_B)$ as in (2.2). However, once we reach a finite cutoff value Φ_B , we can allow $G(\Phi_B)$ to be more arbitrary, which defines a set of possible deformed theories. Below we specialize in one of them due to its applications for studying the stretched horizon conjecture of Susskind [1].

We will be interested in the case $\eta = \pm 1$, as this allows us to introduce an analogous type of deformation as $T\bar{T}(+\Lambda_2)$ [137, 139, 141, 143] deformations, which we define below as

$$T^2(+\Lambda_1) \text{ deformations} : \quad U(\Phi) \quad \text{fixed} , \quad G(\Phi_B) \rightarrow \pm G(\Phi_B) , \quad (2.18)$$

resulting in $\eta = \pm 1$ in (2.15). We note that the solutions to the flow equation when η is a fixed parameter are

$$E_y = \frac{1}{y} \left(1 \pm \sqrt{\eta - 2yf(E)} \right) . \quad (2.19)$$

where $f(E)$ is a function determined by initial conditions.

T^2 deformation The best studied case from the lower dimensional perspective corresponds to $\eta = +1$. The deformed energy spectrum in terms of the seed theory takes the form

$$E_y^{\eta=+1}(\theta) = \frac{1}{y} \left(1 \pm \sqrt{1 - 2yE} \right) . \quad (2.20)$$

The solution with a relative $-$ sign represents the energy spectrum at a finite cutoff in the holographic dual (see e.g. [18, 22]), as seen from the on-shell action (2.31), which is smoothly connected to the seed theory in the limit $y \rightarrow 0$. Meanwhile, the solution with the relative $+$ sign represents the complementary spacetime region with respect to the finite cutoff. Both of them are represented in Fig. 1.

$T\bar{T} + \Lambda_1$ deformations When $\eta = -1$, this corresponds to a s-wave reduction of $T\bar{T} + \Lambda_2$ deformations [41, 136, 139, 142, 143], which we refer to as $T^2 + \Lambda_1$ deformations. In this case $\eta = -1$ means that at some finite radial distance in the flow, we modify the boundary counterterm in the action (2.1) with $G(\Phi_B) \rightarrow -G(\Phi_B)$, while retaining the same dilaton

potential $U(\Phi) \rightarrow U(\Phi)$.¹¹ The energy spectrum takes the form

$$E_y^{\eta=-1} = \frac{1}{y} \left(1 \pm \sqrt{2yE - 1} \right). \quad (2.21)$$

As before, there are two relative signs; we will adopt the one with the relative + sign since it is continuously connected to the deformed theory with $\eta = +1$. The transition between the deformations appears where the argument in the square root vanishes, meaning that

$$y = 1/(2E). \quad (2.22)$$

Note that since there are no modifications in the dilaton potential in the $\eta = -1$ case, it describes the same bulk metric as its $\eta = +1$ analog, similar to [136, 138] (in contrast to other approaches [137, 139–141, 143]).

We illustrate the two-step bulk interpretation of the T^2 and $T^2 + \Lambda_1$ deformation in Fig. 1.

2.3 Thermodynamics

In this subsection, we specialize the previous results to study the semiclassical thermodynamics of the deformed DSSYK model from its partition function to evaluate its energy spectrum, thermodynamic entropy, density of states, and heat capacity as a function of its temperature. This leads to conditions when the deformed theory is thermodynamically stable. We do not assume a specific dual dilaton gravity theory (2.1) to the DSSYK model in this section (see App. C for considerations in sine dilaton gravity).

Energy spectrum, entropy and temperature Consider the partition function of the deformed DSSYK model which we evaluate in the semiclassical limit as¹²

$$Z_y(\beta) \equiv \langle \Omega | e^{-\beta \hat{H}_y} | \Omega \rangle = \int_{\lambda \rightarrow 0} dE(\theta) e^{-\beta E_y(\theta)} \rho(\theta). \quad (2.23)$$

¹¹The bulk interpretation of the $T\bar{T} + \Lambda_2$ deformation in CFT_2 is somewhat debated. It has been interpreted as changing the bulk being an AdS black hole to dS₃ space [41, 139, 142, 143]; while there is an alternative interpretation where one instead probes the black hole interior without recovering complex energy levels [136]. In the dilaton gravity context, given that the potential is unchanged, while the boundary counterterm changes sign, the more recent interpretation [136] is the one which we adopt.

¹²There is a proposal for improvement in partition function in finite cutoff holography in [37] where one includes the perturbative and non-perturbative branches of the one-dimensional T^2 deformation with an appropriate contour of integration with a cutoff in the energy integration to regularize the integral. The contour is subtle for periodic potentials such as in sine dilaton gravity. Moreover, this prescription is not necessary for the DSSYK model whose partition function is UV finite, so it will not be discussed.

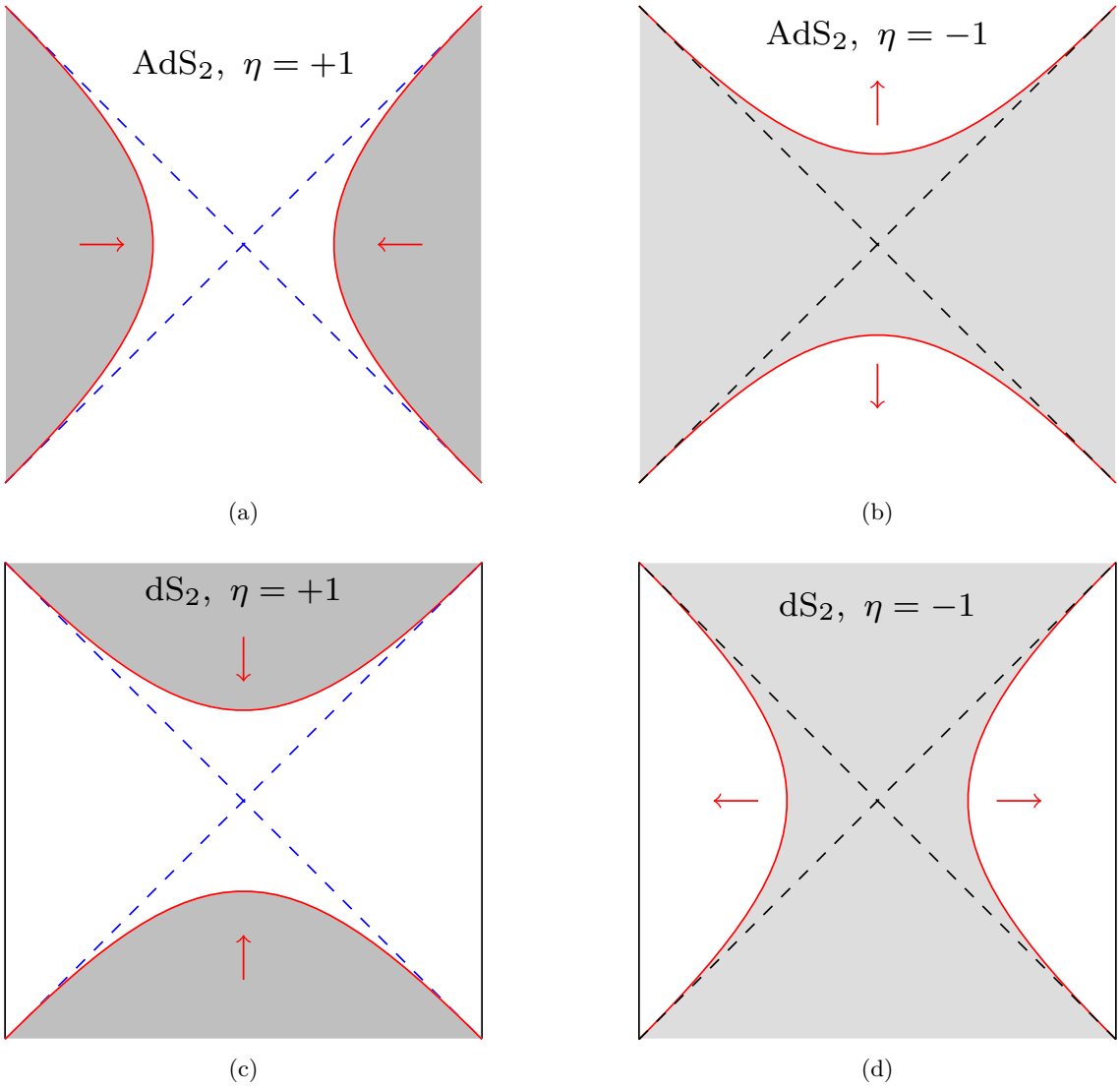


Figure 1. Bulk interpretation of the T^2 and $T^2 + \Lambda_1$ flow in the boundary theory (concretely explained in Sec. 3.5) describing (a,b) an AdS_2 black hole, and (c, d) dS_2 space. The gray regions represent the parts of the bulk that are cut out. (a) By implementing the T^2 deformation, with spectrum (2.20), there is a finite boundary cutoff (red solid curve) in the Rindler- AdS_2 patch til it reaches the horizon. (b) We implement the $T^2 + \Lambda_1$ deformation (2.21) which moves the boundary inside the black hole horizon. A similar procedure applies for dS_2 space for (c) T^2 and (d) $T^2 + \Lambda_1$ deformations. In the latter, the cosmological stretched horizon [1] is realized when the Dirichlet boundaries are very close to the dS_2 horizon.

where $E(\theta)$ is the energy spectrum of the seed theory; $\rho(\theta) = e^{S(\theta)}$ is the semiclassical density of states, and $S(\theta)$ is the thermodynamic entropy, given by [183],¹³

$$E(\theta) \equiv -\frac{2J \cos(\theta)}{\sqrt{\lambda(1-q)}} , \quad S(\theta) \equiv S_0 + \frac{2\theta}{\lambda}(\pi - \theta) , \quad \theta \in [0, \pi] , \quad (2.24)$$

¹³Note that the entropy is proportional to $1/\lambda = N/(2p^2)$ at all temperature scales, where N is the number of degrees of freedom in the SYK and p the number of all-to-all interacting Majorana fermions. While it has

where $J, \lambda \equiv -\log q \geq 0$ are constant parameters of the theory, which will be specified in Sec. 3.1, and we have introduced S_0 , resulting from an overall normalization of the partition function. The microcanonical inverse temperature in this theory is given by¹⁴

$$\beta_y(\theta) \equiv \frac{dS}{dE_y} = \beta(\theta) \frac{dE}{dE_y} , \quad \beta(\theta) \equiv \frac{2\pi - 4\theta}{J \sin \theta} , \quad (2.25)$$

where there is a redshift factor

$$\frac{dE}{dE_y} = \begin{cases} \sqrt{1 - 2yE(\theta)} , & \eta = +1 , \\ \sqrt{2yE(\theta) - 1} , & \eta = -1 . \end{cases} \quad (2.26)$$

Given that β_y is the periodicity of the thermal circle, the T^2 deformation effectively shrinks it. One can similarly recast (2.23) in the form:

$$Z_y(\beta) = \int dE_y(\theta) e^{-\beta E_y(\theta)} \rho_y(\theta) , \quad (2.27a)$$

$$\rho_y(\theta) \equiv \rho(\theta) \frac{dE(\theta)}{dE_y(\theta)} , \quad (2.27b)$$

where ρ_y can be interpreted as the density of states in the deformed theory [27]. Note that since the redshift factor is $\mathcal{O}(1)$, it does not modify the thermodynamic entropy which is $\mathcal{O}(\lambda^{-1})$ in the limit where $\lambda \rightarrow 0$.

We include Fig. 2 to exemplify the resulting thermodynamic properties of the T^2 deformed DSSYK model for generic values of the deformation parameter y appearing in the flow equation (2.15) for $\eta = +1$.¹⁵

First law of thermodynamics The previous results can be used to express variations of the energy spectrum with respect to the parameters of the model. We include details about the relevant calculations in App. F.

Heat capacity Next, we use the previous results to determine the thermal stability of the system, using the definition of the heat capacity

$$C_y(\theta) \equiv -\beta_y(\theta)^2 \frac{dE_y(\theta)}{d\beta_y(\theta)} . \quad (2.28)$$

been debated (see e.g. [116, 117]) if the DSSYK model at infinite temperature should behave like any other system of N qubits at infinite temperature, the entropy would instead scale as $S \propto N$. The double scaling introduces the $1/p^2$ factor (as seen explicitly in partition function in Sec. 2.3). I thank Takanori Anegawa and Jiuci Xu for useful discussions related to this point.

¹⁴This is a Boltzmann temperature, in contrast to the temperature scale in the correlation functions, which we discuss in Sec. 4.2.

¹⁵It would be interesting to match them with the sine-dilaton gravity [61] at finite cutoff with massive scalar fields. We leave this for future directions.

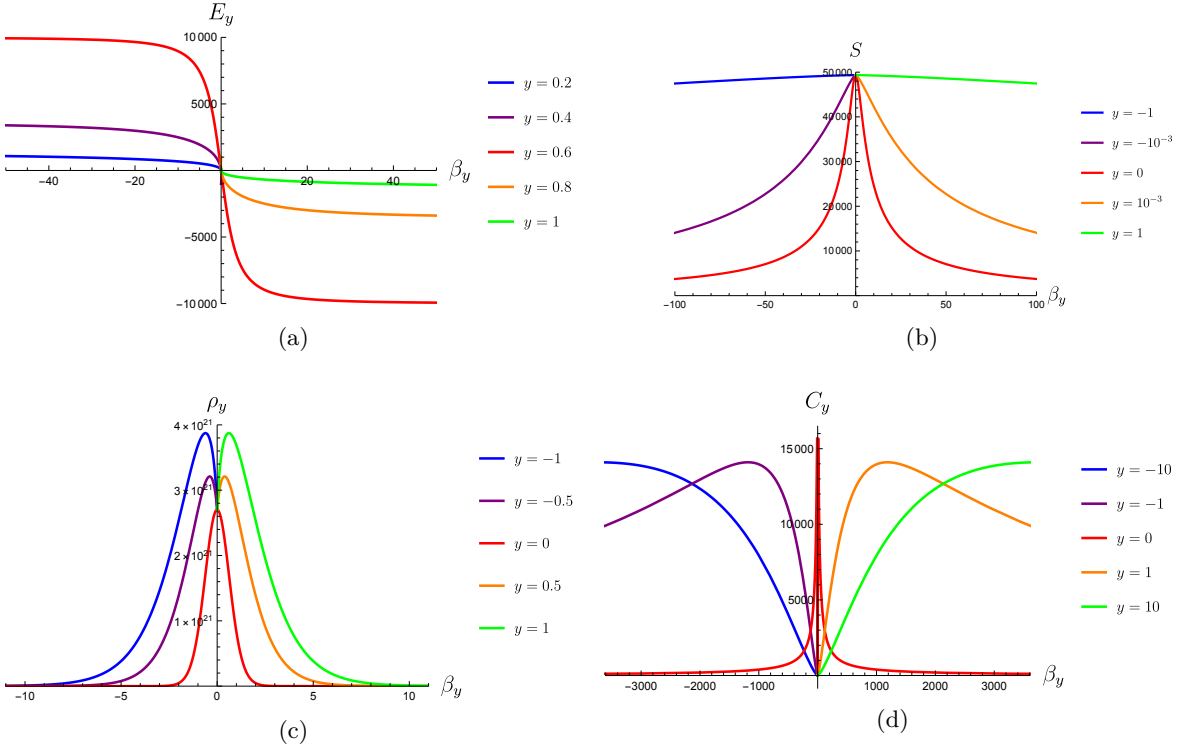


Figure 2. (a) The energy spectrum (3.13), (b) thermodynamic entropy (2.24), (c) density of states (2.27b), and (d) heat capacity (2.28) for generic values of the deformation parameter y (2.16) (shown in the legends) and fixing $\eta = +1$. We use $\lambda = 10^{-4}$ in all subfigures, except in (c) where $\lambda = 0.1$ for visualization purposes.

For concreteness, we consider the main cases of interest where $\eta = \pm 1$ so that E_y is given by (3.13) ($\eta = +1$) and (2.21) ($\eta = -1$) respectively, so that (2.28) becomes

$$C_y(\theta) = \frac{\eta(J \sin \theta \beta_y(\theta))^2}{2Jy \sin \theta(\pi - 2\theta) + 4Jy \cos \theta(2 + (\pi - 2\theta) \cot \theta) + 2(2 + (\pi - 2\theta) \cot \theta \sqrt{\lambda(1 - q)})} \quad (2.29)$$

The argument in the numerator is positive definite when $y \in \mathbb{R}$, $\lambda > 0$ and $\theta \in [0, \pi]$. Note that the case where $\eta = +1$ has a positive heat capacity while $\eta = -1$ a negative one assuming that E_y can be interpreted as the conserved energy spectrum of the deformed theory.

It is important to distinguish when $C_y(\theta)$ physically corresponds to heat capacity when performing the T^2 and $T^2 + \Lambda_1$ flow. For instance in dS₂, one performs the T^2 deformation, associated with $E_y^{\eta=+1}$, using the Dirichlet boundaries in the Milne patch which are spacelike [138]; while during the $T^2 + \Lambda_1$ flow, associated to $E_y^{\eta=-1}$, the finite cutoff boundaries are located in the static patch of dS₂ and they are timelike, so that $E_y^{\eta=-1}$ can indeed be associated with a quasilocal BY energy [184]. Then, (2.29) is indeed physically associated with a heat capacity and the system can thus be thermodynamically unstable, as found in different parts of the literature, see e.g. Sec 6.1. As additional comparison, when $T\bar{T}$ deforming CFTs, one

finds negative heat capacities at high energies for T^2 -deformed CFTs and quantum mechanical systems in [185]; while in this system, the energy spectrum is bounded. To make more contrast, opposite observations appear in the AdS_2 case, one performs the T^2 deformation when the boundaries are timelike, and thus the system is stable since (2.29) indeed corresponds to a positive heat capacity, and $T^2 + \Lambda_1$ when the boundaries are spacelike, similar to [136].

Finite cutoff Holographic Interpretation We now provide a bulk interpretation of (2.25) from finite cutoff holography. Let us consider the dilaton gravity theory (2.1), where the metric solution to the equations of motions without matter sources is

$$ds^2 = F(\Phi)d\tau + \frac{d\Phi}{F(\Phi)} , \quad F(x) = \int_{r_h}^x U(\Phi)d\Phi , \quad (2.30)$$

where r_h is the horizon radius. This can be used to evaluate the on-shell action from (2.1) resulting in

$$I_E^{(\text{on})} = -\frac{1}{2\kappa^2} \left(2\pi(\Phi_0 + r_h) + \beta \left(F(\Phi_B) - \sqrt{F(\Phi_B) G(\Phi_B)} \right) \right) , \quad (2.31)$$

where we have used the fact that \mathcal{M} has a disk topology when $\Phi_0 \gg |\Phi|$ everywhere in \mathcal{M} . From (2.31) we find:

$$\beta_T E_{\text{BY}} = \left(\beta \sqrt{\frac{F(\Phi_B)}{G(\Phi_B)}} \right) \left(\frac{G(\Phi_B)}{2\kappa^2} \left(1 - \sqrt{\frac{F(\Phi_B)}{G(\Phi_B)}} \right) \right) , \quad (2.32)$$

where we identified the inverse the BY quasi-local energy and *Tolman temperature* (i.e. the respective energy and temperature that an observer in a bulk spacetime would associate with a given system at a finite distance Φ_B from it [180]) as

$$E_{\text{BY}} \equiv \frac{1}{2\kappa^2} \left(\sqrt{G(\Phi_B)} - \sqrt{F(\Phi_B)} \right) , \quad \beta_T \equiv \beta \sqrt{F(\Phi_B)} . \quad (2.33)$$

Comparing (2.33) with the microcanonical temperature of the deformed theory in (2.25) due to (2.16), we identify the parameters:

$$E_y = \sqrt{G(\Phi_B)} E_{\text{BY}} , \quad \beta_y = \frac{\beta_T}{\sqrt{G(\Phi_B)}} . \quad (2.34)$$

For these relations to hold, we have that

$$\lambda = \kappa^2 , \quad (2.35)$$

which is consistent with [105].¹⁶

Thus, we find a holographic dictionary at the level of finite cutoff thermodynamics. In contrast with previous literature, we include a more general counterterm $G(\Phi_B)$ in the above expressions, which permits the analysis for non-trivial η in the flow equations (2.15).

¹⁶See e.g. (2.32) [105] where $\pi \mathbf{b}^2 = \kappa^2/2\pi$ in our notation.

Moreover, it follows from (2.34) that the specific heat in the bulk at a fixed finite radial cutoff can be expressed as

$$C_{r_B} \equiv -\beta_T^2 \frac{dE_{BY}}{d\beta_T} = -(\beta_y)^2 \frac{dE_y}{d\beta_y} = C_y . \quad (2.36)$$

This means that there is a direct relation between the heat capacity in the boundary theory at a fixed deformation parameter y (as well as η) (2.28) with respect to the heat capacity in the bulk. Similar results were recovered in related settings by [33].

Hagedorn growth Before closing the section, we make contrast with other results in the literature, we analyze the semiclassical partition function with $\eta = -1$ (2.21)

$$\int_{-\frac{2J}{\lambda}}^{\frac{2J}{\lambda}} dE(\theta) e^{S(\theta) - \beta E_y^{\eta=-1}(\theta)} = \int_{-\frac{2J}{\lambda}}^{\frac{2J}{\lambda}} dE(\theta) e^{S(\theta) - \frac{\beta}{y} (1 + \sqrt{2yE(\theta) - 1})} . \quad (2.37)$$

Notably, there no divergence associated to Hagedorn growth for the $T^2 + \Lambda_1$ deformed theory, in contrast to other studies [136]. The reason that there is no divergence even when $\beta \rightarrow 0$ is that the integration is performed over a finite energy range and the factor $e^{S(\theta)}$ is finite, thus the model remains UV finite. It was interpreted by [136], that one reaches a divergence once the boundary in the dual theory reaches a curvature singularity, which is not present in JT gravity, seen as a s-wave reduction of higher dimensional charged black hole, nor in sine dilaton gravity.

3 Deforming the DSSYK Model: Chord Basis, Bulk Length & Complexity

Following up the last subsection, we specialize in chord Hamiltonian deformations of the DSSYK model. Based on finite cutoff holography, we define a natural chord number basis. In this representation, the deformed chord Hamiltonian in the IR triple-scaling limit takes the same form as the ADM Hamiltonian of JT gravity in canonical variables at a finite cutoff.¹⁷ In this formulation, the chord number reproduces the corresponding wormhole length in the semiclassical limit of the path integral of theory. This motivates us to develop a new definition of state complexity based on the new chord number basis.

Outline In Sec. 3.1 we briefly review the DSSYK model, including its Hilbert space extension with matter chords. Next, in Sec. 3.2 we define a chord basis motivated by finite cutoff holography. In Sec. 3.3 we study the path integral formulation of the model. Sec. 3.4 contains a proposal for state complexity based on our previous results. It reproduces a wormhole length in finite cutoff holography. In Sec. 3.5 we define the IR/UV triple-scaling limits of the deformed theory.

¹⁷There is ongoing work by a different group following up [37], which has some overlap with the deformed DSSYK chord Hamiltonian in this section and its IR triple-scaling limit from a bulk perspective. I thank the authors for pointing it out.

3.1 Review of the DSSYK model

In this subsection, we briefly review the DSSYK model.

The SYK model [45–48, 186] is a system with N Majorana fermions in $(0+1)$ -dimensions, and p -body all-to-all interactions. The theory is given by

$$\hat{H}_{\text{SYK}} = i^{p/2} \sum_I J_I \hat{\psi}_I , \quad (3.1)$$

where $I = i_1, \dots, i_p$ is a collective index, $1 \leq i_1 < \dots < i_p \leq N$; and similarly $\hat{\psi}_I \equiv \hat{\psi}_{i_1} \dots \hat{\psi}_{i_p}$ is a string of Majorana fermions, obeying the Clifford algebra

$$\{\hat{\psi}_i, \hat{\psi}_j\} = 2\delta_{ij} \mathbb{1} ; \quad (3.2)$$

and the coupling constants $J_I = J_{i_1 \dots i_p}$ follow a Gaussian distribution

$$J_I = 0 , \quad \langle J_I J_J \rangle = \binom{N}{p}^{-1} \frac{J^2 N}{2p^2} \delta_{IJ} , \quad (3.3)$$

with $J \in \mathbb{R}$ being a constant, and the expectation values denote annealed averaging over the couplings. We also introduce matter operators (also called matter chords, or cords), which have the form:

$$\hat{O}_\Delta \equiv i^{\frac{p'}{2}} \sum_{I'} K_{I'} \hat{\psi}_{I'} . \quad (3.4)$$

Here $I' = i_1, \dots, i_{p'}$; and $K_{I'}$ represents Gaussian random couplings that are independent of J_I . We also define $\Delta \equiv p'/p$, so that we can express

$$\langle K_I \rangle = 0 , \quad \langle K_I J_{I'} \rangle = 0 , \quad \langle (K_I)^2 \rangle = \frac{\mathcal{K}^2}{\Delta^2 \lambda} \binom{N}{p'}^{-1} , \quad (3.5)$$

where $\mathcal{K} \in \mathbb{R}$. In the following, we will set $\mathcal{K} = 1$, which can be restored back with dimensional analysis. Importantly for us, once we consider the double scaling regime, where:

$$N, p \rightarrow \infty , \quad q = e^{-\lambda} \equiv e^{-\frac{2p^2}{N}} \text{ fixed} . \quad (3.6)$$

The SYK model becomes analytically solvable even away from the low energy regime; its ensemble averaged Hamiltonian moments can be described with chord diagrams techniques [49–52] which leads to an auxiliary quantum mechanical theory containing thermal information about the physical system.¹⁸ The auxiliary chord Hilbert space without matter insertions is

$$\mathcal{H}_0 = \text{span}\{|n\rangle \mid n \in \mathbb{Z}\} = L^2([0, \pi], d\mu(\theta)) , \quad (3.7)$$

¹⁸Other models in the same universality class as the DSSYK model can be solved using the same type of chord counting techniques [176, 187–190].

where n denotes the number of open chords at a given time slice in the chord diagram (see e.g. [191] for a review). From now on we will denote the zero chord number state as

$$|n=0\rangle \equiv |\Omega\rangle . \quad (3.8)$$

By an appropriate orthogonal transformation, $\{|n\rangle\}$ can be orthonormalized (i.e. $\langle n|m\rangle = \delta_{nm}$), such that the Hamiltonian takes a symmetric form (see e.g. [51])

$$\hat{H}|n\rangle = -\frac{J}{\sqrt{\lambda}} \left(\sqrt{[n]_q} |n-1\rangle + \sqrt{[n+1]_q} |n+1\rangle \right) , \quad (3.9)$$

where $[n]_q \equiv \frac{1-q^n}{1-q}$. We can now define the chord number operator \hat{n} and its conjugate momentum, \hat{p} :

$$e^{\pm i\hat{p}} |n\rangle = |n \mp 1\rangle , \quad \hat{n} |n\rangle = n |n\rangle , \quad (3.10)$$

which obey the commutation relation:

$$[\hat{n}, e^{i\hat{p}}] = e^{i\hat{p}} , \quad [\hat{n}, e^{-i\hat{p}}] = -e^{-i\hat{p}} . \quad (3.11)$$

The Hamiltonian can be then expressed as

$$\hat{H} = -\frac{J}{\sqrt{\lambda}} \left(e^{i\hat{p}} \sqrt{[\hat{n}]_q} + \sqrt{[\hat{n}]_q} e^{-i\hat{p}} \right) . \quad (3.12)$$

One can also find the energy basis $|\theta\rangle$ of \hat{H} , whose eigenvalues are given as [51, 52]

$$\hat{H}|\theta\rangle = E(\theta)|\theta\rangle , \quad E(\theta) \equiv -\frac{2J \cos(\theta)}{\sqrt{\lambda(1-q)}} , \quad \theta \in [0, \pi] . \quad (3.13)$$

Solving the eigenvalue problem in (3.12) one can then find that the inner product between the energy basis $\{|\theta\rangle\}$ and the chord number $\{|n\rangle\}$ is given by

$$\langle \theta | n \rangle = \frac{H_n(\cos \theta | q)}{\sqrt{(q; q)_n}} , \quad (3.14)$$

with $(a; q)_n$ the q-Pochhammer symbol:

$$(a; q)_n \equiv \prod_{k=0}^{n-1} (1 - aq^k) , \quad (a_0, \dots, a_N; q)_n \equiv \prod_{i=1}^N (a_i; q)_n , \quad (3.15)$$

and $H_n(x|q)$ is the q-Hermite polynomial:

$$H_n(\cos \theta | q) \equiv \sum_{k=0}^n \begin{bmatrix} n \\ k \end{bmatrix}_q e^{i(n-2k)\theta} , \quad \begin{bmatrix} n \\ k \end{bmatrix}_q \equiv \frac{(q; q)_n}{(q; q)_{n-k} (q; q)_k} . \quad (3.16)$$

The $|\theta\rangle$ basis is normalized such that

$$\langle \theta | \theta_0 \rangle = \frac{1}{\mu(\theta)} \delta(\theta - \theta_0) , \quad \mathbb{1} = \int_0^\pi d\theta \mu(\theta) |\theta\rangle \langle \theta| , \quad (3.17)$$

$$\mu(\theta) = \frac{(q, e^{\pm 2i\theta}; q)_\infty}{2\pi} \equiv \frac{1}{2\pi} (q, q)_\infty (e^{2i\theta}, q)_\infty (e^{-2i\theta}, q)_\infty . \quad (3.18)$$

For later convenience, we introduce a simple generalization when considering that the DSSYK model with matter insertions [53], which we denote as

$$\mathcal{H}_{\text{full}} \equiv \bigoplus_{m=0}^{\infty} \mathcal{H}_m , \quad \mathcal{H}_m \equiv \text{span} \left\{ \left| \tilde{\Delta}, n_0, n_1, \dots, n_m \right\rangle \right\} , \quad (3.19)$$

where $\tilde{\Delta} = \{\Delta_1, \dots, \Delta_m\}$ is a set of conformal dimensions, and Δ_i characterizes each matter chord operator \hat{O}_{Δ_i} which is the ensemble averaged analog of the SYK operator (3.4).

It is also useful to define a total chord number operator

$$\hat{N} \left| \tilde{\Delta}, n_0, \dots, n_m \right\rangle = \sum_{i=0}^m n_i \left| \tilde{\Delta}, n_0, \dots, n_m \right\rangle , \quad (3.20)$$

which will be applied in later sections to evaluate correlation functions.

Next, we consider the two-sided chord Hamiltonian with m operator insertions:

$$\hat{H}_{L/R} = -\frac{J}{\sqrt{\lambda}} \left(\hat{a}_{L/R} + \hat{a}_{L/R}^\dagger \right) , \quad \text{where} \quad (3.21a)$$

$$\hat{a}_L^\dagger = \hat{a}_0^\dagger , \quad \hat{a}_L = \sum_{i=0}^m \hat{\alpha}_i [\hat{n}_i]_q q^{\hat{n}_i^<} , \quad \text{with} \quad \hat{n}_i^< = \sum_{j=0}^{i-1} (\hat{n}_j + \Delta_{j+1}) , \quad (3.21b)$$

$$\hat{a}_R^\dagger = \hat{a}_m^\dagger , \quad \hat{a}_R = \sum_{i=0}^m \hat{\alpha}_i [\hat{n}_i]_q q^{\hat{n}_i^>} , \quad \text{with} \quad \hat{n}_i^> = \sum_{j=i+1}^m (\hat{n}_j + \Delta_j) , \quad (3.21c)$$

where the creation and annihilation operators for the chord number sectors (3.21) in (3.19) act as,

$$\hat{a}_i^\dagger \left| \tilde{\Delta}; n_0, \dots, n_i, \dots, n_m \right\rangle = \left| \tilde{\Delta}; n_0, \dots, n_i + 1, \dots, n_m \right\rangle , \quad (3.22a)$$

$$\hat{\alpha}_i \left| \tilde{\Delta}; n_0, \dots, n_i, \dots, n_m \right\rangle = \left| \tilde{\Delta}; n_0, \dots, n_i - 1, \dots, n_m \right\rangle . \quad (3.22b)$$

For instance, in terms of the above basis, the one-particle chord Hamiltonian, corresponding to $m = 1$ in (3.21) becomes

$$\hat{H}_{L/R} = \frac{J}{\sqrt{\lambda(1-q)}} \left(e^{-i\hat{P}_{L/R}} + e^{i\hat{P}_{L/R}} (1 - e^{-\hat{\ell}_{L/R}}) + q^\Delta e^{i\hat{P}_{R/L}} e^{-\hat{\ell}_{L/R}} (1 - e^{-\hat{\ell}_{R/L}}) \right) . \quad (3.23)$$

where we expressed

$$\hat{a}_i^\dagger = \frac{e^{-i\hat{P}_i}}{\sqrt{1-q}} , \quad \hat{\alpha}_i = \sqrt{1-q} e^{i\hat{P}_i} , \quad q^{\hat{n}_i} = e^{-\hat{\ell}_i} , \quad i = L, R . \quad (3.24)$$

At last, there is an energy basis conjugate to the one-particle chord number basis, diagonalizing the two-sided Hamiltonians (3.21a), i.e.

$$\hat{H}_{L/R} |\Delta; \theta_L, \theta_R\rangle = E(\theta_{L/R}) |\Delta; \theta_L, \theta_R\rangle . \quad (3.25)$$

where $E(\cdot)$ appears in (3.13). We will apply the above definitions to evaluate different properties and observables of the theory under a Hamiltonian deformation in the remainder of the manuscript.

3.2 Chord Basis and Hamiltonian Representations

We now explore the structure of the chord Hilbert space after a generic Hamiltonian deformation

$$\hat{H} \rightarrow \hat{H}_y \equiv f_y(\hat{H}) |\Omega\rangle , \quad (3.26)$$

for some analytic function f_y . For instance, in the particular case of a T^2 deformation [27]

$$f_y(x) = \frac{1}{y} \left(1 - \sqrt{1 - 2yx} \right) . \quad (3.27)$$

While the deformed and seed theories have the same Hilbert space, the chord basis can take different forms, and the Hamiltonian (3.26) can have different representations depending on the basis that we choose. For instance, consider the chord number basis as

$$|n\rangle = f_n \left(\hat{h} \equiv \frac{\sqrt{\lambda(1-q)}}{-J} \hat{H} \right) |\Omega\rangle , \quad (3.28a)$$

$$\frac{x}{\sqrt{1-q}} f_n(x) = \sqrt{[n+1]_q} f_{n+1}(x) + \sqrt{[n]_q} f_{n-1}(x) , \quad f_0(x) = 1, \quad f_{-1}(x) = 0 , \quad (3.28b)$$

where the recursive function $f(x)$ can be associated to normal ordering [54] in terms of the creation and annihilation operators \hat{a} and \hat{a}^\dagger . In this representation, we recover the same representation for the seed theory chord Hamiltonian in (3.12).

Motivated by recent progress on finite cutoff holography [37], we define a new chord basis

$$|n\rangle_y \equiv g_n \left(\hat{h} \equiv \frac{\sqrt{\lambda(1-q)}}{-J} \hat{H} \right) |\Omega\rangle , \quad (3.29)$$

where $g_n(x)$ is a polynomial function defined recursively

$$x g_n(x) = g_{n+1}(x) + \left(1 - R(y)^2 \operatorname{sech}^2 \frac{\lambda n}{2} \right) g_{n-1}(x) , \quad (3.30)$$

with $R(y)$ a constant dependent on the deformation parameter y , and we impose as initial conditions,¹⁹

$$g_0(x) = 1 , \quad g_{-1}(x) = 0 . \quad (3.32)$$

The explicit holographic dictionary between the arbitrary parameter $R(y)$ and the bulk radial cutoff will be determined below.

Using the basis (3.29), the seed theory Hamiltonian is then expressed as,²⁰

$$\hat{H} = \frac{-J}{\sqrt{\lambda(1-q)}} \left(2 \cos \hat{P}_y - R(y)^2 e^{i\hat{P}_y} \operatorname{sech}^2 \frac{\lambda \hat{n}_y}{2} \right) , \quad (3.34)$$

¹⁹For instance:

$$g_1(x) = R(y)^2 \operatorname{sech}^2 \left(\frac{\lambda}{2} \right) x , \quad (3.31)$$

and the higher-order polynomials, $g_{n \geq 2}$, follow iteratively.

²⁰Note that by imposing

$$\lim_{y \rightarrow 0} \frac{\cosh(L_y/2)}{R(y)} = e^{L/2}/2 , \quad (3.33)$$

one recovers the corresponding chord Hamiltonian (3.39) in the appropriate limit after a canonical transformation [67]. Importantly, (3.34) remains as a Hermitian Hamiltonian with respect to the chord inner product [68, 69].

where

$$e^{\mp i\hat{P}_y} |n\rangle_y \equiv |n \pm 1\rangle_y, \quad \hat{n}_y |n\rangle_y \equiv n |n\rangle_y. \quad (3.35)$$

We remark (3.34) is just a representation; whose deformation corresponds to \hat{H}_y (3.26). As we will see, there is a useful physical interpretation for the above operator representations.

First, note there is a map between the different chord basis, given by

$$|n\rangle_y = g_n(\hat{h}) |\Omega\rangle = \sum_{m=0}^{\infty} a_{nm} |m\rangle, \quad (3.36)$$

where

$$a_{nm} \equiv \langle m|n\rangle_y = \int_0^\pi d\theta \mu(\theta) g_n(2\cos\theta) \frac{H_n(\cos\theta|q)}{\sqrt{(q;q)_n}}. \quad (3.37)$$

While the chord Hamiltonian (3.34) is tridiagonal in the new chord basis (3.29), which is not an orthonormal basis, as we show in Sec. 3.4. The reason for representing the Hamiltonian in the basis $|n\rangle_y$ is that, as we will see, the chord number in this basis is related to a Einstein-Rosen bridge connecting the boundaries of an AdS_2 black hole with a finite radial cutoff with Dirichlet boundary conditions [37] (7.5) (see also App. B), and it also has an interpretation in terms of minimal length geodesics in dS_2 JT gravity (Sec. 6.2). We elaborate these perspectives below.

3.3 Path Integral Formulation of the Deformed DSSYK

As previously mentioned, the chord basis for the new Hamiltonian representation (3.34) allows us to associate the expectation value of the chord number

$$\hat{n}_y \equiv \sum_{n=0}^{\infty} n |n\rangle_y \langle n|_y, \quad (3.38)$$

in the deformed HH state

$$|\psi(\tau)\rangle = e^{-\tau\hat{H}_y} |\Omega\rangle, \quad (3.39)$$

with a geodesic length in finite cutoff holography. To see this, we study the path integral of the theory

$$Z = \int [dL_y] [dP_y] \exp \left[\int d\tau \left[\frac{i}{\lambda} P_y \partial_\tau L_y - H_y \right] \right], \quad (3.40a)$$

$$H_y = f_y \left(\frac{J}{\lambda} \left(2 \cos P_y - \frac{R(y)^2 e^{iP_y}}{\cosh^2 \frac{L_y}{2}} \right) \right). \quad (3.40b)$$

where $\tau \equiv \frac{\beta}{2} + it$. Here, we represent L_y as the semiclassical expectation value of the chord number, namely

$$L_y \equiv \lambda \frac{\langle \Omega | e^{-\tau^* \hat{H}_y} \hat{n}_y e^{-\tau \hat{H}_y} | \Omega \rangle}{\langle \Omega | e^{-\beta \hat{H}} | \Omega \rangle}, \quad (3.41)$$

and P_y is the corresponding conjugate momenta. The saddle point solutions of (3.40a) are then

$$\frac{1}{\lambda} \frac{dL_y}{dt} = \frac{\partial H_y}{\partial P_y} = f'_y(H) \frac{\partial H}{\partial P_y} , \quad (3.42a)$$

$$\frac{1}{\lambda} \frac{dP_y}{dt} = -\frac{\partial H_y}{\partial L_y} = -f'_y(H) \frac{\partial H}{\partial L_y} . \quad (3.42b)$$

Note that we have used the chain rule. Using the explicit form in (3.34) we recover

$$\frac{dL_y}{dt_y} = 2i(\cos \theta - e^{iP_y}) , \quad (3.43a)$$

$$-i \frac{de^{-iP_y}}{dt_y} = R(y)^2 \operatorname{sech}^2 \left(\frac{L_y}{2} \right) \tanh \left(\frac{L_y}{2} \right) , \quad (3.43b)$$

where

$$t_y \equiv J f'_y(H) t . \quad (3.44)$$

In particular for T^2 deformations (3.27) we have that the redshift factor is $f'_y(H) = 1/\sqrt{1-2yH}$, and for $T^2 + \Lambda_1$ $f'_y(H) = 1/\sqrt{2yH-1}$.

The differential equations in (3.43) are supplemented by boundary conditions

$$L_y(0) \equiv L_0 , \quad L'_y(0) = 0 , \quad (3.45)$$

where the second condition follows from the comutation relation

$$\begin{aligned} \frac{d}{dt} \langle \psi(\tau) | \hat{n}_y | \psi(\tau) \rangle \Big|_{t=0} &= \langle \Omega | e^{-\frac{\beta}{2} \hat{H}_y} [\hat{H}_y, \hat{n}_y] e^{-\frac{\beta}{2} \hat{H}_y} | \Omega \rangle \\ &= 2 \sum_{n=0}^{\infty} n \left(\langle \Omega | e^{-\beta \hat{H}_y} | n \rangle_y \langle n |_y \frac{de^{-\beta \hat{H}_y}}{d\beta} | \Omega \rangle - \langle \Omega | \frac{de^{-\beta \hat{H}_y}}{d\beta} | n \rangle_y \langle n |_y e^{-\frac{\beta}{2} \hat{H}_y} | \Omega \rangle \right) \\ &= 2 \sum_{n=0}^{\infty} n (\psi_n(\beta, y) \psi'_n(\beta, y) - \psi_n(\beta, y) \psi'_n(\beta, y)) = 0 , \end{aligned} \quad (3.46)$$

where we expanded the chord number as $\hat{n}_y \equiv \sum_n n |n\rangle_y \langle n|_y$ and we defined $\psi_n(\beta, y) \equiv \langle \Omega | e^{-\frac{\beta}{2} \hat{H}_y} | n \rangle_y$, which is real as long as \hat{H}_y is Hermitian, and $\psi'_n(\beta, y) = d\psi_n(\beta, y)/d\beta$; which thus leads to the second initial condition in (3.45).

Meanwhile, L_0 in (3.45) is a numerical constant determined from initial conditions and conservation of energy. Namely, consider (3.43a) and the second initial condition in (3.45) for $t = 0$ implies

$$\frac{dL_y}{dt_y} \Big|_{t_y=0} = 0 , \quad e^{iP_y(0)} = \cos \theta . \quad (3.47)$$

Then, by introducing (3.47) and the first initial condition in (3.45) to (3.40b), it follows that

$$R(y)^2 \operatorname{sech}^2 \frac{L_0}{2} = \sin^2 \theta . \quad (3.48)$$

Combining them, we recover

$$\frac{d^2 L_y}{dt_y^2} = 2R(y)^2 \tanh\left(\frac{L_y}{2}\right) \operatorname{sech}^2\left(\frac{L_y}{2}\right). \quad (3.49)$$

The solution to the above ordinary differential equation subject to the boundary conditions (3.45) is

$$L_y = 2 \operatorname{arcsinh}\left(\sqrt{\frac{R(y)^2}{\sin^2 \theta} - 1} \cosh(t_y \sin \theta)\right), \quad (3.50)$$

which is precisely the spacelike geodesic length between the finite cutoff boundaries of AdS_2 black holes [37, 148] with a black hole horizon at $\rho = \sin \theta$ in the coordinates

$$ds_{\text{eff}}^2 = (\rho^2 - \sin^2 \theta) d\tau^2 + \frac{d\rho^2}{\rho^2 - \sin^2 \theta}. \quad (3.51)$$

In fact, we show that (3.50) is also valid to describe timelike geodesics connecting finite cutoff boundaries inside the AdS_2 black hole (3.51), see App. B.

In the AdS_2 interpretation, $\rho = R(y)$ (3.50) corresponds to the radial cutoff parameter in the effective AdS_2 metric. Thus, while the original chord Hamiltonian in canonical variables measure lengths/momenta with respect to the boundaries [53], we can implement the canonical transformation in the Hamiltonian (3.34) to the new chord basis (3.29) to describe the deformed theory.²¹

T^2 vs $T^2 + \Lambda_1$ Deformations Note that in the derivation of the semiclassical chord number (3.50) we have made no assumptions about the explicit form of f_y ; the expression is valid for both general deformations in finite cutoff holography. In particular, the difference between T^2 and $T^2 + \Lambda_1$ deformation is contained in the factor t_y (3.44) which depends on the explicit form of the deformation. Also, from the bulk perspective, we will be interested in the cases where $R(y) \geq \sin \theta$ for the T^2 case, and $R(y) \leq \sin \theta$ for $T^2 + \Lambda_1$, resulting real-valued and pure imaginary lengths, as we elaborate later in Sec. 3.5.

3.4 State Complexity

In this subsection, we seek to interpret the expectation value of the chord number operator $|n\rangle_y$ (3.38) in terms of state complexity (similar to [53, 63] in the seed theory) to clarify its place in

²¹For example, in the specific case of the sine dilaton gravity proposal [85], the map between the AdS_2 black hole metric (3.51) to the geometry where we identified $y = 2\lambda/G(r_B)$ based on (2.16) and (2.35) is given by

$$r_B = \frac{\pi}{2} + i \log(R(y) + i \cos \theta), \quad y = \frac{-\lambda}{\cos(r_B)}, \quad (3.52)$$

where we are using $G(x) = -2 \cos(x)$ (2.2) for sine dilaton gravity. The above relation means that

$$\frac{\lambda}{y} = \frac{i}{2} \left(R(y) + i \cos \theta - \frac{1}{R(y) + i \cos \theta} \right), \quad (3.53)$$

if the DSSYK model were dual to sine dilaton gravity at the disk level.

the finite cutoff holographic dictionary. While there have been significant insights gained by studying Krylov (state and operator) complexity in the DSSYK model [63, 65–70, 73–76, 192], we will take a broader perspective before discussing Krylov spread complexity and proposing a notion of state complexity which is particularly suited to study finite cutoff holography.

State Complexity From Cost Function In general, following [81] and [193] we refer to the cost function of an ordered basis $\{|B_0\rangle, |B_1\rangle, \dots, |B_n\rangle, \dots\}$ with respect to a reference state $|\psi(\tau)\rangle$ as

$$\mathcal{C} \equiv \sum_{n=0}^{\infty} c_n \frac{|\langle B_n | \psi(\tau) \rangle|^2}{\langle \psi(\tau) | \psi(\tau) \rangle} , \quad (3.54)$$

where $\{c_n \in \mathbb{R}\}$ is a monotonically increasing sequence, and we allow that the reference state evolves in complex-valued time τ as [193]

$$|\psi(\tau)\rangle \equiv e^{-\tau \hat{\mathcal{L}}} |\psi(0)\rangle , \quad (3.55)$$

where $\tau \equiv \frac{\beta}{2} + it$, with β and $t \in \mathcal{R}$, leading to standard Schrödinger evolution when $\beta = 0$, and $\hat{\mathcal{L}}$ is the corresponding generator of evolution in terms of the parametrization τ . State complexity in [81] is defined by minimizing the cost function (3.54) over all possible basis sets, which occurs when $\{|B_n\rangle\}$ is the Krylov basis, defined below.

Krylov Spread Complexity Now, we specialize in Krylov spread complexity [81] in deformed DSSYK, so that $\hat{\mathcal{L}} = \hat{H}_y$ in (3.55). We seek to build a Krylov basis $\{|K_n\rangle\}$ with $|K_0\rangle = |\psi(\tau = 0)\rangle$ as the initial state in the basis, which we may choose as the zero-chord state $|\Omega\rangle$. The other elements in the Krylov basis are obtained recursively through the Lanczos algorithm in the form,

$$|K_n\rangle \equiv f_n \left(\hat{h}_y \equiv \frac{\sqrt{\lambda(1-q)}}{-J} \hat{H}_y \right) |\Omega\rangle , \quad (3.56a)$$

$$x f_n(x) = b_{n+1} f_{n+1}(x) + b_n f_{n-1}(x) + a_n f_n(x) , \quad (3.56b)$$

which is initialized by the condition $b_0 = 0$, $f_0(x) = 1$; and b_n and a_n are the Lanczos coefficients. One can then use the above algorithm to find the explicit coefficients in terms of Hamiltonian moments (see e.g. [194])

$$\begin{aligned} a_0 &= m_1 , \quad b_1 = m_2 - m_1^2 , \quad a_1 = \frac{m_3 + m_1^3 - 2m_1 m_2}{m_2 - m_1^2} , \\ b_2 &= \frac{m_2 m_4 - m_2^3 - m_3^2 - m_1^2 m_4 - 2m_1^2 m_2 m_4}{(m_2 - m_1^2)^2} \end{aligned} \quad (3.57)$$

where

$$m_n = (-1)^n \left. \frac{\partial^n \mathcal{Z}_y(\beta)}{\partial \beta^n} \right|_{\beta=0} , \quad \mathcal{Z}(\beta) \equiv \frac{\langle \psi(t=0) | e^{-\beta \hat{H}_y} | \psi(t=0) \rangle}{\langle \psi(t=0) | \psi(t=0) \rangle} . \quad (3.58)$$

Then, based on (3.54) with $\{B_n\} = \{|K_n\rangle\}$ and $c_n = n$, Krylov spread complexity is simply defined as

$$\mathcal{C}_S = \sum_{n=0}^{\infty} n \frac{|\langle K_n | \psi(t) \rangle|^2}{\langle \psi(t) | \psi(t) \rangle}. \quad (3.59)$$

By deducing the form of the Lanczos coefficients one can then work in the semiclassical limit, where $\ell \equiv \lambda \mathcal{C}_y$ ((3.66)) is fixed as $\lambda \rightarrow 0$ as

$$Z = \int [d\ell] [dp] \exp \left[\int d\tau \left(\frac{i}{\lambda} p \partial_\tau \ell - H_y \right) \right], \quad H_y = \frac{J}{\lambda} (b(\ell) \cos p + a(\ell)). \quad (3.60)$$

One then finds the equations of motion

$$\frac{1}{\lambda} \frac{d\ell}{dt} = -2 \sin p \, b(\ell), \quad \frac{1}{\lambda} \frac{dp}{dt} = 2 \cos p \, b'(\ell) + a'(\ell), \quad (3.61a)$$

$$-\frac{1}{\lambda^2} \frac{d^2\ell}{dt^2} = 2 \frac{d}{d\ell} (b(\ell)^2) + a'(\ell), \quad (3.61b)$$

where $b'(\ell) = \frac{db}{d\ell}$. However, in our case of interest, due to the deformation in the energy spectrum, there are additional complications in deriving the explicit form of the Krylov basis from the Lanczos coefficients (3.57). It would be very interesting to find a close form of the Lanczos coefficients in the semiclassical limit and solving (3.61) explicitly to check if it agrees with the expectation value of the chord number in the $|n\rangle_y$ basis (3.50). Below, we take a different approach where we define a notion of state complexity in the DSSYK model which has an arguably clear bulk interpretation in finite cutoff holography.

A Proposal for State Complexity Now, we develop a chord basis closely related to $|n\rangle_y$ (3.29) that obeys the recurrence relation in the Lanczos algorithm (3.56b). For concreteness, consider the reference state

$$|\psi(\tau)\rangle = e^{-\tau \hat{H}_y} |\psi(0)\rangle, \quad (3.62)$$

where, for instance, one may select the zero-particle HH state as the reference $|\psi(0)\rangle = |\Omega\rangle$. In general, we construct a chord basis of the form

$$|n, y\rangle \equiv \tilde{g}_n \left(\hat{h} \equiv \frac{\sqrt{\lambda(1-q)}}{-J} \hat{H} \right) |\psi(0)\rangle, \quad (3.63)$$

where \tilde{g}_n obeys a recurrence relation

$$x \tilde{g}_n(x) = \sqrt{1 - R(y)^2 \operatorname{sech}^2 \frac{\lambda(n+1)}{2}} \tilde{g}_{n+1}(x) + \sqrt{1 - R(y)^2 \operatorname{sech}^2 \frac{\lambda n}{2}} \tilde{g}_{n-1}(x), \quad (3.64)$$

$$\tilde{g}_0(x) = 1, \quad \tilde{g}_{-1}(x) = 0,$$

Note (3.64) adopts the same form as the recurrence relation in the Lanczos algorithm (3.56b). The crucial difference is that the resulting basis $\{|n, y\rangle\}$ is not orthonormal, as seen by inserting the resolution of the identity in the energy basis (3.17),

$$\langle n, y | m, y \rangle = \int_0^\pi d\theta \, \mu(\theta) \tilde{g}_n(2 \cos \theta) \tilde{g}_m(2 \cos \theta). \quad (3.65)$$

The result of the integral would be δ_{nm} if and only if $\tilde{g}_n(2\cos\theta)$ were substituted for (3.14) due to the measure $\mu(\theta)$ in (3.17). Thus, despite that $\{|n, y\rangle\}$ satisfies a recurrence relation of the same form as that in the Lanczos algorithm (3.56b), it is not orthonormal and thus, not a Krylov basis. Nevertheless, $|n, y\rangle$ and plays a role in finite cutoff holography. To see this, we define the state complexity associated to the basis $|n, k\rangle$ in a similar way as (3.59),²²

$$\mathcal{C}_y \equiv \sum_{n=0}^{\infty} \frac{n|\langle\psi(\tau)|n, y\rangle|^2}{\langle\psi(\tau)|\psi(\tau)\rangle} . \quad (3.66)$$

We can then evaluate (3.66) in the semiclassical limit, i.e. λn fixed as $\lambda \rightarrow 0$. For convenience in the evaluation, note that the recurrence relation (3.64) is equivalent to the one defining $|n\rangle_y$ in (3.30) after a rescaling of the operators,

$$e^{-i\hat{P}_y} \rightarrow \sqrt{1 - R(y)^2 \operatorname{sech}^2 \frac{\lambda \hat{n}_y}{2}} e^{-i\hat{P}_y} , \quad e^{i\hat{P}_y} \rightarrow e^{i\hat{P}_y} \sqrt{1 - R(y)^2 \operatorname{sech}^2 \frac{\lambda \hat{n}_y}{2}} , \quad (3.67)$$

where the rescaled $e^{-i\hat{P}_y}$ acts on the $|n, y\rangle$ basis in the same way as for $|n\rangle_y$ in (3.35). This means that the zero-particle chord Hamiltonian is represented by

$$\hat{H} = \frac{-J}{\sqrt{\lambda(1-q)}} \left(e^{i\hat{P}_y} \sqrt{1 - R(y)^2 \operatorname{sech}^2 \frac{\lambda \hat{n}_y}{2}} + \sqrt{1 - R(y)^2 \operatorname{sech}^2 \frac{\lambda \hat{n}_y}{2}} e^{i\hat{P}_y} \right) \quad (3.68)$$

in the basis $|n, y\rangle$ generated from the recurrence relation (3.64).

We can then evaluate state complexity (3.66) from

$$\ell(t) \equiv \frac{\lambda \langle\psi(\tau)|\hat{n}_y|\psi(\tau)\rangle}{\langle\psi(\tau)|\psi(\tau)\rangle} \Big|_{\tau=\frac{\beta}{2}+it} = \lambda \mathcal{C}_y , \quad (3.69)$$

where ℓ satisfies the equation of motion in (3.61b), which can be evaluated by identifying the corresponding Lanczos coefficients from (3.68),

$$b(\ell) = \frac{-J}{\lambda} \sqrt{1 - R(y)^2 \operatorname{sech}^2 \frac{\ell}{2}} , \quad a(\ell) = 0 . \quad (3.70)$$

Thus, $\ell(t)$ satisfies the same equation of motion as L_y (3.49), and given that the reference state in the algorithm is the zero-particle HH state, it follows that ℓ satisfies the same initial conditions as L_y (3.45) from the same argument as (3.46) to show that $\ell'(0) = 0$ and from conservation of the Hamiltonian (3.68) at the semiclassical level for $\ell(0) = L_0$ (3.48). It

²²However, since $\{|n, y\rangle\}$ is not an orthonormal basis, (3.66) is not a cost function (3.54) and thus not state complexity per the definition in [81]. Nevertheless, we refer to (3.66) as state complexity in a broader sense, given that $\{|n, y\rangle\}$ satisfies a recurrence relation of the same form as that in the Krylov basis (3.56b), albeit these two basis have different properties.

follows that $\ell(t)$ evolves in the same way as L_y (3.50). Using (3.69), this means that the state complexity of the HH state $\psi(\tau)$ in the $|n, y\rangle$ basis is given by

$$\mathcal{C}_y = \frac{2}{\lambda} \operatorname{arcsinh} \left(\sqrt{\frac{R(y)^2}{\sin^2 \theta} - 1} \cosh(t_y \sin \theta) \right). \quad (3.71)$$

Thus, our proposal for state complexity is constructed to reproduce a wormhole length at finite cutoff (3.50) (Fig. 3) in the semiclassical limit, i.e. where $\lambda \mathcal{C}_y$ is fixed as $\lambda \rightarrow 0$. In particular in the limit $y = 0$ we recover the Krylov spread complexity of the seed DSSYK model (see footnote 20).

Note however that the definition (3.66) is simply an interpretation of the chord basis (3.29) that reproduces a wormhole length (3.50). To probe finite cutoff holography, it is more interesting to relate the deformed DSSYK chord Hamiltonian (3.26) with the wormhole length (3.50). A natural expectation is that the Krylov spread complexity of the reference state (3.62) given the deformed Hamiltonian (3.26) would reproduce the new state complexity definition (3.66) in the seed theory. However, the technical analysis is more complex, we have not performed an all order derivation of the corresponding Krylov basis in this manuscript.

3.5 IR/UV Triple-Scaling Limits and $T^2(+\Lambda_1)$ Deformations

Since the expectation value of the chord number (3.38) is related to a bulk geodesic, we now propose the following definition of IR/UV triple-scaling limit to further examine its properties:

$$\text{IR : } \operatorname{sech}^2 \frac{\hat{L}_y}{2} \rightarrow \lambda^2 \operatorname{sech}^2 \frac{\hat{L}_{\text{IR}}}{2}, \quad \hat{P}_y \rightarrow \lambda \hat{P}_{\text{IR}}, \quad (3.72a)$$

$$\text{UV : } \operatorname{sech}^2 \frac{\hat{L}_y}{2} \rightarrow \lambda^2 \operatorname{sech}^2 \frac{i\hat{L}_{\text{UV}}}{2}, \quad \hat{P}_y \rightarrow \pi - i\lambda \hat{P}_{\text{UV}}, \quad (3.72b)$$

where the eigenvalues of the operators \hat{L}_{IR} , \hat{P}_{IR} and \hat{L}_{UV} , \hat{P}_{UV} are fixed as $\lambda \rightarrow 0$.

We note that by subtracting the zero-energy contribution in the IR and UV limits of the chord Hamiltonian in the $|n\rangle_y$ basis (3.34) and considering leading order terms, we recover

$$\hat{H}_{\text{IR}} \equiv \frac{1}{2J\lambda} \left(\hat{H} + \frac{2J}{\sqrt{\lambda(1-q)}} \right) \Big|_{\mathcal{O}(1), \text{IR}} = \frac{\hat{P}_{\text{IR}}^2}{2} + \frac{R(y)^2}{2} \operatorname{sech}^2 \frac{\hat{L}_{\text{IR}}}{2}, \quad (3.73a)$$

$$\hat{H}_{\text{UV}} \equiv \frac{1}{2J\lambda} \left(\hat{H} - \frac{2J}{\sqrt{\lambda(1-q)}} \right) \Big|_{\mathcal{O}(1), \text{UV}} = -\frac{\hat{P}_{\text{UV}}^2}{2} + \frac{R(y)^2}{2} \operatorname{sec}^2 \frac{\hat{L}_{\text{UV}}}{2}. \quad (3.73b)$$

\hat{H}_{IR} is isomorphic to the canonically quantized JT gravity Hamiltonian at finite cutoff in [37] (\hat{H}_{IR}) in terms of the finite cutoff length and its canonical conjugate,²³ and \hat{H}_{UV} is its

²³Alternatively, it is suggested in [37] that the JT gravity ADM Hamiltonian at finite cutoff is

$$\hat{H}_y^{(\text{JT})} = \frac{1}{y} \left(1 - \tanh \frac{\hat{L}_y}{2} \cos \hat{p}_y \right), \quad (3.74)$$

dS_2 counterpart, which is the boundary operator dual to the generator of spatial translations along \mathcal{I}^\pm in dS JT gravity [77, 92], as a s-wave dimensional reduction of dS_3 space [77]. Note that both are manifestly Hermitian.

For either of these cases, we can consider the sequence of a T^2 deformation and $T^2 + \Lambda_1$ deformation once the cutoff boundary reaches the corresponding AdS_2 black hole and dS_2 cosmological horizons, namely

$$\hat{H}_{IR/UV,y} = \begin{cases} \frac{1}{y} \left(1 - \sqrt{1 - 2y\hat{H}_{IR/UV}} \right) & 0 \leq y \leq y_0, \\ \frac{1}{y} \left(1 + \sqrt{2y\hat{H}_{IR/UV} - 1} \right) & y \geq y_0, \end{cases} \quad (3.75)$$

We represent the energy spectrum introducing the parameters $\theta_{IR} \equiv \theta \ll 1$ and $\theta_{UV} \equiv \pi - \theta \ll 1$ in the corresponding triple-scaling limits, so that the deformed energy spectrum becomes

$$E_{IR/UV,y} = \begin{cases} \frac{1}{y} \left(1 - \sqrt{1 - y\theta_{IR/UV}^2} \right) & 0 \leq y \leq y_0, \\ \frac{1}{y} \left(1 + \sqrt{y\theta_{IR/UV}^2 - 1} \right) & y \geq y_0. \end{cases} \quad (3.76)$$

Here, y_0 is the critical value of the deformation parameter y (2.16) where the spectrum of the Hamiltonian of the T^2 deformation equals that of the $T^2 + \Lambda_1$ deformed theory; i.e. when the square root in (3.75) and the Hamiltonians $\hat{H}_{IR/UV}$ are replaced by its eigenvalues $\theta_{IR/UV}^2/2$. Namely

$$IR : y_0 = \theta_{IR}^{-2}, \quad UV : y_0 = \theta_{UV}^{-2}. \quad (3.77)$$

In particular, given that we describe the static patch of dS_2 space in the UV case with the $T^2 + \Lambda_1$ deformation, we then have an explicit boundary theory realization of the stretched horizon holographic proposal by Susskind [1], as explained below.

To make connection with our discussion of state complexity, we also define the expectation value of the IR and UV length operators in (3.72) in the deformed HH state $e^{-\tau\hat{H}_y}|\Omega\rangle$ as

$$L_{IR}(t) \equiv \frac{\langle \Omega | e^{-\tau^* \hat{H}_y} \hat{L}_{IR} e^{-\tau \hat{H}_y} | \Omega \rangle}{\langle \Omega | e^{-\beta \hat{H}_y} | \Omega \rangle}, \quad L_{UV}(t) \equiv \frac{\langle \Omega | e^{-\tau^* \hat{H}_y} \hat{L}_{UV} e^{-\tau \hat{H}_y} | \Omega \rangle}{\langle \Omega | e^{-\beta \hat{H}_y} | \Omega \rangle}, \quad (3.78)$$

which can be seen as the UV and IR limits of expectation value of the chord number in the $|n\rangle_y$ basis in (3.50).

To carry out their evaluation, we use the explicit solution for the wormhole length L_y in (3.50) with $R(y)$ identified as the boundary cutoff an AdS_2 black hole metric (3.51) in the IR and UV triple-scaling limits (3.72), which describe JT ($U(\Phi) = 2\Phi$) and dS JT gravity ($U(\Phi) = -2\Phi$) respectively. Using the counterterm $G(\Phi_B)$ (2.2) (corresponding to $\eta = +1$) and the deformation parameter y through (2.16) we have that

$$\eta = +1 : IR : y = R(y)^{-2}, \quad UV : y = -R(y)^{-2}. \quad (3.79)$$

This form differs from our discussion about the triple-scaling limit of the DSSYK chord Hamiltonian since the momentum is always periodic, and thus the spectrum of ℓ_y is discrete, even in the triple-scaling limit. [37] mentions (3.74) may be isometrically dual to the Hamiltonian in a matrix model. It would be interesting to connect their interpretation with our approach.

Meanwhile, for $T^2 + \Lambda_1$ deformations, we invert the sign of $G(\Phi_B)$ in both the IR and UV cases (2.21), resulting in

$$\eta = -1 : \quad \text{IR} : y = -R(y)^{-2}, \quad \text{UV} : y = R(y)^{-2}. \quad (3.80)$$

It follows that the wormhole length (3.50) in each of the corresponding triple-scaling limits (3.78) becomes²⁴

$$L_{\text{IR}}(t) = \begin{cases} 2\text{arcsinh}\left(\sqrt{\frac{1}{y\theta_{\text{IR}}^2} - 1} \cosh\left(\frac{J\theta_{\text{IR}}t}{\sqrt{1-y\theta_{\text{IR}}^2}}\right)\right), & 0 \leq y \leq y_0, \\ 2i \arcsin\left(\sqrt{1 - \frac{1}{y\theta_{\text{IR}}^2}} \cosh\left(\frac{J\theta_{\text{IR}}t}{\sqrt{y\theta_{\text{IR}}^2 - 1}}\right)\right), & y \geq y_0, \end{cases} \quad (3.81\text{a})$$

$$L_{\text{UV}}(t) = \begin{cases} 2i \text{arcsinh}\left(\sqrt{\frac{1}{y\theta_{\text{UV}}^2} - 1} \cosh\left(\frac{J\theta_{\text{UV}}t}{\sqrt{1-y\theta_{\text{UV}}^2}}\right)\right), & 0 \leq y \leq y_0 \\ 2\arcsin\left(\sqrt{1 - \frac{1}{y\theta_{\text{UV}}^2}} \cosh\left(\frac{J\theta_{\text{UV}}t}{\sqrt{y\theta_{\text{UV}}^2 - 1}}\right)\right), & y \geq y_0. \end{cases} \quad (3.81\text{b})$$

Note that L_{IR} and L_{UV} are real and pure imaginary respectively for the T^2 deformation, and they exchange to pure imaginary and real for the $T^2 + \Lambda_1$ flow. This is in accordance to the geometric interpretation where the expectation value of the chord number is a bulk length. The latter becomes spacelike or time-like depending on whether the cutoff boundaries are located outside or inside the black hole respectively, as displayed in Fig. 3. The results show that the rescaled chord number in the IR triple-scaling limit L_{IR} grows eternally in the $\eta = +1$ case, while in the $\eta = -1$, there is a finite growth in terms of the t parametrization. In both cases, the deformation parameter y modifies the rate of growth of L_{IR} . This reflects that the Tolman temperature in the bulk is the thermal scale accompanying t . In the $\eta = +1$ case as we approach $y \rightarrow y_0$ the rate of growth increases since the cutoff surface approaches the black hole horizon, increasing the Tolman temperature. Meanwhile, in the $\eta = -1$ case, corresponding to the interior of the black hole in the AdS₂ description, the imaginary value of L_{IR} can be interpreted in terms of the growth of the timelike geodesics. Note the growth of L_{IR} stops when the argument in \arcsin of (3.81a) is greater than 1 (which we discuss further in Sec. 6.2). This signals that the geodesics in the bulk dual reach $r \rightarrow \infty$ in Rindler-AdS₂ space, as this corresponds to the maximum value of the renormalized length in the AdS₂ description in Fig. (3). Similar findings occur in dS₂ space, as discussed in Sec. 6.3.

4 Correlation Functions

In this section, we study n -point correlation functions of the deformed DSSYK model. They are directly defined in the chord theory with Hamiltonian deformations. We evaluate them in the semiclassical limit. Consistent with the literature, the semiclassical results are modified only by a redshift factor associated with the Tolman temperature in the bulk.

²⁴Note that in (3.81b) we are using the fact that the conformal transformation between Rindler-AdS₂ (3.51) and static patch coordinates is given by a $-$ sign, instead applying the map in sine dilaton gravity of (3.53).

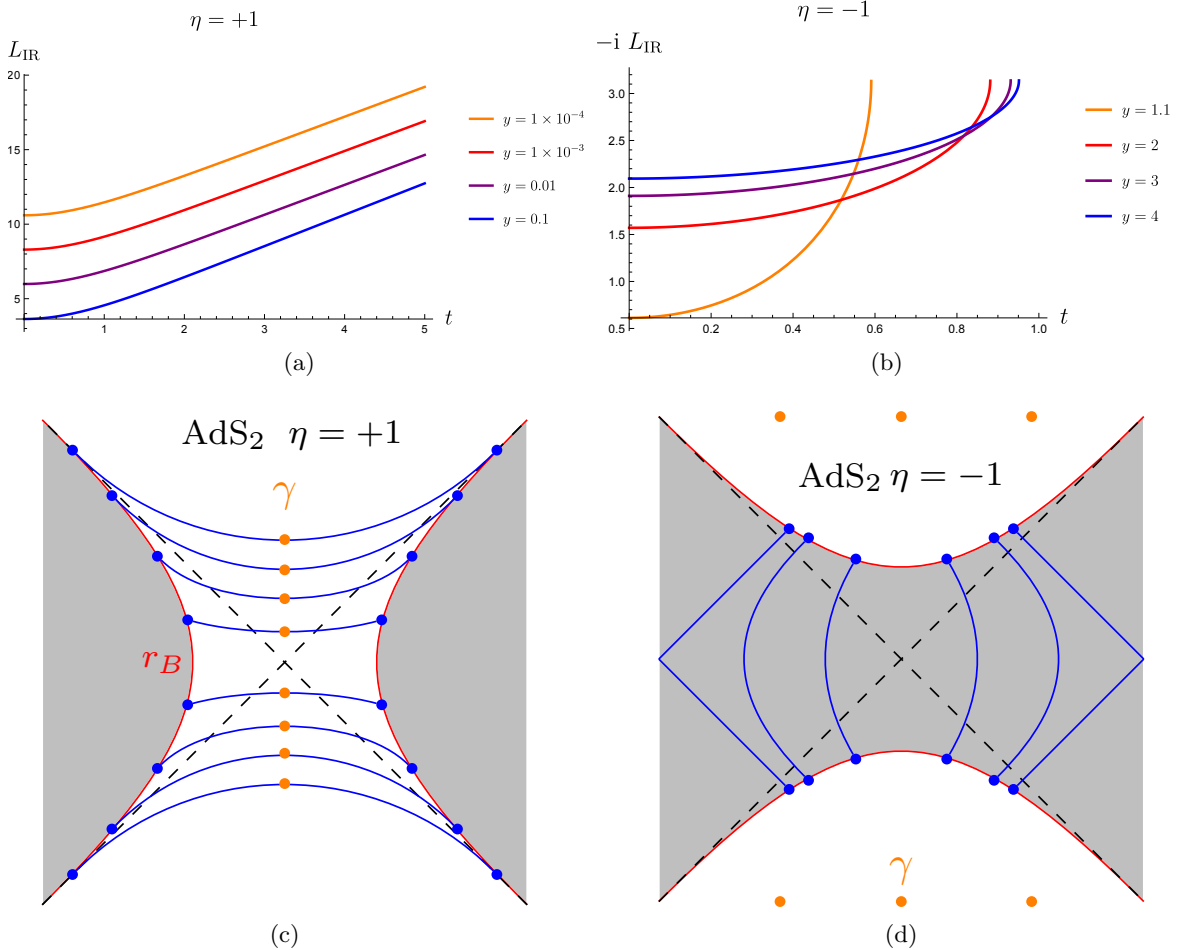


Figure 3. *Top:* Expectation value of the chord number \hat{n}_y (3.38) in the IR limit (3.81a) of the deformed HH state (3.78) after (a) a T^2 ($\eta = +1$) and (b) $T^2 + \Lambda_1$ ($\eta = -1$) deformation. *Bottom:* Corresponding bulk interpretation in terms of (c) spacelike and (d) timelike extremal Einstein-Rosen bridges (blue solid curves) connecting the finite Dirichlet boundaries (red solid curve), located at a constant $r = r_B$ in the Rindler-AdS₂ coordinates (B.2)). We marked the minimal extremal codimension-two area (measured by the dilaton) surfaces γ (orange dots) subject to the homology constraint to the entangling surface (blue dots at the Dirichlet boundaries). Increasing the deformation parameter y (2.16) enhances the rate of growth of the wormhole length for the $\eta = +1$ case. In finite cutoff holography, this is moves the location of the boundaries towards the corresponding black hole horizon, which increases the Tolman temperature, which determines the growth of the length with respect to the boundary time. Meanwhile for the $\eta = -1$ case, increasing y moves the boundary cutoff away from the horizon in the bulk, leading to a decrease in the Tolman temperature. However, there is no eternal growth unlike the $\eta = +1$ case, since the timelike geodesic eventually reaches $r \rightarrow \infty$ in Rindler-AdS₂ space (B.3) as one increases the spacelike coordinate t .

Outline In Sec. 4.1 we define n -point correlation functions in the chord theory after the deformation. In Sec. 4.2 we perform the semiclassical evaluation of the correlation functions

from a path integral argument, which leads to the expected redshift parameter. At last, in Sec. 4.3 we discuss the triple-scaling limits of the expressions.

4.1 n-Point Correlation Functions

In the following, we generalize the original flow equation (2.15) for the chord Hamiltonian with matter (3.21a),

$$\partial_y \hat{H}_{L/R,y} = \frac{\hat{H}_{L/R,y}^2 + (\eta - 1)/y^2}{2(1 - y\hat{H}_{L/R,y})}. \quad (4.1)$$

The holographic dictionary entry relating the deformation parameter y with a finite Dirichlet cutoff in the bulk, such as in (2.16), may be modified since we need to account for matter in the dilaton gravity action (2.1). In this case, finite cutoff holography is less understood in general [22]; and one in principle may use a different holographic interpretation of (4.1) related to mixed boundary conditions [21]. Regardless of the bulk interpretation, we will study the solutions of (4.1) as a deformed chord theory by itself.

While correlation functions are originally defined by taking the double-scaling limit of operators in the physical SYK model, since we are interested in evaluating correlation functions in the ensemble averaged theory, we work directly in chord space. For a simple illustration, we define a (unnormalized) two-point function by simply deforming the chord Hamiltonian, while keeping the matter operators unchanged

$$G_2 = \langle \Omega | \hat{O}_\Delta e^{-\tau^* \hat{H}_{L,y}} e^{-\tau \hat{H}_{L,y}} \hat{O}_\Delta | \Omega \rangle, \quad (4.2)$$

where \hat{O}_Δ represents \hat{O}_Δ^L , and $\tau \equiv \frac{\beta}{2} + it$.

Note that the above definition has the same structure as the two-point function of the seed theory [51], where we simply replace the corresponding Hamiltonians as $\hat{H}_{L/R} \rightarrow \hat{H}_{L/R,y}$.

To evaluate the correlation function in the one-particle space (4.2) we can use the resolution of the identity

$$1 = \int d\theta_L d\theta_R \mu(\theta_L) \mu(\theta_R) \hat{\mathcal{F}}_\Delta^\dagger(|\theta_L\rangle \otimes |\theta_R\rangle) (\langle \theta_L | \otimes \langle \theta_R |) \hat{\mathcal{F}}_\Delta, \quad (4.3)$$

where we use a chord intertwiner [62, 68]:

$$\hat{\mathcal{F}}_\Delta |\Delta; \theta_L, \theta_R\rangle = \sqrt{\langle \theta_L | q^{\Delta \hat{n}} |\theta_R \rangle} |\theta_L\rangle \otimes |\theta_R\rangle. \quad (4.4)$$

Then, (4.2) becomes

$$\begin{aligned} G_2 &= \prod_{i=1}^2 \int d\theta_i \mu(\theta_i) e^{-\tau^* E_y(\theta_1) - \tau E_y(\theta_2)} \langle \theta_1 | q^{\Delta \hat{n}} |\theta_2 \rangle \\ &= \langle \Omega | e^{-\tau^* \hat{H}_y} q^{\Delta \hat{n}} e^{-\tau \hat{H}_y} | \Omega \rangle, \end{aligned} \quad (4.5)$$

where we used the resolution of the identity in the zero-particle space (3.17) in the last line.

Therefore, since the chord number in the original chord basis without deformation $\hat{n} = \sum_{n=0}^{\infty} n |n\rangle \langle n|$ appears in the above expressions, we can perform the evaluation of the correlation functions with path integral methods using the representation of the Hamiltonian in the original basis. This implies that correlation functions in the deformed theory defined above might not capture the behavior of geodesic lengths in finite cutoff holography. As we will see, this is consistent with the commonly employed definitions in the literature.²⁵

Next, applying (4.5), it follows that higher-point functions can be expressed [53, 56]

$$\begin{aligned} G_{2m} &= \langle \Omega | e^{-\tau_m^* \hat{H}_{L,y}} \dots \hat{\mathcal{O}}_{\Delta} e^{-\tau_2^* \hat{H}_{L,y}} \hat{\mathcal{O}}_{\Delta} e^{-\tau_1^* \hat{H}_{L,y}} e^{-\tau_1 \hat{H}_{R,y}} \hat{\mathcal{O}}_{\Delta} e^{-\tau_2 \hat{H}_{L,y}} \hat{\mathcal{O}}_{\Delta} \dots e^{-\tau_m \hat{H}_{L,y}} | \Omega \rangle \\ &= \langle \Omega | e^{-\tau_m^* \hat{H}_{L,y}} \dots \hat{\mathcal{O}}_{\Delta} e^{-(\tau_1 + \tau_2)^* \hat{H}_{L,y}} q^{\Delta \hat{N}} e^{-(\tau_1 + \tau_2) \hat{H}_{L,y}} \hat{\mathcal{O}}_{\Delta} \dots e^{-\tau_m \hat{H}_{L,y}} | \Omega \rangle \end{aligned} \quad (4.6)$$

where

$$\tau_i = \frac{\beta_i}{2m} + it_i, \quad t_i \in \mathbb{R}, \quad 2 \sum_{i=1}^m \beta_i = \beta, \quad (4.7)$$

with β being the periodicity of the thermal circle, and \hat{N} is the total chord number operator (3.20).

4.2 Semiclassical Evaluation

Having found that correlation functions in the deformed theory can be treated in terms of the chord number in the Krylov basis, we will now proceed to evaluate them in the semiclassical limit [53], i.e. λn fixed as $\lambda \rightarrow 0$.

The $(2m+2)$ -correlation function of interest is,²⁶

$$G_{\tilde{\Delta}}^{\Delta_0} = \frac{\langle \Psi_{\tilde{\Delta}}^y(\tau_0, \tau_1, \dots, \tau_m) | q^{\Delta_0 \hat{N}} | \Psi_{\tilde{\Delta}}^y(\tau_0, \tau_1, \dots, \tau_m) \rangle}{\langle \Psi_{\tilde{\Delta}}^y(\tau_0, \tau_1, \dots, \tau_m) | \Psi_{\tilde{\Delta}}^y(\tau_0, \tau_1, \dots, \tau_m) \rangle}, \quad (4.9a)$$

$$|\Psi_{\tilde{\Delta}}^y(\tau_0, \tau_1, \dots, \tau_m)\rangle \equiv e^{-\tau_m \hat{H}_{L,y}} \hat{\mathcal{O}}_{\Delta_m} \dots e^{-\tau_1 \hat{H}_{L,y}} \hat{\mathcal{O}}_{\Delta_1} e^{-\tau_0 \hat{H}_{L,y}} | \Omega \rangle, \quad (4.9b)$$

with \hat{N} in (3.20), $\tau_i \in \mathbb{C}$ and $\sum_{i=0}^m \tau_i = \beta$ where β represents the periodicity of the thermal circle. Meanwhile, $\hat{\mathcal{O}}_{\Delta_1}, \dots, \hat{\mathcal{O}}_{\Delta_m}$ are general matter chord operators, which may be light or heavy (i.e. $\lambda \Delta_{1 \leq i \leq m} \sim \mathcal{O}(1)$ as $\lambda \rightarrow 0$). We display the representation of the correlation function (4.9a) in Fig. 4 (based on [68]),

²⁵It might be interesting to use alternative definitions for the correlation functions, for instance, by promoting the chord number \hat{n} in (4.5) to the one associated with finite cutoff geodesics in the bulk \hat{n}_y (3.38).

²⁶In the bulk, this correlation function is associated with a bulk propagator being that of a probe massive scalar coupled in the effective geometry as [85, 104],²⁷

$$I_{\text{matter}} = \int d^2x \sqrt{g_{\text{eff}}} (g_{\text{eff}}^{\mu\nu} \partial_\mu \tilde{\phi} \partial_\nu \tilde{\phi} + m^2 \tilde{\phi}^2), \quad (4.8)$$

$\beta_y(\theta = \pi) \rightarrow \infty$. It would be interesting to do an explicit matching between the finite cutoff sine dilaton gravity with the $T\bar{T}$ deformed DSSYK model; or more general multitrace deformations for the DSSYK model corresponding to other modifications in the boundary conditions in the bulk.

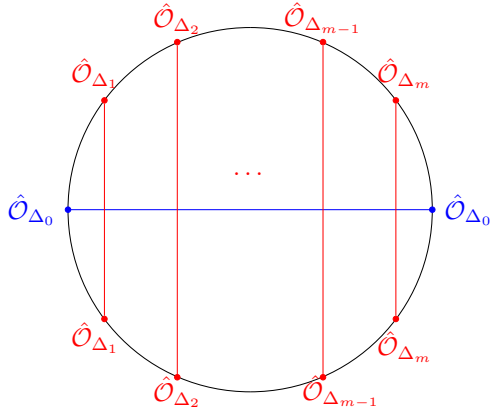


Figure 4. $(2m+2)$ -correlation function in (4.9a) with $\hat{\mathcal{O}}_{\Delta_0}$ (blue) being light operators and $\hat{\mathcal{O}}_{\Delta_{1 \leq i \leq m}}$ (red) at different locations within the thermal circle.

To evaluate the general correlation function (4.9a), we are interested in the semiclassical regime where

$$\left\langle f\left(\hat{N}\right)\right\rangle _{\lambda\rightarrow0}f\left(\left\langle \hat{N}\right\rangle \right)=f\left(\frac{\ell}{\lambda}\right),\quad\ell\equiv\sum_{i=0}^m\ell_i. \quad (4.10)$$

Here, we denote f as a generic function; the expectation value is taken in a generic state (which in our case of interest corresponds to (4.9a)); and at last we defined

$$\ell_{0 \leq i \leq m} \equiv \lambda \langle \hat{n}_i \rangle , \quad (4.11)$$

as expectation values of the rescaled chord number for each chord subsector, defined in (3.20); and note that the quantum fluctuations for the parameter \hat{N} are suppressed in the $\lambda \rightarrow 0$ limit.

We evaluate the expectation value of the length from the path integral of the DSSYK model with matter as

$$\int \prod_{i=0}^m [d\ell_i] [dP_i] \exp \left[\int d\tau_L d\tau_R \left(\frac{i}{\lambda} \sum_{i=0}^m (P_i (\partial_{\tau_L} + \partial_{\tau_R}) \ell_i) + H_{L, y} + H_{R, y} \right) \right], \quad (4.12)$$

where $H_{L/R, y}$ are the deformed chord Hamiltonians with one particle insertion (3.23) $m = 1$

$$H_{L/R,y} \equiv f_y(H_{L/R}) , \quad (4.13a)$$

$$H_{L/R} = \frac{J}{\sqrt{\lambda(1-q)}} \left(e^{-iP_{L/R}} + e^{iP_{L/R}} \left(1 - e^{-\ell_{L/R}} \right) + q^\Delta e^{iP_{R/L}} e^{-\ell_{L/R}} \left(1 - e^{-\ell_{R/L}} \right) \right). \quad (4.13b)$$

In the $\lambda \rightarrow 0$ limit, we evaluate the path integral through saddle points that split into the left/right chord sectors

$$\frac{1}{\lambda} \frac{\partial \ell}{\partial t_{L/R}} = \sum_{i=0}^m \frac{\partial H_{L/R, y}}{\partial P_i} , \quad \frac{1}{\lambda} \frac{\partial P_i}{\partial t_{L/R}} = - \frac{\partial H_{L/R, y}}{\partial \ell_i} , \quad (4.14)$$

given that $\hat{H}_{L/R}$, y are the translation generators in $t_{L/R}$.

Using (4.13a) it follows that (4.14) can be expressed as

$$\frac{1}{\lambda} \frac{\partial \ell}{\partial t_{L/R}} = f'_y(\hat{H}_{L/R}) \sum_{i=0}^m \frac{\partial H_{L/R}}{\partial P_i} , \quad \frac{1}{\lambda} \frac{\partial P_i}{\partial t_{L/R}} = -f'_y(\hat{H}_{L/R}) \frac{\partial H_{L/R}}{\partial \ell_i} , \quad (4.15)$$

It is clear from this derivation of the saddle points of the path integral (4.12) that $f'_y(\hat{H}_{L/R})$ are just overall constant factors since the two-sided Hamiltonian $H_{L/R}$ is conserved (3.13). This means that the correlation function (4.9a) for the deformed theory is the same the seed correlation function after rescaling the $t_{L/R} \rightarrow f'_y(E_{L/R})t_{L/R}$. Given that the temperature is the only energy scale in the correlation functions, the effect of the deformation is equivalent to rescaling the temperature by an appropriate redshift factor. This means

$$\frac{t}{\beta} \rightarrow \frac{t}{\beta_y} , \quad \text{when} \quad t \rightarrow f'_y(E)t , \quad (4.16)$$

where $\beta_y = f'_y(E)\beta$ (2.25) as we defined in the semiclassical thermodynamic analysis in Sec. 2.3. This means that the rate of growth is modified by the Hamiltonian deformation. A similar finding was reported in $T\bar{T}$ deformations to study OTOCs in the shockwave BTZ black hole geometry [136, 196]. We should note that (4.16) is consistent with finite cutoff holography [18], given that the factor $\beta \rightarrow \beta_y$ corresponds to a change in the Tolman temperature in the bulk, as we discussed at the end of Sec. 2.3.

Using the above results we can immediately evaluate all the correlation functions of the type (4.12) in the deformed theory based on those in the seed theory. This follows from solving ℓ based on the specific equations of motion in (4.15) with appropriate boundary conditions and then applying (4.10) to evaluate correlation functions, as we specify below.

Two-Point Functions Consider (4.9a) for $m = 1$ with an analytic continuation in the parameter

$$\tau = \frac{\beta(\theta)}{2} + it , \quad (4.17)$$

where $\beta(\theta)$ is the semiclassical temperature (2.25) to compute Lorentzian correlators in the microcanonical ensemble. Based on our results from the saddle point analysis above, and using the semiclassical seed theory two-point correlation function at finite temperature in [183], the corresponding correlation function in the deformed theory is given by

$$G_2(t, \theta) \equiv G^{\Delta_0}(\tau) \Big|_{\tau=\frac{\beta(\theta)}{2}+it} = \frac{\langle \Omega | e^{-\tau^* \hat{H}_y} q^{\Delta_0 \hat{n}} e^{-\tau \hat{H}_y} | \Omega \rangle}{\langle \Omega | e^{-\beta(\theta) \hat{H}_y} | \Omega \rangle} \Big|_{\tau=\frac{\beta(\theta)}{2}+it} \quad (4.18)$$

$$\stackrel{\lambda \rightarrow 0}{=} \frac{\exp(-\Delta_0 \ell)}{\langle \Omega | e^{-\beta(\theta) \hat{H}_y} | \Omega \rangle} = \left(\sin \theta \operatorname{sech} \frac{2\pi t}{\tilde{\beta}_y(\theta)} \right)^{2\Delta_0} ,$$

where $\tilde{\beta}_{y=0}$ above is termed as fake temperature [85], which in our case contains a redshift factor

$$\tilde{\beta}_y(\theta) \equiv \frac{2\pi}{J \sin \theta} \frac{dE}{dE_y} = \begin{cases} \frac{2\pi}{J \sin \theta} \sqrt{1 - 2yE(\theta)} & \eta = +1 , \\ \frac{2\pi}{J \sin \theta} \sqrt{2yE(\theta) - 1} & \eta = +1 . \end{cases} \quad (4.19)$$

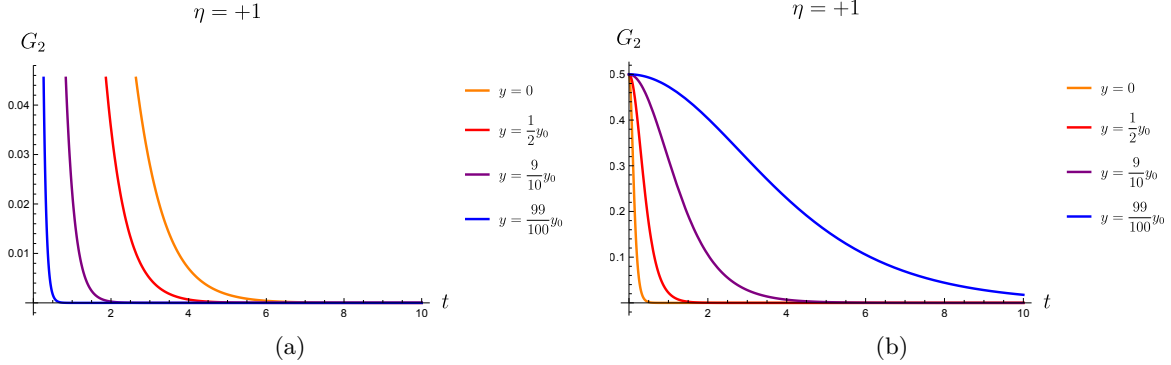


Figure 5. Evolution of the two-point correlation function (4.18) for (a) T^2 , and (b) $T^2 + \Lambda_1$ deformations. As the deformation parameter reaches the critical value y_0 (3.77) the fake temperature (4.19) increases resulting in faster decay of the correlation function. The parameters in this evaluation are: $\lambda = 10^{-4}$, $J = 1$, $\Delta = 1$ and $\theta = 3\pi/4$.

and $\ell \equiv \lambda \langle \Omega | e^{-\tau^* \hat{H}_y} \hat{n} e^{-\tau \hat{H}_y} | \Omega \rangle$ as in (4.10); while the last step comes from solving the equations of motion for ℓ in (4.15) (in the case $m = 0$), which follows analogously to [67] with the fake temperature in (4.19).

We illustrate the behavior of the above expressions in Fig. 5. The fake temperature, which corresponds to the inverse rate of decay of two-point functions, is argued to represent the black hole temperature in the bulk so that the system is only maximally chaotic with respect to $\tilde{\beta}_y$ [85]. In particular, Fig. 5 indicates that as the deformation parameter reaches its critical value y_0 (3.77) the boundary cutoff in the bulk approaches the location of a black hole horizon, which has infinite Tolman temperature (2.33) in accordance with finite cutoff holography. In contrast, the system is submaximally chaotic with respect to the physical temperature as defined from the partition function β_y (2.25), as we find below.

Crossed Four-Point Functions Similarly, we can evaluate explicitly (4.9a) for $m = 2$ to recover a Lorentzian crossed four-point function using the analytic continuation (4.17) when $\lambda \rightarrow 0$ based on the seed theory result for the crossed four-point function of matter chord operators in [67] and the time rescaling in (4.16). Similaly to (4.19), this gives:

$$G_4(t_L, t_R; \theta_L, \theta_R) \equiv G_{\Delta_1}^{\Delta_0}(\tau_L, \tau_R) \Big|_{\tau_{L/R} = \frac{\beta(\theta_{L/R})}{2} + it_{L/R}} = \begin{aligned} & \stackrel{\lambda \rightarrow 0}{=} \left(\frac{e^{-\ell_*(q^{\Delta_1}, \theta_L, \theta_R)/2}}{\cosh\left(\frac{2\pi t_L}{\tilde{\beta}_{L,y}}\right) \cosh\left(\frac{2\pi t_R}{\tilde{\beta}_{R,y}}\right) + \frac{e^{-\ell_*(q^{\Delta_1}, \theta_L, \theta_R)} q^{\Delta_1}}{\sin \theta_L \sin \theta_R} \sinh\left(\frac{2\pi t_L}{\tilde{\beta}_{L,y}}\right) \sinh\left(\frac{2\pi t_R}{\tilde{\beta}_{R,y}}\right)} \right)^{2\Delta_0} \end{aligned} \quad (4.20)$$

where $\tilde{\beta}_{L/R,y} \equiv \tilde{\beta}_y(\theta_{L/R})$ which appears in (4.19), while

$$\begin{aligned} e^{-\ell_*(q^{\Delta_1}, \theta_L, \theta_R)} &= \frac{q^{-2\Delta_1}}{2} \left(1 + q^{2\Delta_1} - 2q^{\Delta_1} \cos \theta_L \cos \theta_R \right. \\ &\quad \left. - \sqrt{1 + q^{4\Delta_1} + 2q^{2\Delta_1}(1 + \cos(2\theta_L) + \cos(2\theta_R)) - 4q^{\Delta_1}(1 + q^{2\Delta_1}) \cos \theta_L \cos \theta_R} \right). \end{aligned} \quad (4.21)$$

In particular, when $t_L = -t_R := t$ and $\beta_L = -\beta_R = \beta(\theta)/2$ then (4.20) takes the form

$$G_4(-t, t; \theta, \pi - \theta) \underset{\lambda \rightarrow 0}{=} \left(\frac{e^{-\ell_0}}{\cosh^2 \left(\frac{2\pi}{\tilde{\beta}_y} t \right) - \frac{q^{\Delta_1} e^{-\ell_0}}{\sin^2 \theta} \sinh^2 \left(2\pi t / \tilde{\beta}_y \right)} \right)^{2\Delta_0}, \quad (4.22)$$

where we denote $e^{-\ell_0} \equiv e^{-\ell_*(q^{\Delta_1}, \theta, \pi - \theta)}$.²⁸

The expression (4.22) can then be approximated as

$$G_4(-t, t; \theta, \theta) \simeq \begin{cases} e^{-2\Delta_0 \ell_0} \left(1 - 2\Delta_0 \left(1 - \frac{q^{\Delta_1} e^{-\ell_0}}{\sin^2 \theta} \right) \left(\frac{2\pi t}{\tilde{\beta}_y} \right)^2 \right), & t \ll \frac{\tilde{\beta}_y}{2\pi}, \\ \left(\frac{2\sin^2 \theta e^{-\ell_0}}{\sin^2 \theta + q^{\Delta_1} e^{-\ell_0}} \right)^{2\Delta_0} \left(1 - \Delta_0 \frac{\sin^2 \theta - q^{\Delta_1} e^{-\ell_0}}{\sin^2 \theta + q^{\Delta_1} e^{-\ell_0}} e^{\frac{4\pi t}{\tilde{\beta}_y}} \right), & \frac{\tilde{\beta}_y}{2\pi} \ll t \ll t_{\text{sc}}, \\ \left(\frac{e^{-\ell_0}}{\sin^2 \theta - q^{\Delta_1} e^{-\ell_0}} \right)^{2\Delta_0} e^{-\frac{8\pi \Delta_0 t}{\tilde{\beta}_y}}, & t \gg t_{\text{sc}}, \end{cases} \quad (4.24)$$

where in the second line we approximated

$$\sinh^2 \frac{2\pi}{\tilde{\beta}_y} \simeq \frac{1}{4} e^{\frac{4\pi t}{\tilde{\beta}_y}} - \frac{1}{2}, \quad e^{\frac{4\pi t}{\tilde{\beta}_y}} \gg 1, \quad (4.25)$$

up to the scrambling time,

$$t_{\text{sc}} \equiv \frac{1}{2J \sin \theta} \log \frac{2 \left(\sin^2 \theta + q^{\Delta_1} e^{-\ell_0} \right)}{\sin^2 \theta - q^{\Delta_1} e^{-\ell_0}}, \quad (4.26)$$

which is the time scale of validity for the Taylor expansion used to derive the exponential growth in (4.24).

Note that the chaos bound [197] in the deformed theory is satisfied in terms of the fake temperature $\tilde{\beta}_y$ since the OTOC decays by a rate $2\pi/\tilde{\beta}_y$ fixed by the Tolman temperature in the bulk dual theory (as we have discussed in Sec. 2.3). In contrast, if we compare the rate of growth with respect to the physical temperature of the deformed DSSYK model, given by

²⁸Note that (4.22) in the $y \rightarrow 0$ limit corresponds to a crossed four-point correlation function in the physical SYK model [51]

$$G_4 = \text{Tr} \left[\hat{\mathcal{O}}_{\Delta_1}(t) e^{-\frac{\beta(\theta)}{4}} \hat{\mathcal{O}}_{\Delta_0}(0) e^{-\frac{\beta(\theta)}{4}} \hat{\mathcal{O}}_{\Delta_1}(t) e^{-\frac{\beta(\theta)}{4}} \hat{\mathcal{O}}_{\Delta_0}(0) e^{-\frac{\beta(\theta)}{4}} \right], \quad (4.23a)$$

$$\hat{\mathcal{O}}_{\Delta_0}(t) \equiv e^{it\hat{H}_{\text{SYK}}} \hat{\mathcal{O}}_{\Delta_0} e^{-it\hat{H}_{\text{SYK}}}, \quad (4.23b)$$

which is evaluated in the double-scaling limit and with annealed ensemble averaging in [51].

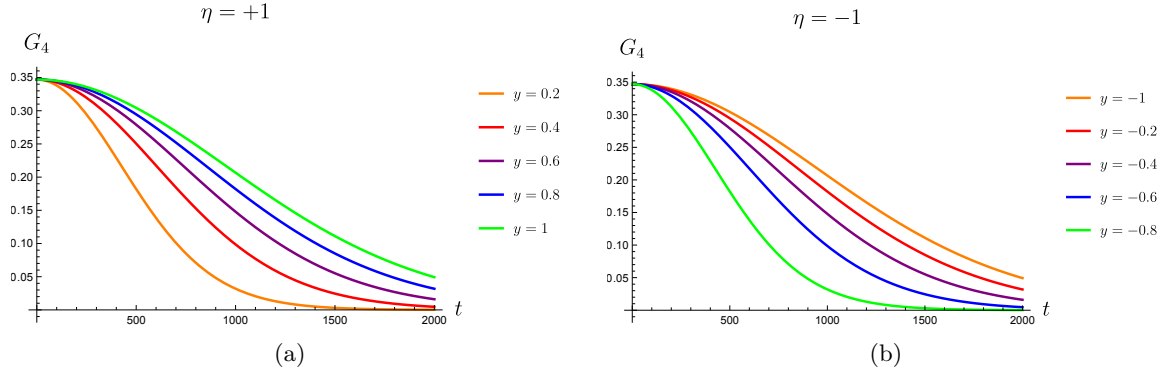


Figure 6. Evolution of the OTOC (4.22) based on the energy spectrum of the deformed theory E_y for (a) $\eta = +1$ (2.20), and (b) $\eta = -1$ (2.21). The parameters applied in the plot are $\theta = \pi/4$, $\lambda = 10^{-6}$, $J = 1$, $\Delta_0 = 1$, $\lambda\Delta_1 = 1$. We observe that the rate of decay is slower as the deformation parameter increases.

$1/\beta_y$, then the system is submaximally chaotic given that $\tilde{\beta}_y(\theta) \geq \beta_y(\theta)$, as seen from (4.19), (2.25)), when $\theta \in [0, \pi]$. This result has been observed in the seed theory [68].

To exemplify the results, we display the growth of the OTOCs using the energy spectrum of the deformed theory E_y in (2.21) ($\eta = -1$) and (2.20) ($\eta = +1$) in Fig. 6. Note that we recover the expected behavior as the solution smoothly connected to the $y = 0$ solution when $y \geq 0$ for $\eta = +1$ and $y \leq 0$ for $\eta = -1$. The reason for this is that the redshift factor dE_y/dE (determined from (2.20) ($\eta = +1$) and (2.21) ($\eta = -1$)) can become imaginary when $y \leq 0$ for $\eta = +1$ and $y \geq 0$ for $\eta = -1$, which modifies the evolution (as exponential functions become trigonometric ones). When the redshift factor is complex-valued the assumptions that $\hat{H}_{L/R, y}$ has a conserved energy spectrum are not valid.

As we elaborate further in App. C, when $y \geq 0$ and $\eta = +1$ (2.16) one describes timelike boundaries in the bulk at finite cutoff, as well as for $y \geq 0$ and $\eta = -1$, when $\hat{H}_{L/R, y}$ can be interpreted as a generator of time translations. Furthermore, we note from the results that the decay rate decreases as the magnitude of the deformation parameter y increases in both cases.

Similarly, for higher point functions in (4.9a) one can perform the evaluation using the time rescaling by the redshift factor in (4.16) and the semiclassical correlation functions for the seed theory in [68]. However, since this is not necessary for the subsequent analysis.

4.3 Triple-Scaling Limit of Crossed Four-Point Functions

For later convenience, we analyze an extension of the UV and IR triple-scaling limits (3.72) in the canonical variables of the one-particle Hamiltonian (3.23)

$$\text{IV : } e^{i\hat{P}_{L/R}} \rightarrow e^{i\lambda\hat{P}_{\text{IR}}^{(L/R)}}, \quad q^{\hat{n}_{L/R}} \rightarrow \lambda e^{-\hat{L}_{\text{IR}}^{(L/R)}}, \quad (4.27a)$$

$$\text{UV : } e^{i\hat{P}_{L/R}} \rightarrow e^{-\hat{P}_{\text{UV}}^{(L/R)}}, \quad q^{\hat{n}_{L/R}} \rightarrow \lambda e^{i\hat{L}_{\text{UV}}^{(L/R)}} \quad (4.27b)$$

where the eigenvalues of the operators $\hat{L}_{\text{IR}}^{(L/R)}$, $\hat{L}_{\text{UV}}^{(L/R)}$, $\hat{P}_{\text{IR}}^{(L/R)}$, $\hat{P}_{\text{UV}}^{(L/R)}$, and the conformal dimension of matter chord Δ_1 , are $\mathcal{O}(1)$ as $\lambda \rightarrow 0$. This means that the one-particle chord Hamiltonian (3.23) can be expressed as

$$\begin{aligned}\hat{H}_{\text{IR}}^{(L/R)} &\equiv \frac{1}{2J\lambda} \left(\hat{H}_{L/R} + \frac{2J}{\sqrt{\lambda(1-q)}} \mathbb{1} \right) \\ &\xrightarrow{\text{IR}} \frac{1}{2} \left(\left(\hat{P}_{\text{IR}}^{(L/R)} \right)^2 + e^{-\hat{L}_{\text{IR}}^{(\text{tot})}} + \left(\Delta_1 + i \left(\hat{P}_{\text{IR}}^{(L/R)} - \hat{P}_{\text{IR}}^{(R/L)} \right) \right) e^{-L_{\text{IR}}^{(L/R)}} \right),\end{aligned}\quad (4.28\text{a})$$

$$\begin{aligned}\hat{H}_{\text{UV}}^{(L/R)} &\equiv \frac{1}{2J\lambda} \left(\hat{H}_{L/R} - \frac{2J}{\sqrt{\lambda(1-q)}} \mathbb{1} \right) \\ &\xrightarrow{\text{UV}} \frac{1}{2} \left(\left(\hat{P}_{\text{UV}}^{(L/R)} \right)^2 - e^{i\hat{L}_{\text{UV}}^{(\text{tot})}} - \left(\Delta_1 + \left(\hat{P}_{\text{UV}}^{(L/R)} - \hat{P}_{\text{UV}}^{(R/L)} \right) \right) e^{iL_{\text{IR}}^{(L/R)}} \right),\end{aligned}\quad (4.28\text{b})$$

and we denote

$$L_{\text{IR}/\text{UV}}^{(\text{tot})} = L_{\text{IR}/\text{UV}}^{(L)} + L_{\text{IR}/\text{UV}}^{(R)}. \quad (4.29)$$

The corresponding correlation functions in the IR/UV triple-scaling limit can be solved based on the same procedure leading to (4.20) for the crossed four-point function, and, for instance, for the IR case one finds

$$G_4(t_L, t_R; \theta_L, \theta_R) \xrightarrow{\text{IR}} \left(\frac{e^{-\ell_0/2}}{\cosh\left(\frac{2\pi t_L}{\tilde{\beta}_{\text{IR},y}^L}\right) \cosh\left(\frac{2\pi t_R}{\tilde{\beta}_{\text{IR},y}^R}\right) + \frac{2e^{-\ell_0}}{\tilde{\theta}_{\text{IR}}^{(L)} \tilde{\theta}_{\text{IR}}^{(R)}} \sinh\left(\frac{2\pi t_L}{\tilde{\beta}_{\text{IR},y}^L}\right) \sinh\left(\frac{2\pi t_R}{\tilde{\beta}_{\text{IR},y}^R}\right)} \right)^{2\Delta_0}, \quad (4.30)$$

where $\tilde{\theta}_{\text{IR}}^{(L/R)} \equiv \theta_{L/R}/\lambda$ is a fixed constant in the triple-scaling limit; while the fake temperature (4.19) in the IR limit takes the form

$$\tilde{\beta}_{\text{IR},y}^{L/R} \xrightarrow{\text{IR}} \frac{2\pi}{J\tilde{\theta}_{\text{IR}}^{(L/R)}} \begin{cases} \sqrt{1 - y\left(\tilde{\theta}_{\text{IR}}^{(L/R)}\right)^2}, & \eta = +1, \\ \sqrt{y\left(\tilde{\theta}_{\text{IR}}^{(L/R)}\right)^2 - 1}, & \eta = +1. \end{cases} \quad (4.31)$$

with the deformation parameter y (2.16) (with $2\kappa^2 = 1$ from (4.28)) being related to the radial cutoff in JT gravity by $y = r_B^{-2}$. Meanwhile, the constant ℓ_0 is determined from energy conservation in the corresponding triple-scaled Hamiltonian (4.28). To recover real solutions in the triple-scaling limit, we implement a homogeneous energy condition after the operator insertion (such as that used in shockwave geometries [198]) $\tilde{\theta}_{\text{IR}}^L = \tilde{\theta}_{\text{IR}}^R \equiv \tilde{\theta}_{\text{IR}}$, which leads to

$$e^{-\ell_0} = \frac{1}{2} \left(\tilde{\theta}_{\text{IR}}^2 + \Delta_1^2 - \Delta_1 \sqrt{2\tilde{\theta}_{\text{IR}}^2 + \Delta_1^2} \right). \quad (4.32)$$

The $y \rightarrow 0$ limit of the above results has appeared previously in [192]. Similar outcomes are recovered in the UV limit, which we discuss in Sec. 6.3 in the context of the stretched horizon, i.e. when $y \rightarrow y_0$ (3.77). This leads to an infinite temperature limit (already noticed in [18]) enhancing the rate of growth of the OTOC (4.30).

Summary Our findings show that all the correlation functions at the semiclassical level experience the same evolution as the correlation functions in the seed theory; where the temperature is affected by a redshift factor, in agreement with the existing literature on finite cutoff holography. The results also highlight the analytic control on the DSSYK model. In $CFT_{d \geq 2}$ real-time correlation functions at finite temperature are known only in terms of perturbative expansions in the deformation parameter [15]. In contrast, in this specific system we evaluate the correlation functions at a non-perturbative order in the deformation parameter y .

Additionally, we discuss how to apply the results in this section to evaluate ETW brane partition functions and correlation functions, including trumpet geometries, in App. D.

5 Holographic Entanglement Entropy from Double-Scaled Algebra

In this section, we study the entanglement entropy between the double-scaled algebras of the DSSYK [53, 54], defined below, given a chord state and we analyze its finite cutoff holographic interpretation. The analysis is based on recent developments in von Neumann algebras and generalized entropies in quantum gravity [199–203]; see [204–207] for modern reviews. Note that while a $T\bar{T}$ deformation generates spatial non-locality in higher-dimensional theories, which is an important component for defining holographic entanglement entropy, we consider a theory without spatial dimensions, which remains local, at least from the boundary theory perspective. This might be a reason that there is a precise match between the boundary and bulk evaluations; even non-perturbatively in the cutoff parameter.

Outline In Sec. 5.1 we discuss the double-scaled algebra of the (deformed) DSSYK model and define entanglement entropy between the algebras given a pure global state. We illustrate the definitions considering the HH state. In Sec. 5.2 we then evaluate entanglement entropy using the chord number state in the basis that reproduces a wormhole length with finite cutoff, particularly its IR triple-scaling limit. In Sec. 5.3 we show that the expressions have a bulk interpretation.

5.1 Double-Scaled Algebra & Entanglement Entropy

As argued in the previous sections, in general the chord operators in the deformed theory belong to the operator algebra of the seed theory since we study chord Hamiltonian deformations encoded in the flow equation (2.17). This means the double-scaled algebras [53, 54] can be expressed in terms of the (un)deformed Hamiltonian

$$\mathcal{A}_{L/R} = \left\{ \hat{H}_{L/R, y}, \hat{\mathcal{O}}_{\Delta}^{(L/R)} \right\}, \quad (5.1)$$

where $\hat{\mathcal{O}}_{\Delta}^{(L/R)}$ are matter chord operators. Moreover, we know that $\mathcal{A}_{L/R}$ is a type II₁ algebra [54], where the $|\Omega\rangle$ is the cyclic separating state in both the deformed and seed theories. This allows us to define traces

$$\text{Tr}(\hat{w}_{L/R}) = \langle \Omega | \hat{w}_{L/R} | \Omega \rangle, \quad \forall \hat{w}_{L/R} \in \mathcal{A}_{L/R}. \quad (5.2)$$

We may then define the density matrix in $\hat{\rho}_{L/R} \in \mathcal{A}_{L/R}$ associated to a state $|\Psi\rangle \in \mathcal{H}_{\text{chord}}$ as [199]

$$\text{Tr}\left(\hat{\rho}_{L/R} \hat{w}_{L/R}\right) = \langle \Psi | \hat{w}_{L/R} | \Psi \rangle , \quad \forall \hat{w}_{L/R} \in \mathcal{A}_{L/R} , \quad (5.3)$$

Next, from the Gelfand–Naimark–Segal construction [208, 209], we can express any state in the chord Hilbert space by applying a string of the operators in the double-scaled algebras to the cyclic separating state,

$$|\psi\rangle = f\left(\hat{H}_{L/R,y}, \hat{\mathcal{O}}_{\Delta}^{(L/R)}\right) |\Omega\rangle \in \mathcal{H}_{\text{chord}} , \quad (5.4)$$

where f is a generic function, then combining (5.3) and (5.4) we identify

$$\hat{\rho}_{L/R} = f\left(\hat{H}_{L/R,y}, \hat{\mathcal{O}}_{\Delta}^{(L/R)}\right) f\left(\hat{H}_{L/R,y}, \hat{\mathcal{O}}_{\Delta}^{(L/R)}\right)^{\dagger} , \quad (5.5)$$

where we applied cyclicity of the trace (5.2).

Given that $|\Omega\rangle$ is the tracial state in the double-scaled algebra, the von Neumann entropy of (5.5) can be defined as

$$S \equiv \log \langle \Omega | \hat{\rho} | \Omega \rangle - \frac{\langle \Omega | \hat{\rho} \log \hat{\rho} | \Omega \rangle}{\langle \Omega | \hat{\rho} | \Omega \rangle} , \quad (5.6)$$

where we have suppressed the L/R index since both density matrices lead to the same result. For this reason, we associate (5.6) as a notion of algebraic entanglement entropy [210].

Note that while we can evaluate entanglement entropy between the double-scaled algebras in the seed and deformed theory in the same way, the main difference is the physical interpretation of the entropies which depend on the form that $\hat{\rho}$ takes, given that it can either involve the (un)deformed chord Hamiltonian.

Thermodynamic Entropy For instance, there is a thermodynamic entropy that can be computed from the partition function of the deformed theory

$$S = (1 - \beta \partial_{\beta}) \log Z_y(\beta) \quad Z_y(\beta) = \langle \Omega | e^{-\beta \hat{H}_y} | \Omega \rangle \quad (5.7)$$

where $e^{-\frac{\beta}{2} \hat{H}_y} |\Omega\rangle$ is the HH state in the zero-particle chord space.

The above result can also be interpreted as entanglement entropy between the double-scaled algebra using the definition of the density matrix:

$$Z_y(\beta) = \text{Tr}(\hat{\rho}_{\text{HH}}) , \quad \hat{\rho}_{\text{HH}} = e^{-\beta \hat{H}_y} . \quad (5.8)$$

Note that the density matrix is not normalized. The von Neumann entropy in the corresponding state (5.6) is thus the thermal entropy in the deformed theory (5.7). Holographically, since the effect of a T^2 deformation represents a finite cutoff in the bulk [18], the above expressions would have a natural geometric interpretation in terms of a finite cutoff AdS_2 black hole effective geometry, similar to the partition functions computed in finite cutoff holography for JT gravity [29, 37].

Additionally, there are simple extensions to evaluate the algebraic entanglement entropy (5.6) using particle insertions in the HH state, which follows similarly to our discussion, and which were connected to the partially-entangled thermal state [183, 211] in the DSSYK model in [92].

5.2 Boundary Perspective: Entropy from Chord Number State

In this subsection, we will investigate the holographic nature of the algebraic entropy (5.6) by considering the state $|n\rangle_y$ and its corresponding density matrix (5.5) in the double-scaled algebra

$$|\Psi\rangle = |n\rangle_y = g_n(\hat{h}) |\Omega\rangle, \quad \hat{\rho} = g_n(\hat{h})^2, \quad (5.9)$$

where g_n appears in (3.30).

From the general expression for algebraic entanglement entropy (5.6), we get

$$S(L) \equiv - \int_0^\pi d\theta \mu(\theta) \frac{g_n(2 \cos \theta)^2}{\langle \Psi | \Psi \rangle} \log \frac{g_n(2 \cos \theta)^2}{\langle \Psi | \Psi \rangle}, \quad (5.10)$$

where the energy measure appears in (3.17).

For analytic progress, we study the triple-scaling limit of the above result; see [91] for similar considerations, and [92].²⁹ For concreteness, we focus on the IR triple-scaling limit (3.72); very similar arguments can be implemented for the UV limit; which we discuss in Sec. 6.4.

To study the IR triple-scaling limit of the different terms in (5.10), let us first find solutions to the inner product $\langle k | L \rangle$, where $|L\rangle$ represents the eigenstates of \hat{L}_{IR} , and $|k\rangle \equiv |\theta = \lambda k\rangle$ the eigenstates of \hat{H}_{IR} , i.e.

$$\hat{L}_{\text{IR}} |L\rangle = L_{\text{IR}} |L\rangle, \quad \hat{H}_{\text{IR}} |k\rangle = \frac{k^2}{2} |k\rangle, \quad (5.11)$$

Plugging these states in the corresponding Hamiltonian in (3.73),

$$\langle k | \hat{H}_{\text{IR}} | L \rangle = \left(\frac{-1}{2} \partial_{L_{\text{IR}}}^2 + \frac{R(y)^2}{2} \operatorname{sech}^2 \frac{L_{\text{IR}}}{2} \right) \langle k | L \rangle = \frac{k^2}{2} \langle k | L \rangle, \quad (5.12)$$

where we used $\hat{P}_{\text{IR}} = -i\partial_{L_{\text{IR}}}$, and $\theta \equiv k\lambda$ in the IR triple-scaling limit (3.72), so that (5.12) can be seen as a Schrödinger equation. The solutions are associated Legendre functions of first ($P_\nu^\mu(x)$) and second ($Q_\nu^\mu(x)$) kind,

$$\langle k | L \rangle = c_1 P_{\frac{1}{2}(\sqrt{1-16R(y)^2}-1)}^{2ik} \left(\tanh \left(\frac{L_{\text{IR}}}{2} \right) \right) + c_2 Q_{\frac{1}{2}(\sqrt{1-16R(y)^2}-1)}^{2ik} \left(\tanh \left(\frac{L_{\text{IR}}}{2} \right) \right), \quad (5.13)$$

where c_1 and c_2 are constants. We are interested in solutions that are square integrable, so we keep $c_2 = 0$ and take c_1 such that

$$c_1 = \left(\int_0^\infty dk \rho(k) \left| P_{\frac{1}{2}(\sqrt{1-16R(y)^2}-1)}^{2ik} \left(\tanh \left(\frac{L_{\text{IR}}}{2} \right) \right) \right|^2 \right)^{-1/2}, \quad (5.14)$$

where $\rho(k)$ is the density of states of JT gravity

$$\rho(k) \equiv 4k \sin(2\pi k). \quad (5.15)$$

²⁹We expect that the evaluation in the $\lambda \rightarrow 0$ limit leads to a RT formula in sine dilaton gravity at finite cutoff, which has not been addressed even in the seed theory case.

Then, (5.10) becomes

$$\Delta S \xrightarrow{IR} -\lambda \int_0^\infty dk p(L_{IR}, k) \log \frac{p(L_{IR}, k)}{\mu(\theta \equiv \lambda k)} . \quad (5.16)$$

where we use that

$$\mu(\theta \equiv \lambda k) \xrightarrow{IR} \frac{\lambda^{1/2}}{\sqrt{2\pi}} e^{-\frac{\pi^2}{2\lambda}} (\rho(k) + \mathcal{O}(\lambda)) , \quad (5.17a)$$

$$\mu(\theta) \frac{g_n(2 \cos \theta)^2}{\langle \Psi | \Psi \rangle} \xrightarrow{IR} p(L_{IR}, k) . \quad (5.17b)$$

Here, (5.17a) is known in [53], and (5.17b) follows the fact that $\langle \theta | n \rangle_y$ satisfies the recurrence relation (3.30) where $x = -\lambda E(\theta)/(2J)$, while $\langle k | L \rangle$ satisfies the IR triple-scaled version of the same equation, namely (5.12).

To make more analytic progress, we apply the Wentzel-Kramers-Brillouin (WKB) approximation [212–214], where we look for semiclassical solutions to the Schrödinger equation (5.12). We consider energy scales away from the one where the kinetic energy vanishes, meaning $\hat{P}_{IR}^2 = 0$ in (3.73a). This can be expressed in terms of a cutoff scale

$$k_{\text{crit}} \equiv R(y) \operatorname{sech} \frac{L_{IR}}{2} , \quad (5.18)$$

so that the wavefunction in (5.12) can be approximately described by a particle trapped in a potential given by the $R(y)^2 \operatorname{sech}^2 \frac{L_{IR}}{2}$ term in the Schrödinger equation (5.12), resulting in

$$p(L_{IR}, k) \simeq \begin{cases} \frac{1}{2\pi} \sqrt{\frac{k^2}{R(y)^2 \operatorname{sech}^2 \frac{L_{IR}}{2} - k^2}} \exp\left(-2 \int_{L_{IR}}^{L_0} dL' \sqrt{R(y)^2 \operatorname{sech}^2 \frac{L}{2} - k^2}\right) & k \lesssim k_{\text{crit}} , \\ \frac{2}{\pi} \sqrt{\frac{k^2}{k^2 - R(y)^2 \operatorname{sech}^2 \frac{L_{IR}}{2}}} \sin^2\left(\int^{L_{IR}} dL' \sqrt{k^2 - R(y)^2 \operatorname{sech}^2 \frac{L}{2}}\right) & k > k_{\text{crit}} , \end{cases} \quad (5.19)$$

where

$$L_0 \equiv 2 \operatorname{arccosh}\left(\frac{R(y)}{k}\right) \quad (5.20)$$

results from inverting (5.18), and the proportionality constant in (5.19) is chosen for normalization. By evaluating the integrals in the approximation where

$$\begin{aligned} R(y) \operatorname{sech} \frac{L_{IR}}{2} &\gg k , \quad k \lesssim k_{\text{crit}} , \\ R(y) \operatorname{sech} \frac{L_{IR}}{2} &\ll k , \quad k > k_{\text{crit}} , \end{aligned} \quad (5.21)$$

then the corresponding probability distribution in the WKB approximation (5.19) becomes

$$p(L_{IR}, k) \simeq \begin{cases} 0 & k \lesssim k_{\text{crit}} , \\ \frac{2}{\pi k} \sin^2(L_{IR} k) & k > k_{\text{crit}} . \end{cases} \quad (5.22)$$

We can now evaluate the following entropy difference based on (5.16)

$$\Delta S \equiv S(L) - S(L \rightarrow \infty) , \quad (5.23)$$

using the triple-scaled probability distribution in the following terms inside (5.16),

$$\lambda \int_0^\infty dk (p(L_{\text{IR}}, k) \log p(L_{\text{IR}}, k) - p_\infty(k) \log p_\infty(k)) = \mathcal{O}(\lambda) , \quad (5.24)$$

where

$$p_\infty(k) \equiv p(L_{\text{IR}} \rightarrow \infty, k) = \frac{1}{\pi} , \quad (5.25)$$

as seen from (5.22); and the last equality in (5.24) follows from $p(L_{\text{IR}}, E) \sim \mathcal{O}(1)$.

Thus, the leading order terms contributing to the entropy difference (5.23) are

$$\Delta S \simeq 2 \int_0^\infty dk (p(L_{\text{IR}}, k) - p_\infty(k)) \lambda \log(\mu(\theta = \lambda k)) . \quad (5.26)$$

We can implement the following relation from (5.17a)

$$\lambda \log \mu(\theta = \lambda k) \xrightarrow{UV} -\frac{1}{2}\pi^2 + \mathcal{O}(\lambda \log \lambda) . \quad (5.27)$$

Therefore, to leading order in the semiclassical expansion, the entropy difference (5.26) with (5.22, 5.24, 5.27) becomes

$$\Delta S \simeq -\pi^2 \int_0^\infty dk (p(L_{\text{IR}}, k) - p_\infty(k)) \simeq \pi \int_0^{k_{\text{crit}}} dk . \quad (5.28)$$

Then, the WKB approximation gives

$$\Delta S \simeq \pi R(y) \operatorname{sech} \frac{L_{\text{IR}}}{2} . \quad (5.29)$$

Moreover, since, in general, traces are defined up to a proportionality constant (equivalently with respect to the choice of normalization of $|\Omega\rangle$), we can perform the following rescaling

$$\operatorname{Tr} \rightarrow \frac{2}{\lambda} \operatorname{Tr} , \quad (5.30)$$

so that (5.29) after the rescaling becomes

$$\Delta S \xrightarrow{IR} \frac{2\pi}{\lambda} R(y) \operatorname{sech} \frac{L_{\text{IR}}}{2} . \quad (5.31)$$

The specific choice of overall constant is motivated by the RT formula used just below.

5.3 Bulk Perspective: RT Formula

In the following, we search for the minimal area surface γ in the (A)dS₂ space, using the finite cutoff boundary as the entangling surface to evaluate holographic entanglement entropy. The extremal surfaces in two dimensional quantum gravity are point-like. We investigate the different configurations depending on the location of boundary cutoff surfaces in the corresponding spacetime.

Timelike Boundaries in an AdS Black Hole First, considering timelike finite cutoff boundaries, as illustrated in Fig. 3 (c) as the entangling surface to evaluate the RT formula in JT gravity, which corresponds to (2.1) with $U(\Phi) = 2\Phi$,

$$S_{\text{AdS}} \equiv \frac{\Phi_{\text{AdS}}(\gamma)}{4G_N} , \quad (5.32)$$

with G_N being the two-dimensional Newton's constant, Φ_{AdS} is the dilaton in JT gravity, and γ the extremal surface. To locate the latter, we use global and Rindler-AdS₂ coordinates,

$$ds^2 = -(1 + X^2)dt^2 + \frac{dX^2}{1 + X^2} = -(r^2 - r_{\text{BH}}^2)dt^2 + \frac{dr^2}{r^2 - r_{\text{BH}}^2} , \quad (5.33)$$

where the dilaton in JT gravity is given by

$$\Phi_{\text{AdS}} = r_{\text{BH}}\sqrt{1 + X^2} \cos T . \quad (5.34)$$

Due to symmetry, γ is located at $X = 0$ in global AdS₂ coordinates for a given Cauchy slice, as seen by minimizing the dilaton (5.34) ($\partial_X \Phi_{\text{AdS}} = 0$ with T fixed).

Let us then relate the time t and T at the location of the entangling region, $r = r_B$, using the following coordinate transformation between global and Rindler-AdS coordinates

$$\tan T = \frac{r_{\text{BH}}}{r} \sqrt{\frac{r^2}{r_{\text{BH}}^2} - 1} \sinh(r_{\text{BH}}t) , \quad r < r_{\text{BH}} . \quad (5.35)$$

Next, from the explicit form of the wormhole length in terms of Rindler-AdS₂ time t (3.50), we have that the dilaton at $X = 0$ is

$$\Phi_{\text{AdS}} \Big|_{X=0} = r_B \operatorname{sech} \frac{L_{\text{IR}}}{2} , \quad \text{where} \quad \sinh \frac{L_{\text{IR}}}{2} = \sqrt{\frac{r_B^2}{r_{\text{BH}}^2} - 1} \cosh(r_{\text{BH}}t) . \quad (5.36)$$

Then, from (5.32) we recover

$$S_{\text{AdS}} = \frac{r_B}{4G_N} \operatorname{sech} \frac{L_{\text{IR}}}{2} . \quad (5.37)$$

Thus, we find exactly the same result as the boundary theory (5.31) following the holographic dictionary between DSSYK and sine dilaton gravity [105], including the relationship between the deformation parameter y and r_B in (2.16) for the counterterm $G(\Phi_B) = \Phi_B^2$ (2.2) in JT gravity

$$\lambda = 8\pi G_N , \quad R(y) = \frac{1}{\sqrt{y}} = r_B . \quad (5.38)$$

In particular, the limit $r_R \rightarrow r_{\text{BH}}$ leads to the Bekenstein-Hawking (BH) entropy of a Bañados-Teitelboim-Zanelli (BTZ) black hole,

$$S_{\text{BH}} = \frac{2\pi r_{\text{BH}}}{4G_3} , \quad (5.39)$$

where the two and three-dimension Newton's constants are related by $G_3 = 4\pi G_N$ [184], and we can recognize the factor $2\pi r_{\text{BH}}$ as the codimension-two area of the BTZ black hole, corresponding to the perimeter of a circle with radius r_{BH} . This can be interpreted from the boundary theory answer (5.37) when $y \rightarrow y_0$.

Spacelike Boundaries in an AdS Black Hole Next, we return to the JT gravity case with spacelike cutoff boundaries inside the black hole interior, illustrated in Fig. 3 (d), interpreted as the bulk dual to a $T^2 + \Lambda_1$ deformed DSSYK model in the IR limit.

An attempt might be made to evaluate the holographic entanglement entropy of (5.32) in a similar way to the previous case. However, if we extremize the dilaton (5.34) with T fixed and varying X to obey the homology constraint ($\partial_T \Phi = 0$) one would find $T = 0$ as the location for the RT surface. This corresponds to a maximum dilaton value instead of a minimum one. In fact, the minimum value is reached when $T = \pm\pi/2$, where $\Phi = 0$ for any X . However, the dilaton in the minimal area surface cannot describe holographic entanglement entropy, it would not even be smoothly connected to the extremal area when the timelike boundaries approach the black hole horizon (5.37). This means that the RT formula does not apply when the boundaries are located in the black hole interior. Thus, while we expect that the algebraic entanglement entropy for a chord number in the $T^2 + \Lambda_1$ deformed DSSYK (5.31) has a bulk interpretation, it does not correspond to the minimal area in the RT formula measured by the dilaton at the corresponding extremal surface.

6 Stretched Horizon Holography From the Deformed DSSYK Model

We collect the lessons from the previous sections to explicitly realize the stretched horizon conjecture by Susskind [1]. We perform the T^2 and $T^2 + \Lambda_1$ deformation procedure in the DSSYK chord Hamiltonian in the UV triple-scaling limit (3.72), which is isomorphic to the dS JT gravity generator of spatial translations along \mathcal{I}^\pm . After the $T^2 + \Lambda_1$ deformation, the finite cutoff boundary moves inside the static patch of dS₂ space, which takes the role of the cosmological stretched horizon [1]. We evaluate the rate of growth of the state complexity defined in Sec. 3.4; OTOCs (based on Sec. 4.2), as well as the algebraic entanglement entropy for the chord number state in Sec. 5.2. We show that the state complexity and OTOCs display hyperfast growth and hyperfast scrambling respectively as the boundary approaches the cosmological horizon. Meanwhile, the entanglement entropy matches the dilaton in dS JT gravity at finite cutoff if the boundaries are spacelike, and it reproduces the expected formula in the Gibbon-Hawking entropy in dS₃ space in the stretched horizon limit.

Outline In Sec. 6.1 we compare general aspects and the thermodynamic properties between the UV limit of the deformed DSSYK model after T^2 and $T^2 + \Lambda_1$ deformations with dS₂ JT gravity with a stretched horizon in the static patch. In Sec. 6.2 we discuss our proposal for state complexity of the deformed HH state in this theory and its bulk interpretation as a geodesic length; particularly its hyperfast growth. In Sec. 6.3 we evaluate the OTOCs in the UV triple-scaling limit and its Lyapunov exponent. At last, in Sec. 6.4 we evaluate algebraic entanglement entropy for a chord number state in the basis $|n\rangle_g$; we match it to the dilaton in dS₂ JT gravity, confirming the RT formula.

A summary of results in this section in connection with the stretched horizon holographic proposal [1] is shown in Tab. 1.

6.1 UV Limit of the DSSYK Model vs dS Space at Finite Cutoff

To realize the stretched horizon proposal in the UV limit (3.72), as explained in Sec. 3.5, we apply the T^2 deformation in to the UV chord Hamiltonian (3.73b). Once the deformation parameter reaches the critical value $y = y_0$ (3.77), we apply the $T^2 + \Lambda_1$ deformation. We thus specialize in the deformed theory in (3.73b, 3.75), namely

$$\hat{H}_{\text{UV},y} \equiv \begin{cases} \frac{1}{y} \left(1 - \sqrt{1 - 2y \left(\frac{R(y)^2}{2} \sec^2 \frac{\hat{L}_{\text{UV}}}{2} - \frac{\hat{P}_{\text{UV}}}{2} \right)} \right) & 0 \leq y \leq y_0, \\ \frac{1}{y} \left(1 + \sqrt{2y \left(\frac{R(y)^2}{2} \sec^2 \frac{\hat{L}_{\text{UV}}}{2} - \frac{\hat{P}_{\text{UV}}}{2} \right) - 1} \right) & y \geq y_0, \end{cases} \quad (6.1)$$

where $y_0 \equiv \theta_{\text{UV}}^{-2}$. We may now interpolate between dS₂/CFT₁ holography at finite cutoff and static patch holography. In particular, when $y = y_0 + \delta$ for $0 < \delta \ll 1$ we recover the stretched horizon conjecture.³⁰

As emphasized in [92], the UV limit of the DSSYK model is an explicit example of a unitary theory which contrasts the dS/CFT correspondence [215–219] in higher dimensions, where a non-unitary CFT dual is expected to live at future/past infinity \mathcal{I}^\pm .³¹ Work in this area indicates that the renormalization group (RG) flow in the dual CFT at \mathcal{I}^\pm allows for an emergent notion of time evolution from the bulk [240] (recently debated by [175]). Similarly, the T^2 flow in (6.1) indicates one can associate an emergent global time generated by the T^2 deformation.

Next, we apply our results in Sec. 2 to compare the thermodynamics in the deformed boundary theory (6.1) to those in the bulk at a finite cutoff, discussed below.

First, consider the geometry of the dS₂ static patch (resulting from the s-wave reduction of dS₃ space), which is given by:

$$ds^2 = -f(r)dt_{L/R}^2 + \frac{dr^2}{f(r)}, \quad f(r) = r_{\text{CH}}^2 - r^2, \quad \Phi = r \in [0, r_{\text{CH}}], \quad (6.2)$$

where r_{CH} is a parametrization of the cosmological horizon radius.³² We illustrate the geometry of dS₂ and the cosmological stretched horizon in Fig. 1 (d). Note that in writing (6.2) we may assume a gauge fixing where $t_L = t_R = t$. Adopting a gauge-fixing choice for the coordinate system is not necessary for the evaluation of diffeomorphism invariant observables, all other gauge choices are equivalent.

³⁰This resonates with similar ideas presented in [138], which views $T\bar{T} + \Lambda_2$ deformations in dS₃/CFT₂ as a way to unify it with static patch holography.

³¹There have been explicit realizations of the dS/CFT correspondence in different approaches, including higher spin gravity [220, 221] where dS₄ space [222–224] is dual to $\text{Sp}(N)$ CFT₃s; as well as proposal of higher spin dS₃ space being dual to a SU(2) Wess-Zumino-Witten model [225–228] from an analytic continuation of Euclidean AdS₃ space; and from transitions between Euclidean AdS₄ space to dS₄ space [229–231]. A different approach involves geometries interpolating from asymptotically AdS₂ and dS₂ spacetimes, often referred to as centaur geometries [148, 164, 232–236], whose holographic dual has been recently investigated in [237, 238]. See [239] for a review and references therein.

³²This parameter is associated with the mass of SdS₃ space [241], where a value $r_{\text{CH}} \neq 1$ implies the existence of a conical deficit.

Let us now evaluate the Euclidean on-shell action of the half-reduction dS_2 JT gravity model with a finite time-like Dirichlet surface, $r = r_B$, using (6.2, 2.31) with $U(\Phi) = -2\Phi$, and a counterterm $G(\Phi_B) = \Phi_B^2$ for the dual T^2 deformation, or $G(\Phi_B) = -\Phi_B^2$ for $T^2 + \Lambda_1$,³³ which, like (2.31), results in

$$I_E = S_{dS} - \beta_T E_{BY}(r_B) , \quad (6.3)$$

where $S_{dS} = r_{CH}/(4G_2)$ is the Gibbons-Hawking (GH) entropy [242, 243] (which does not include a topological contribution, unlike the term Φ_0 in (2.24)). Meanwhile the BY [180] quasi-local energy with respect to the Dirichlet wall is given by

$$E_{BY} = \begin{cases} \frac{1}{8\pi G_2} \left(r_B + \sqrt{r_{CH}^2 - r_B^2} \right) , & \text{when } r_{CH} > r_B , \\ \frac{1}{8\pi G_2} \left(r_B + \sqrt{r_B^2 - r_{CH}^2} \right) , & \text{when } r_{CH} < r_B , \end{cases} \quad (6.4)$$

which is directly related to the energy spectrum of the triple-scaled SYK (3.76) as expected from the holographic dictionary at a finite cutoff (2.33).

The corresponding inverse Tolman temperature is then given by

$$\beta_T = \beta \begin{cases} \sqrt{r_B^2 - r_{CH}^2} , & \text{when } r_{CH} > r_B , \\ \sqrt{r_{CH}^2 - r_B^2} , & \text{when } r_{CH} < r_B , \end{cases} \quad \beta = \frac{2\pi}{r_{CH}} . \quad (6.5)$$

Performing a similar analysis of the heat capacity with a Dirichlet wall with a fixed radial location $r = r_B$, as in (2.28), results in

$$C_{r_B} = -\frac{r_B}{8\pi G_2} \frac{4\pi^2 \beta_T^2}{(4\pi^2 - \beta_T^2)^{3/2}} . \quad (6.6)$$

Notice that the heat capacity for fixed location r_B is always negative, in contrast with (2.28).

Thermodynamic properties of dS_2 space are indeed in agreement with the analysis of the UV behavior of the deformed boundary theory in Sec. 3.5. Particularly, given $G(\Phi_B) = \pm\Phi_B^2$ then the dictionary entry for the deformation parameter (2.16)

$$y = \pm 1/r_B^2 , \quad (6.7)$$

allow us to explicitly check of the dictionary (2.33) relating BY quasi-local energy (6.4) and Tolman temperature (6.5) to the energy spectrum of the T^2 deformed (2.20) and $T^2 + \Lambda_1$ deformed (2.21) theories and microcanonical temperature (2.25) respectively, as well as the corresponding heat capacity at fixed y (2.29) with that at fixed r_B (6.6). Thus, there is an exact match at the level of thermodynamic properties. We will extend this to dynamical observables and holographic entanglement entropy in the rest of the section.

³³Note that this is the same boundary term choice as [33], which can be motivated for defining a notion of ADM mass for SdS_3 space with respect to \mathcal{I}^+ , as elaborated in [241], and it has also been applied in $T\bar{T} + \Lambda_2$ deformations in [141, 143].

6.2 Hyperfast State Complexity Growth

Let us now discuss the expectation value of the chord number \hat{n}_y in the HH state with a $T^2(+\Lambda_1)$ deformation (3.81b), which we repeat for the convenience of the reader,

$$L_{\text{UV}} \equiv \frac{\langle \Omega | e^{-\tau^* \hat{H}_y} \hat{L}_{\text{UV}} e^{-\tau \hat{H}_y} | \Omega \rangle}{\langle \Omega | e^{-\beta \hat{H}_y} | \Omega \rangle} = \sum_{n=0}^{\infty} n \left| \frac{\langle \Omega | e^{-\tau^* \hat{H}_y} | n \rangle_y}{Z_y(\beta)} \right|^2 \Big|_{\tau = \frac{\beta(\theta)}{2} + it} \quad (6.8)$$

$$\stackrel{UV}{\rightarrow} \begin{cases} 2i \operatorname{arcsinh} \left(\sqrt{\frac{1}{y\theta_{\text{UV}}^2} - 1} \cosh \left(\frac{\theta_{\text{UV}} t}{\sqrt{1-y\theta_{\text{UV}}^2}} \right) \right), & 0 \leq y \leq y_0, \\ 2 \operatorname{arcsin} \left(\sqrt{1 - \frac{1}{y\theta_{\text{UV}}^2}} \cosh \left(\frac{\theta_{\text{UV}} t}{\sqrt{y\theta_{\text{UV}}^2 - 1}} \right) \right), & y \geq y_0. \end{cases}$$

As mentioned in Sec. 3.2, the expectation of the chord number takes the role of a generalized notion of state complexity for states obeying the recurrence relation (3.28) obeyed by the $|n\rangle_y$ basis given the seed state $|\Omega\rangle$. We display the growth of this observable in Fig. 7. As seen in (6.8) and in contrast to Sec. 3.5, L_{UV} is pure imaginary for the $\eta = +1$ case and real in the $\eta = -1$ case. However, similar to L_{IR} there is eternal growth in the former, and a limit in the evolution of L_{UV} . The first observation is in agreement with [77] (for the seed theory case), who finds that the expectation value of the chord number in the regime we have considered as Krylov spread complexity of the corresponding state. The authors interpret this as a geodesic length in dS_2 space, which is thus a concrete manifestation of the CV conjecture [90]. It eternally evolves in terms of the spacelike coordinate t in (6.2). Our results can be seen as a finite cutoff realization. Meanwhile, by performing the $T^2 + \Lambda_1$ deformation, the rescaled chord number becomes real-valued. In the bulk interpretation, this means that the corresponding geodesic curves become spacelike instead of timelike. This indicates that the cutoff surface has crossed the cosmological horizon in the bulk dual, as depicted in Fig. 7, which is consistent with the $T\bar{T} + \Lambda_2$ interpretation [136, 138] in one lower spacelike dimension, as well as our findings in the AdS_2 case. Meanwhile, the maximal range of evolution from (3.81b) is:

$$t \in [-t_{\text{crit}}, t_{\text{crit}}], \quad t_{\text{crit}} \equiv \frac{\sqrt{y\theta_{\text{UV}}^2 - 1}}{\theta_{\text{UV}}} \operatorname{arccosh} \left(\sqrt{1 - \frac{1}{y\theta_{\text{UV}}^2}} \right). \quad (6.9)$$

The result agrees with the hyperfast complexity growth conjecture (iii) and (iv) in Sec. 1; the state complexity reaches its maximum at a critical time t_{crit} which is order one in units of the dS length scale.

In the bulk interpretation, (6.9) is consistent with previous results in the CV conjecture in $dS_{d+1 \geq 3}$ with a cosmological stretched horizon [149]. While the previous proposal do not discuss an explicit boundary dual, it was noticed that the extremal volume surfaces do not evolve eternally since there is a maximum value for the timelike coordinate, similar to $t = t_{\text{crit}}$ above. At this point, the extremal surfaces reach \mathcal{I}^\pm , as seen in Fig. 1 and they generically diverge in higher dimensions. Thus, our results provide an explicit confirmation

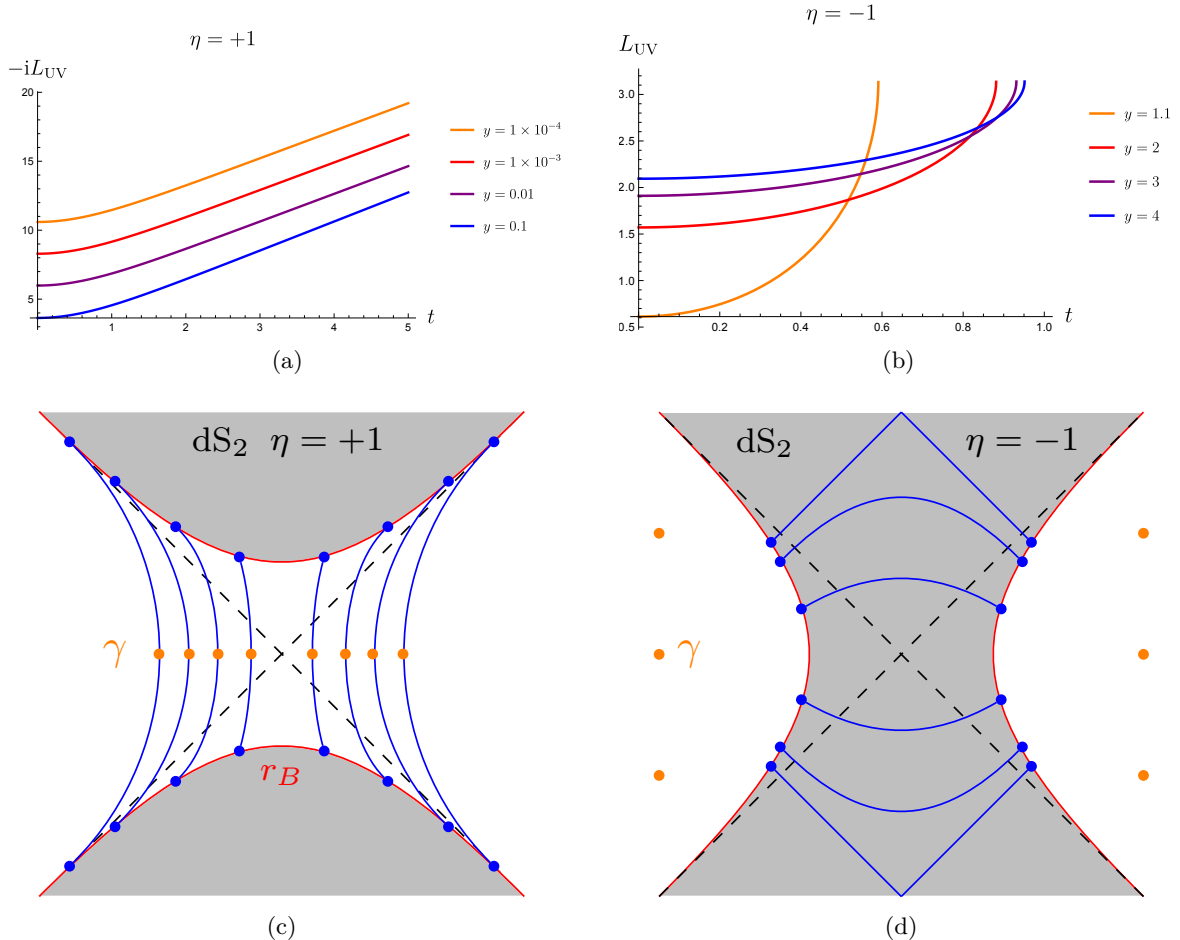


Figure 7. *Top:* UV triple-scaling limit of the chord number in the $|n\rangle_y$ basis from (a) T^2 , and (b) $T^2 + \Lambda_1$ deformations of the DSSYK model using $\theta_{\text{UV}} = 1$. *Bottom:* Corresponding bulk interpretation of the T^2 and $T^2 + \Lambda_1$ deformations in terms of (c) timelike and (d) spacelike extremal length geodesics at a finite cutoff in dS_2 space. We marked minimal codimension-two area (measured by the dilaton) points γ homologous to the finite boundaries as orange dots, and the entangling surfaces as blue dots in the corresponding boundaries.

of the proposal for the CV conjecture in dS_2 space, and it displays the hyperfast growth expected by [1]

6.3 Hyperfast Scrambling From OTOCs

The crossed four-point function of the deformed DSSYK model in the semiclassical limit was calculated in (4.22) and its scrambling time in (4.26). Now, we are interested in its UV triple-scaling limit (3.72), where $\tilde{\theta}_{\text{UV}} \equiv (\pi - \theta)/\lambda$ is fixed as $\lambda \rightarrow 0$. Since the analysis follows similarly to the IR limit of the crossed four-point function (4.20) with two operators of conformal dimension Δ_0 and two with dimension Δ_1 , we specialize in the OTOC case,

where $t_L = -t_R \equiv t$, as explained in (4.22). Using the corresponding canonical variables, the UV triple-scaling limit of (4.20) becomes

$$G_4(t, -t; \theta, \pi - \theta) \xrightarrow{UV} \left(\frac{e^{-\ell_0/2}}{1 + \left(1 - \frac{2e^{-\ell_0}}{\tilde{\theta}_{UV}^2} \right) \sinh^2(\frac{\lambda_L}{2}t)} \right)^{2\Delta_0}, \quad (6.10)$$

where, similar to (4.32), we the constant $\ell_0 = \ell_*(q_1^\Delta, \theta, \pi - \theta)$ in becomes

$$e^{-\ell_0} \equiv e^{-\ell_*(q_1^\Delta, \theta, \pi - \theta)} \xrightarrow{UV} \frac{1}{2} \left(\tilde{\theta}_{UV}^2 + \Delta_1^2 - \Delta_1 \sqrt{2\tilde{\theta}_{UV}^2 + \Delta_1^2} \right), \quad (6.11)$$

with ℓ_* defined in (4.21), and λ_L is the corresponding Lyapunov exponent in the scrambling phase of the OTOC (4.22), i.e. when we can Taylor expand (6.10) in powers of $e^{\lambda_L t}$ by

$$G_4 \simeq \left(\frac{2\tilde{\theta}_{UV}^2 e^{-\ell_0}}{\tilde{\theta}_{UV}^2 + 2e^{-\ell_0}} \right)^{2\Delta_0} \left(1 - \Delta_0 \frac{\tilde{\theta}_{UV}^2 - 2e^{-\ell_0}}{\tilde{\theta}_{UV}^2 + 2e^{-\ell_0}} e^{\lambda_L t} \right), \quad t \ll t_{sc}, \quad (6.12)$$

where

$$\lambda_L \equiv \frac{4\pi}{\tilde{\beta}_y} \xrightarrow{UV} \begin{cases} \frac{\tilde{\theta}_{UV}}{\sqrt{1-y\tilde{\theta}_{UV}^2}} & , \quad 0 \leq y_0 \leq y_0 \\ \frac{\tilde{\theta}_{UV}}{\sqrt{y\tilde{\theta}_{UV}^2-1}} & , \quad y \geq y_0 \end{cases}, \quad (6.13a)$$

$$t_{sc} \xrightarrow{UV} \frac{1}{2\lambda_L} \log \frac{2(\tilde{\theta}_{UV}^2 + 2e^{-\ell_0})}{\tilde{\theta}_{UV}^2 - 2e^{-\ell_0}}. \quad (6.13b)$$

Note that the latter expression is consistent with (3.83) in [65]. Manifestly, the result (6.13b) agrees with the hyperfast scrambling conjecture (ii) and (iv) in Sec. 1. The scrambling time of the OTOC is order one, corresponding to the dS scale, instead of order $\log S \propto \log N$ [92, 183] the expected scrambling time for fast scrambler, which diverges in the double-scaling limit. Next, we see that the presence of the redshift factor in λ_L , the limit $y \rightarrow y_0$ reproduces the infinite temperature limit, similar to that in the hyperfast state complexity growth in the previous subsection.

6.4 Holographic Entanglement Entropy and dS Space

In this section, we discuss the algebraic entanglement entropy (5.6) of the DSSYK model in the UV limit and its holographic interpretation. Similar to the previous discussion, we focus on the chord number state $|n\rangle_y$.

Chord Number State From the boundary side, the algebraic entanglement entropy given the state $|n\rangle_y$ (3.29) in the UV triple-scaling limit (3.72) can be evaluated using very analogous steps as in Sec. 5.3 with the corresponding limit of the Hamiltonian (3.73b) using symmetry

in the integration measure $\mu(\theta)$ (3.17) around $\theta = \pi/2$. Specifically, (5.31) extends to the UV case as

$$\Delta S_{UV} \xrightarrow{\lambda} \frac{2\pi}{\lambda} R(y) \sec \frac{L_{UV}}{2} . \quad (6.14)$$

Now, we discuss its bulk interpretation, including its limit as the GH entropy in the stretched horizon limit.

RT Surfaces From Spacelike Boundaries We are interested in evaluating the RT formula in dS JT gravity, i.e. (2.1) with $U(\Phi) = -2\Phi$ as

$$S_{dS} \equiv \frac{\Phi_{dS}(\gamma)}{4G_N} , \quad (6.15)$$

where the finite cutoff boundaries are spacelike, as displayed in Fig. 7 (c).

First, consider global coordinates, where the metric and the dilaton take the form

$$ds^2 = -dT^2 + \cosh^2 T d\varphi^2 , \quad \Phi_{dS} = r_{CH} \sin \varphi \cosh T . \quad (6.16)$$

To map to static patch coordinates in (6.2) describing the Milne patch (i.e. outside the cosmological horizon in Fig. 1 (d)) we need to use $r_{CH} t \rightarrow r_{CH} t + i\frac{\pi}{2}$ [244], so that

$$\sqrt{\frac{r^2}{r_{CH}^2} - 1} \cosh(r_{CH} t) = \sinh T , \quad \text{when } r > r_{CH} , \quad (6.17a)$$

$$\sqrt{\frac{r^2}{r_{CH}^2} - 1} \sinh(r_{CH} t) = \cos \varphi \cosh T . \quad (6.17b)$$

From symmetry of dS_2 space the finite cutoff boundaries are located at $T = 0$ in global coordinates, as displayed in Fig. 7 (c). Then, using the relation between the coordinates in (6.17) with $r = r_B > r_{CH}$ for the entangling surface we get

$$\Phi_{dS} \Big|_{T=0} = r_B \sec \frac{L_{UV}}{2} , \quad \sinh^2 \frac{iL_{UV}}{2} = \left(\frac{r_B}{r_{CH}} - 1 \right) \cosh^2(r_{CH} t) . \quad (6.18)$$

Then, the evaluation of the RT formula in dS_2 space (6.15) gives

$$S_{dS} = \frac{r_B}{4G_N} \sec \frac{L_{UV}}{2} . \quad (6.19)$$

Note that the only difference with respect to the JT gravity setting (5.37) is in replacing $L_{IR} \rightarrow -iL_{UV}$, which is consistent with the boundary evaluation. Note in particular that in the stretched horizon limit, i.e. $r_B \rightarrow r_{CH}$ we recover the GH entropy of dS_3 space, since $L_{UV} \rightarrow 0$ (6.18)

$$S_{dS} = \frac{2\pi r_{CH}}{4G_3} , \quad (6.20)$$

where we again used that $2\pi G_N = G_3$ [184], and $2\pi r_{CH}$ is the corresponding codimension-two area in dS_3 space. Due to the general correspondence with the entanglement entropy in the deformed theory (6.14) the GH entropy can indeed be interpreted as entanglement entropy from the perspective of the microscopic theory. The BH entropy in the $y \rightarrow 0$ limit can also be recovered as explained in [92].

RT Surfaces From Timelike Boundaries At last, we search to evaluate the RT formula for dS JT gravity (2.1) (with $U(\Phi) = -2\Phi$) in (6.15) using global coordinates (6.16) when the entangling surface are points along the finite cutoff boundaries that reside in the static patch (e.g. the cosmological stretched horizon case) in Fig. 7 (d).³⁴ The relationship between static patch coordinates and global dS₂ coordinates in the case of interest is similar to (6.17) without the analytic continuation between Milne and static patch, namely

$$\sqrt{1 - \frac{r^2}{r_{\text{CH}}^2}} \sinh(r_{\text{CH}} t) = \sinh T, \quad \text{when } r < r_{\text{CH}} \quad (6.21\text{a})$$

$$\sqrt{1 - \frac{r^2}{r_{\text{CH}}^2}} \cosh(r_{\text{CH}} t) = \cos \varphi \cosh T. \quad (6.21\text{b})$$

Analogous to the AdS case in Sec. 5.3, the homology constraint with r timelike boundaries implies that the dilaton in dS JT gravity (6.16) is extremized in the φ direction ($\partial_\varphi \Phi_{\text{dS}} = 0$) and for a fixed T coordinate. This leads to $\varphi = \pi/2$, which is a maximum value for the dilaton (6.16), while the minimum value is reached when $\varphi = 0$ or π , corresponding to the poles of the static patch. However, since the dilaton is trivial for this minimum, this would not even be connected to the previous result the extremal value of the dilaton with spacelike boundaries (6.19), and neither to the boundary result for the algebraic entanglement entropy. This indicates that the RT formula does not apply after the $T^2 + \Lambda_1$ deformation, and one might need a search for a different geometric quantity dual to the algebraic entanglement entropy found in (6.14).

Thus, the result differs from Susskind’s conjectures (i) and (iv) in Sec. 1, which expected the RT formula to hold when the corresponding boundary is inside the static patch instead of the Milne patch. However, in the strict limit where the boundary is at the cosmological horizon one recovers the expected GH entropy. However, in higher dimension, one can have subregions in the stretched horizon and develop a different form of the RT formula in [1], which is not accessible from the two-dimensional analysis

7 Discussion

In summary, we developed chord Hamiltonian deformations based on general dilaton gravity theories with Dirichlet boundaries and different boundary counterterms. In particular, this recovers T^2 deformations in (0+1)-dimension, as well as a lower-dimensional analog of $T\bar{T} + \Lambda_2$ deformations (“ $T^2 + \Lambda_1$ ”) as special cases. While the formalism can be applied in general holographic quantum mechanics, we specialized most of the study in the DSSYK model for concreteness. We evaluated the semiclassical thermodynamic properties of the deformed model from its partition function. We investigated a natural chord basis and the corresponding representation of the chord Hamiltonian, such that the chord number associated to the

³⁴Note that while we use entangling surface points in the two-dimensional context, in higher dimensions one can adopt spatial subregions, which may lead to a larger variety of the minimal codimension-two area with boundaries in the static patch [138, 245].

new basis reproduces a wormhole length with finite cutoff in the bulk. This motivated us to propose a new definition of state complexity in the seed theory. We suspect this definition reproduces the same Krylov spread complexity of the HH state in the deformed theory. We also deduced expressions for general and semiclassical correlation functions in the deformed theory. Remarkably, the algebraic entanglement entropy between the double-scaled algebras of the DSSYK given the new chord number basis precisely matches the dilaton at the extremal surface in the JT and dS JT gravity once we restrict to the IR and UV triple-scaling limits respectively. By combining the previous results in the UV limit of the DSSYK chord spectrum, and applying a sequence of T^2 and $T^2 + \Lambda_1$ deformations, we explicitly realize the stretched horizon proposal by Susskind [1], including its characteristic hyperfast growth for dynamical observables. This provides a direct link between Susskind's conjectures [1] with sine dilaton gravity, which recovers dS_2 space in a specific limit [102] associated with our UV triple-scaling limit, and therefore also with Schwarzschild- dS_3 holography [105]. This allows a more precise connection between different proposals for the bulk dual of the DSSYK model.

Now, we discuss directions for future investigation.

7.1 Outlook

Krylov complexity In the main text, we discussed a proposal for state complexity which has a bulk interpretation in terms of bulk geodesics at finite cutoff in (A) dS_2 space. This connects with literature on holographic complexity with a finite cutoff in the bulk, e.g. [149, 151–155, 157, 158, 246, 247]. It is an important problem to confirm if the bulk geodesics at finite cutoff in dS_2 space, corresponding to the UV limit of the DSSYK model indeed correspond to Krylov spread complexity, which we have elaborated in Sec. 3.4. In the main text, we also explored the effect of the deformations in the semiclassical correlation function, which are only affected by a modification in the inverse temperature to be the Tolman temperature. It is then natural to investigate what would be the effect of the Hamiltonian deformation in Krylov operator complexity.

For concreteness, consider the one-particle HH state in (4.9b) for $m = 1$ which can be expressed as

$$|\Psi_{\Delta_1}(\tau_L = \kappa\tau, \tau_R = \tau)\rangle = e^{-\hat{\mathcal{L}}_{\kappa}\tau} |\Delta_1; 0, 0\rangle = \sum_n \Psi_n^{(\kappa)}(\tau) \left| K_n^{(\kappa)} \right\rangle , \quad (7.1)$$

where

$$\hat{\mathcal{L}}_{\kappa} \equiv \hat{H}_{R,y} + \kappa \hat{H}_{L,y} , \quad \kappa \equiv \tau_L/\tau_R . \quad (7.2)$$

is a Liouvillian operator. Note that

$$\kappa = 1 : \quad |\Psi_{\Delta_1}(\tau_L = \tau, \tau_R = \tau)\rangle = e^{-\tau(\hat{H}_L + \hat{H}_R)} |\Delta_1; 0, 0\rangle , \quad (7.3a)$$

$$\kappa = -1 : \quad |\Psi_{\Delta_1}(\tau_L = -\tau, \tau_R = \tau)\rangle = e^{-\frac{\beta}{2}\hat{H}_{L,y}} \hat{\mathcal{O}}_{\Delta_1}(t) e^{-\frac{\beta}{2}\hat{H}_{L,y}} |\Omega\rangle . \quad (7.3b)$$

where

$$\hat{\mathcal{O}}_{\Delta_1}(t) \equiv e^{it\hat{H}_L} \hat{\mathcal{O}}_{\Delta_1} e^{-it\hat{H}_L} , \quad \tau \equiv \frac{\beta}{2} + it . \quad (7.4)$$

The $\kappa = +1$ case corresponds to Schrödinger evolution with respect to a total Hamiltonian $\hat{H}_L + \hat{H}_R$ in complex-valued time τ ; while $\kappa = -1$ corresponds to Heisenberg evolution with respect to the single-sided Hamiltonian \hat{H}_L . For this reason, based on the Liouvillian evolution operator $\hat{\mathcal{L}}_\kappa$, we can evaluate Krylov complexity for states and operators depending on the value of κ . Other choices of κ are associated with generalized notions of Krylov complexity [67]. We will focus on $\kappa = \pm 1$.

Meanwhile, we refer to $\{ |K_n^{(\kappa)}\rangle\}$ as the Krylov basis for the reference state $|K_0^{(\kappa)}\rangle \equiv |\Delta_1; 0, 0\rangle$, which are defined to satisfy a Lanczos algorithm

$$\hat{\mathcal{L}}_\eta |K_n^{(\kappa)}\rangle = a_n^{(\kappa)} |K_n^{(\kappa)}\rangle + b_{n+1}^{(\kappa)} |K_{n+1}^{(\kappa)}\rangle + b_n^{(\kappa)} |K_{n-1}^{(\kappa)}\rangle , \quad (7.5)$$

with $b_0^{(\kappa)} = 0$, $a_0^{(\kappa)} = \langle K_0^{(\kappa)} | K_0^{(\kappa)} \rangle$, while $a_n^{(\kappa)}$ and $b_n^{(\kappa)}$ are called Lanczos coefficients. We define Krylov operator complexity as

$$\mathcal{C}(t) \equiv \frac{\langle \Psi_\Delta(-\tau, \tau) | \hat{\mathcal{C}}^{(\kappa)} | \Psi_\Delta(-\tau, \tau) \rangle}{\langle \Psi_\Delta(-\tau, \tau) | \Psi_\Delta(-\tau, \tau) \rangle} \Big|_{\tau = \frac{\beta}{2} + it} , \quad \hat{\mathcal{C}}^{(\kappa)} \equiv \sum_n n |K_n^{(\kappa)}\rangle \langle K_n^{(\kappa)}| . \quad (7.6)$$

Similar to the spread complexity case, the effect of the deformation in the Liouvillian operator (7.2) is to scramble the Krylov basis $|K_n^{(\kappa)}\rangle$. It would be interesting to deduce the semiclassical Krylov operator and spread complexity with a one-particle insertion. In particular, this could be useful to learn about these deformations in higher dimensional examples. For instance, it was reported in [248] that the exponential growth of Krylov operator complexity for CFTs might not agree with the OTOC chaos bound [197] when the deformation parameter has the sign associated to superluminal motion [249], unlike in finite cutoff holography.

It would also be interesting to compare the standard definition of Krylov operator complexity above with the work by [250], where the authors use a notion of Krylov operator complexity in a microcanonical window in JT gravity. They find that at leading order in the approximation, the Lanczos coefficients display linear growth, and Krylov complexity grows exponentially with a simple modification in the inverse temperature, which includes the corresponding redshift factor, similar to our findings for the semiclassical correlation functions. This suggests that one might find a redefinition of Krylov operator complexity (7.6) in a microcanonical window which can be expressed as the first derivative of the OTOC at finite temperature in (4.22) based on the seed theory result [67] where one would incorporate the fake temperature with the corresponding redshift factor in (4.19). This redefinition of Krylov operator complexity would be associated to the wormhole length connecting the asymptotic boundaries of an AdS_2 black hole instead of the one with finite Dirichlet boundary (3.50) even when $\Delta \rightarrow 0$. For this reason, it might also be fruitful to develop in detail the definition of Krylov operator complexity in (7.6) without fixing an energy window, which might be more closely related to finite cutoff holography.

Generalized Boundary Conditions in Finite Cutoff Holography Our work has focused on the finite cutoff interpretation of Hamiltonian deformations, when the bulk dual has

Dirichlet boundary conditions. There is literature regarding how to extend holography between Dirichlet through multitrace deformations, which is expected to modify the boundary conditions in the bulk [38–40, 43, 251, 252]. In particular, there has been significant interest in developing conformal boundary conditions and its extensions [41, 42, 144, 144, 253–262, 262, 263] to obtain well-posed solutions in general relativity when Dirichlet boundary conditions are ill-posed. Finite cutoff in AdS space with conformal boundary conditions was investigated in [39–42]. Given that the DSSYK model is a useful analytically solvable model at different energy scales, it might be convenient to generalize our study, incorporating cutoff holography with conformal boundary conditions instead of Dirichlet in the dilaton-gravity theories, possibly along the lines of [259], and analyze how the thermodynamics properties of the model and its correlation functions are modified. Given the connection between the deformations in the DSSYK model and stretched horizon holography, this study could help us gain general lessons for static patch holography, since, as we saw, the theory is otherwise thermodynamically unstable. It is also relevant to study the perturbative stability of the solutions under background fluctuations [144], which could be incorporated following previous studies in the dilaton-gravity context by [264, 265].

Additionally, it should be possible to adapt our study in the mixed boundary condition interpretation where the DSSYK would stay at the original asymptotic boundary location (i.e. r_B). The development of this interpretation in (1+0)-dimensional systems has been previously performed in [28].

We hope to come back to these point in future work to implement this interpretation in the sine dilaton gravity model.

Entanglement entropy in $T^2 + \Lambda_1$ Deformation As emphasized in the main text, the algebraic entanglement entropy in the double-scaled algebras associated to a chord number state (which reproduces bulk geodesics at a finite cutoff) leads to a precise matching between the bulk entanglement entropy in the T^2 deformed theory and the dilaton in JT and dS JT gravity at the extremal surface predicted by the RT formula. However, once we move to $T^2 + \Lambda_1$ deformations, the RT formula does not longer apply as the minimal value of the dilaton becomes trivial, as explained in Secs. 5.3 and 6.4. It would be interesting to find a geometric quantity that one can associate with the corresponding algebraic entanglement entropy (5.6) given the chord state in the natural chord basis $|n\rangle_y$ in the $T^2 + \Lambda_1$ case, although the system is not even thermodynamically stable. For instance, a central part in Susskind’s conjectures are rules to implement RT formula calculations in stretched horizon holography in the bilayer vs monolayer proposals [1, 161–163]. These rules rely on angular dependence in dS_3 space, and they are thus inaccessible from the dS_2 perspective which is dual to the UV limit of the DSSYK model. In principle one may connect these additional RT proposals with the dS_3 embedding of sine dilaton gravity [105], which we leave for future directions.

Additionally, we suspect that one does not need to limit the evaluations to a triple-scaling limit to be able to interpret the algebraic entanglement entropy in the chord number state holographically. We would like to extend this result for the semiclassical regime in the

DSSYK model [53], which is expected to have a bulk interpretation in sine dilaton gravity. One might derive further results in this direction by developing a Lewkowycz-Maldacena path integral derivation of the corresponding RT formula in the bulk [266], or possibly through a factorization map [267–272]. We hope to follow this closely in future work.

Deforming Before Averaging Throughout our analysis, we considered that we deformed the DSSYK model after ensemble averaging since the Hamiltonian deformation can be interpreted as a radial bulk flow in the sine dilaton gravity theory. However, one might investigate the differences in the theory by applying first the deformation and then the averaging. This would mean a transformation in the SYK Hamiltonian (3.1)

$$\hat{H}_{\text{SYK}} \rightarrow \hat{H}_{\text{SYK},y} = \frac{1}{y} \left(1 - \sqrt{1 - 2y\hat{H}_{\text{SYK}}} \right). \quad (7.7)$$

The ensemble average evaluation is more complicated due the square root factor, although one can make much progress by working in the $G\Sigma$ -formalism, as in [28]. It would be interesting to consider in this alternative case how the different thermodynamic properties and dynamical observables, such as state complexity and correlation functions, in our study are modified, and to understand the corresponding bulk geometry.

Verifying Sine Dilaton at Finite Cutoff Our work has mostly taken a boundary perspective without requiring a specific bulk dual to the DSSYK model beyond its IR and UV triple-scaling limits, as long as it corresponds to a dilaton gravity theory. Nevertheless, we found explicit results that suggest a natural bulk interpretation in terms of sine dilaton gravity, such as the chord number in the semiclassical limit reproducing a wormhole geodesic at finite cutoff (3.50), as well as the RT formula verification for the UV and IR triple-scaling limits in Sec. 3.5. As a next step, one could perform a bulk analysis of correlations functions and thermodynamics to provide a concrete bulk dual interpretation of some of our other results. A simple start would be recovering the functional dependence of correlation functions and thermodynamic observables in the microcanonical ensemble being modified by an overall redshift factor associated to the Tolman temperature in the semiclassical limit, as in the existing literature in JT gravity and higher dimensional cutoff holography [27–29, 33, 136, 196]. However, it is important to make further checks outside the AdS_2 regime of the bulk dual theory. For instance, in sine dilaton gravity, one could carry out a gravitational path integral calculation in the bulk, or study solutions to the Wheeler-DeWitt equation in the bulk at finite cutoff (similar to [29]) to verify our boundary theory results for the partition functions and correlation functions.

Additionally, it was previously pointed out by [85] that there is a defect interpretation of the thermodynamics in sine dilaton gravity related to an infinite degeneracy in the black hole and cosmological horizons due to the periodicity in the dilaton potential. Meanwhile, the finite cutoff interpretation of the Hamiltonian deformations in this work might allow to remove the degeneracy by placing the boundaries in appropriate locations in the complex-valued geometry. It would be interesting to investigate how the properties of the conical

defect associated with the removed horizons can be matched with the exact T^2 deformed partition function in (2.23).

Moreover, while the practical computations are semiclassical, one could repeat our analysis of correlation functions and partition functions beyond the on-shell level by including one-loop corrections as in [183] for the T^2 deformed DSSYK, and comparing them with recent developments [37, 104]. It is also important to extend our investigation with non-perturbative series expansions of our results in terms of Borel resummation and instanton processes following analogous studies in JT gravity [32] to better understand the spectrum of the deformed theory and the putative bulk dual at a finite cutoff.

At last, a related interesting extension would be to explore finite cutoff holography using the chord Hamiltonian (3.12) when $q = e^{ib}$ (where $b \in \mathbb{R}$) (instead of $q \in [0, 1]$ in the main text) which is argued to be dual to a $\sinh \Phi$ dilaton gravity theory [273, 274], and it is closely connected with Liouville gravity [275–280]; see [37] for recent progress.

Narovlansky-Verlinde Model Another interesting proposal for the bulk dual of the DSSYK model was made by V. Narovlansky and H. Verlinde in [108] (see also [88, 89, 105, 110]), who developed an approach towards dS_3 holography by considering a two-copy SYK model with an equal energy constraint. In the double-scaling limit and after ensemble-averaging, the system can be described by the zero-particle chord Hamiltonian (3.12).

In the bulk proposal of [108], the dual dilaton gravity theory has a potential (C.1) of the form:

$$U(\Phi) = -2 \cosh(\Phi) . \quad (7.8)$$

The T^2 deformation parameter is given by (2.16) for the potential with the counterterm (2.2) is

$$y = -\frac{\lambda}{\sinh \Phi_B} . \quad (7.9)$$

It would be interesting to test our boundary theory findings with finite cutoff holography in the NV model to check if it leads to a manifestly different thermodynamics or correlation functions with respect to those in sine dilaton gravity at finite cutoff, and compare both with our boundary theory results. In particular, our results about entanglement entropy at a finite cutoff have a clear geometric interpretation for (A)dS space when we zoom in the UV and IR triple-scaling limits. These limits are naturally compatible with sine dilaton gravity; it would be interesting to find if there are similar limit that can be associated to the dilaton gravity theory described by (7.8), or whether one can show there are none unless $\Phi \rightarrow i(\Phi)$ which would recover an equivalent theory to sine dilaton gravity. It would also be interesting to relate the NV model at finite cutoff to a dimensionally reduced version of the $T\bar{T} + \Lambda_2$ deformations [141, 143] similar to our proposal for $T^2 + \Lambda_1$ deformations of the DSSYK model in the triple-scaling limit (3.73b).

Relational Holographic Flow In the future, we would like to study the relational interpretation in the T^2 flow, focusing on the dressed observables and the finite cutoff holographic

dictionary. It has been noticed that quantum reference frame (QRF) transformation will significantly affect the thermodynamics, and algebraic operator structure of general systems [281, 282] (see also [283]). Given the explicit knowledge of the solution for the DSSYK model, it would be intriguing to study QRF transformations in this system explicitly and how the semiclassical thermodynamics studied here will be modified. More generally, it would be interesting to study the algebra of observables for the T^2 -deformed DSSYK model with matter, as a microscopic realization of [142].

If one interprets the boundary in terms of an observer to define expectation values of gravitationally dressed operators in the bulk algebra; we might view that as we change the location of the cutoff boundary, the observer also changes due to the Hamiltonian deformation of the boundary theory. For instance, based on recent work by [105], we could re-express sine dilaton gravity theory by a pair of Liouville fields; and we study how the flow in the Schrödinger evolution is captured by relational observables. The effect of the $T\bar{T}$ deformation is to change the Hamiltonian but not the proper time measured by a boundary observer. From the relational interpretation of the Liouville-CFT formulation of sine dilaton gravity this means that the collective field description of the DSSYK is modified, but not the time parameter itself corresponding to the observer's clock in the Liouville theory. It would thus be interesting to explore how the $T\bar{T}$ deformation changes the Page-Wootters mechanism [284, 285] in the bulk theory. We expect there is a relational description in the bulk in terms proper time in sine dilaton gravity. In contrast; the boundary theory just experiences Schrödinger evolution since it only has access to gauge invariant data of the bulk.

Deforming Matrix Models T^2 deformations in an ensemble of matrix models have been previously considered in the JT gravity context by [31]; which allowed them to study the energy spectrum of the deformed model for all real values of the deformation parameter without recurring to a mixed boundary condition interpretation in the bulk. It would be interesting to generalize the previous work of [31] to explore how this type of interpretation works in a matrix model dual to the sine dilaton gravity model with a higher genus expansion, which is not well developed. It might also be interesting to perform the T^2 deformation of the two-matrix model of [286, 287] that reproduces certain DSSYK amplitudes (and which has been further developed in [288–290]), to compare with our findings on semiclassical thermodynamics in Sec. 2.3, and possibly to investigate recent connections between JT gravity at finite cutoff with matrix models [37].

Charged DSSYK model and $J\bar{T}$ deformations In line with our analysis of T^2 deformations in the DSSYK model, there also exist $J\bar{T}$ deformations [291] in the literature [292], where J is a chiral $U(1)$ current. It would be interesting to investigate the nature of the bulk dual to the DSSYK model with a $U(1)$ charge [293] (see also [294–296]), which has been recently discussed in [107, 125]. One could then introduce $J\bar{T}$ deformations, or alternatively a combination of T^2 , $J\bar{T}$ deformations in the DSSYK model, and study the thermodynamic properties and correlation functions we have encountered in this work. In particular, it would

be interesting to evaluate the corresponding Krylov spread complexity (away from the vanishing deformation parameter $y \rightarrow 0$ limit, discussed by [71]). A related possibility in this direction is using the $\mathcal{N} = 2$ extension of the DSSYK model [297] which counts with an R-charge. It would be very interesting to extend the results deforming the theory and finding the corresponding bulk length at finite cutoff, particularly for the BPS sector [298], its interpretation as chord number [84] and in terms of Krylov spread complexity [72].

Stretched Horizon in Higher Dimensions Recently, [137] found an extension of $T\bar{T} + \Lambda_2$ deformations in higher dimensions, which we denote $T^2 + \Lambda_d$ deformations. Explicitly, consider deformation the action of a CFT_d as

$$\frac{dI_{\text{bdry}}}{dy} = \int d^{d-1}x \sqrt{-h} \left[\frac{\pi y}{d} : \left(\tilde{T}_{\mu\nu} \tilde{T}^{\mu\nu} - \frac{1}{d-1} (\tilde{T}_\mu^\mu)^2 \right) : - \frac{d^2(d-1)}{4\pi} \frac{\eta-1}{y} + \frac{d}{4\pi} \left(\frac{C_d^2}{y^{d-2}} \right)^{1/d} R^{(d)} \right]. \quad (7.10)$$

with $h_{\mu\nu}$ being the metric of the boundary theory in d space-time dimensions, with an associated Ricci scalar $R^{(d)}$; y is the deformation parameter and the stress tensor is $\tilde{T}_{\mu\nu} = T_{\mu\nu} + \tilde{T}_{\mu\nu}^{\text{CT}}$ where $: :$ represents large- N normal ordering as described in [22], where CT denotes the counterterm contribution.

The authors associate the deformed theory (7.10) to Einstein gravity in (A)dS _{$d+1$} space at finite cutoff:

$$I_{\text{bulk}} = \frac{1}{16\pi G_N} \int_{\mathcal{M}} d^{d+1}x \sqrt{-g} \left(R^{(d+1)} + \frac{d(d-1)}{\ell^2} \eta \right) + \frac{1}{8\pi G_N} \int_{\partial\mathcal{M}} d^d x \sqrt{-h} (K + \text{counterterm}) , \quad (7.11)$$

where \mathcal{M} represents the spacetime manifold, G_N Newton's constant, $g_{\mu\nu}$ the bulk metric, $R^{(d+1)}$ the Ricci scalar, and K the mean curvature.

The authors find an associated (dimensionless) energy spectrum for the deformed theory, which takes the form

$$\mathcal{E}_y = \frac{d(d-1)}{2\pi y} \left[\sqrt{1 + \Omega^{2/(d-1)} (C_d y)^{2/d}} \Big|_{y^{(d-2)/d}} \mp \sqrt{\eta + \Omega^{2/(d-1)} (C_d y)^{2/d} - \frac{4\pi}{d(d-1)} y \mathcal{E}_0} \right] , \quad (7.12)$$

where C_d represents constants determined by the counterterms and \mathcal{E}_0 is the (dimensionless) energy spectrum of the seed theory. Using the available tools to repeat the analysis in this work in higher dimensional settings, it would be interesting to verify our findings on the stretched horizon, such as the hyperfast scrambling in the OTOCs and holographic entanglement entropy from the algebraic perspective in the higher dimensional settings. One difficulty is to identify a specific boundary theory in the dS _{$d+1$} case.

Acknowledgments

I thank Andrew Svesko, and Manus Visser for previous collaboration on [33], which partially motivated this work; to Gonçalo Araújo-Regado, Philipp A. Höhn, Francesco Sartini, Jiayue

Yang and Ming Zhang for collaboration in other works with related themes; to Takanori Anegawa, Andreas Blommaert, Klaas Parmentier, and Jiuci Xu for useful comments on an earlier version of the draft; and to Dio Anninos, Luis Apolo, Micha Berkooz, Arghya Chat-topadhyay, Victor Franken, Damián A. Galante, Eleanor Harris, Taishi Kawamoto, Simon Lin, Masamichi Miyaji, Sangjin Sin, Andrew Rolph, and Gopal Yadav for insightful discussions/comments. I also thank the organizers of the “V Siembra-HoLAGrav Young Frontiers Meeting”, the “Quantum Extreme Universe: Matter, Information and Gravity 2024” workshop in Okinawa Institute of Science and Technology Graduate University (OIST), “New Avenues in Quantum Many-body Physics and Holography” in Asia-Pacific Centre (APCTP) for Theoretical Physics, the “Young Researchers of Quantum Gravity” online seminars, “Strings 2025” in New York University Abu Dhabi; the “QISS 2025 Conference” in Vienna University, and “2025 East Asia Joint Workshop on Fields and Strings” in OIST where part of the work was presented in different formats; to the “XX Modave summer school” for allowing relevant discussions with other participants; and Rikkyo University for hospitality while this work was in finishing stages. SEAG acknowledges support from the APCTP, the Office of Scholarships and the QISS consortium for travel support; as well as partial support by the FWO Research Project G0H9318N and the inter-university project iBOF/21/084 when this project started. SEAG is supported by the Okinawa Institute of Science and Technology Graduate University. This work was made possible through the support of the WOST, WithOut SpaceTime project (<https://withoutspacetime.org>), supported by Grant ID# 63683 from the John Templeton Foundation (JTF), and ID#62312 grant from the JTF, as part of the ‘The Quantum Information Structure of Spacetime’ Project (QISS), as well as Grant ID# 62423 from the JTF. The opinions expressed in this work are those of the author(s) and do not necessarily reflect the views of the John Templeton Foundation.

A Notation

Acronyms

- ADM: Arnowitt–Deser–Misner.
- (A)dS: (Anti-)de Sitter.
- AGH: Almheiri-Goel-Hu
- ASC: Al-Salam Chihara.
- BTZ: Bañados-Teitelboim-Zanelli.
- BH: Bekenstein-Hawking.
- BY: Brown-York.
- CFT: Conformal field theory.
- CV: Complexity=volume.
- (DS)SYK: (Double-scaled) Sachdev-Ye-Kitaev
- ETW: End-Of-The-World
- GH: Gibbons-Hawking.

- HH: Hartle–Hawking
- IR: Infrared
- JT: Jackiw–Teitelboim
- OTOC: Out-of-time-order correlations.
- QFT: Quantum field theory
- SC: Square correlators.
- RT: Ryu–Takayanagi.
- WKB: Wentzel–Kramers–Brillouin.
- UV: Ultraviolet
- WDW: Wheeler–DeWitt

Notation

- $F(r)$ (2.30): Blackening factor.
- $G(\Phi_B)$ (2.1): Boundary counterterm, where $\Phi_B (\equiv r_B)$ denotes the dilaton at the finite or asymptotic boundary.
- $h_{\mu\nu}$ (2.1): Induced metric.
- γ_{ab} (2.13): Boundary metric.
- $U(\Phi)$ (2.1): Dilaton potential.
- \mathcal{H} (2.10): Hamiltonian constraint.
- \tilde{T}_{ab} (2.7a): Bulk matter stress tensor.
- T_{ab} (2.12): Boundary matter stress tensor.
- \mathcal{O}_{Φ_B} (2.7b): Dilaton source.
- K, \mathcal{R} (2.1): Mean curvature, and Ricci scalar.
- $Z_y(\beta)$ (2.27a): Deformed partition function without matter.
- y and η (2.16): Deformation parameters.
- $E(\theta) = \frac{-2J \cos(\theta)}{\sqrt{\lambda(1-q)}}$ (2.24): DSSYK energy spectrum, where θ is a parametrization.
- E_y (2.15): Deformed energy spectrum.
- $\hat{H}_y = f_y(\hat{H})$ (2.17): Deformed Hamiltonian, with f_y a generic analytic function.
- $S(\theta)$ (2.24): Thermodynamic entropy.
- ρ_y (2.27b): Density of states in the deformed theory.
- β_y (2.25): Microcanonical inverse temperature.
- C_y (2.28): Heat capacity for fixed deformation parameter.
- N , and p (3.1): Number of Majorana fermions and all-to-all interactions respectively.
- $q \in [0, 1)$ (3.6): q -deformation parameter, the penalty factor associated to DSSYK Hamiltonian interceptions in chord diagrams.
- $\lambda = 2N/p^2 \equiv -\log q$: Parameter in the double-scaling limit (3.6).
- \mathcal{H}_m and $\mathcal{H}_{\text{chord}}$ (3.18): Chord space with m operators, and an all operator extension.
- $|n\rangle_y$ (3.29): Chord number basis built from the recursive function g_n .
- \hat{n}_y (3.38): Chord number operator associated to bulk lengths at finite cutoff.
- $\hat{h} \equiv -(\sqrt{\lambda(1-q)}/J)\hat{H}$ (3.29): Dimensionless Hamiltonian.

- $|K_n^{(\kappa)}\rangle$, $a_n^{(\kappa)}$, $b_n^{(\kappa)}$ (7.5): Krylov basis and Lanczos coefficients, where κ is a parametrization for one-particle states.
- \mathcal{C} (3.54): Cost function.
- \mathcal{C}_y (3.66): Proposal for state complexity based on the $|n\rangle_y$ basis.
- \mathcal{C}_S (3.59), a_n , b_n (3.56b): Krylov spread complexity in the zero-particle chord space.
- L_y (3.41): Expectation value of rescaled chord number in the HH state.
- t_y (3.44): Rescaled time appearing in the evaluation of L_y in the semiclassical limit (3.50) which reproduces the bulk length between the asymptotic boundaries of an AdS_2 black hole with finite distance boundary locations.
- $|n\rangle$, $|\theta\rangle$ (3.14): Chord number and energy basis for zero-particle states respectively.
- $|\Omega\rangle$ (3.8): Tracial (zero chord number) state.
- $[n]_q = \frac{1-q^n}{1-q}$ (3.9): q-deformed integer.
- $(a; q)_n = \prod_{k=0}^{n-1} (1 - aq^k)$ (3.15): q-Pochhammer symbol.
- $(a_1, a_2, \dots, a_m; q)_n = \prod_{i=1}^N (a_i; q)_n$ (3.15).
- $\tilde{\beta}_y = \frac{\pi}{J \sin \theta}$ (4.19): Fake temperature of the deformed theory.
- $H_n(x|q)$ (3.16): q-Hermite polynomials.
- $\mu(\theta)$ (3.17): Integration measure in the energy parametrization basis θ .
- $\hat{\mathcal{O}}_\Delta$ (3.4): Matter chord operator with conformal dimension Δ .
- \hat{n} (3.10): Chord number operator in the zero-particle sector \mathcal{H}_0 .
- dE/dE_y (2.26): Redshift factor.
- $\hat{L}_{\text{IR}} \equiv \lambda \hat{n} - 2 \log \lambda$, $\hat{L}_{\text{UV}} = i(\lambda \hat{n} - 2 \log \lambda)$ (3.72): Rescaled and rescaled chord number operator used in the UV and IR triple-scaling limits.
- \hat{H}_{IR} (3.73a) and \hat{H}_{UV} (3.73b): Chord Hamiltonian in the IR and UV triple-scaling limit.
- $\theta_{\text{IR}} \equiv \theta \ll 1$ and $\theta_{\text{UV}} \equiv \pi - \theta \ll 1$ (3.76): IR and UV triple-scaled energy parametrizations respectively.
- \hat{a}_i^\dagger and \hat{a}_i (3.22a): Non-Hermitian conjugate creation and annihilation operators in \mathcal{H}_m .
- $\tau_{L/R} = \frac{\beta_{L/R}}{2} + it_{L/R}$ (4.7): Complex-valued time, with $\beta_{L/R}$ the inverse temperature and $t_{L/R}$ as real time.
- $|\Psi_\Delta(\tau_L, \tau_R)\rangle$ (4.9b): Generalization of the HH state with matter chord insertions.
- $\tilde{\Delta} = \{\Delta_1, \dots, \Delta_m\}$ (3.19): Collective index of conformal dimensions.
- \hat{N} (3.20): Total chord number with one or more particle chords.
- $\hat{n}_i^> \equiv \sum_{j=i+1}^m (\hat{n}_j + \Delta_j)$ and $\hat{n}_i^< \equiv \sum_{j=0}^{i-1} (\hat{n}_j + \Delta_{j+1})$ (3.21).
- $\hat{H}_{L/R,y}$ (4.1): Deformed two-sided chord Hamiltonian
- G_{2m} (4.6): $(2m)$ -point correlation function.
- ℓ_* (4.21), ℓ_0 (4.32): Constants in the crossed-correlation function in the double-scaling and triple-scaling limits respectively.
- λ_L (6.13a): Lyapunov exponent.
- t_{sc} (4.26): Scrambling time.
- Tr (5.2): Type II algebraic trace.
- S (5.6): Entanglement entropy between double-scaled algebras given a chord state.

- $\mathcal{A}_{L/R} \equiv \{\hat{H}_{L/R}, \hat{\mathcal{O}}_{\Delta}^{L/R}\}$ (5.1): Double-scaled algebras.
- $\hat{\rho}$ (5.5): Reduced density matrix.
- r_{BH} (5.33), r_{CH} (6.2)): AdS black hole and cosmological horizon radial locations.
- $\Phi_{(\text{A})\text{dS}}$ (5.32): Dilaton Φ (2.1) in (dS) JT gravity.
- γ (5.32): RT surface.
- $\hat{\varphi}_i$ (D.4): Constraints selecting symmetry sectors in the chord Hilbert space.
- \hat{H}_{ASC} (D.1): ASC Hamiltonian. X, Y : Parameters in the ASC Hamiltonian.
- $\tilde{\mu}(\theta)$ (D.13): Integration measure factor in energy basis in systems with ETW branes.
- $Q_l(\cos \theta | X, Y; q)$ (D.11): ASC polynomials.
- $Z_{\text{ETW}}^{(y)}(\beta | X, Y)$ (D.19): Disk partition function with ETW brane.
- χ (C.4): Stretched horizon parameter.

B Evaluation of Time/Space-like Geodesics in (3.50)

In this appendix, we show that the geodesic length in (3.50) describes both spacelike and timelike geodesic lengths connecting the finite cutoff boundaries of AdS_2 black hole. We illustrate different configurations of the minimal length geodesics in Fig. 3.

We define geodesic lengths as

$$L = \int d\xi \mathcal{L}, \quad \mathcal{L} \equiv \sqrt{g_{\mu\nu} \dot{x}^\mu \dot{x}^\nu} = \sqrt{-f(r) \dot{v}_{L/R}^2 + 2\dot{v}_{L/R} \dot{r}}, \quad (\text{B.1})$$

where ξ is a general parameterization, $\dot{x} \equiv \frac{dx}{d\xi}$, the index L/R indicates left/right patches, while

$$ds^2 \equiv g_{\mu\nu} dx^\mu dx^\nu = -f(r) dv_{L/R}^2 + 2dv_{L/R} dr = -f(r) dt_{L/R}^2 + \frac{dr^2}{f(r)}. \quad (\text{B.2})$$

Here we will be interested in the blackening factor

$$f(r) = r^2 - r_{\text{BH}}^2, \quad (\text{B.3})$$

although, we keep some expressions with $f(r)$ general unless otherwise specified.

There is a conserved charge

$$P = \frac{\delta \mathcal{L}}{\delta \dot{v}_{L/R}} = \frac{-f(r) \dot{v}_{L/R} + \dot{r}}{\mathcal{L}}. \quad (\text{B.4})$$

Note that \mathcal{L} is a diffeomorphism invariant function, and it can be thus gauged fixed to any value. In the literature, one commonly chooses $\mathcal{L} = \pm 1$ where $+1$ corresponds to the spacelike case, and -1 to timelike [299]. However, given that \mathcal{L} is diffeomorphism invariant, it is not necessary to make any particular gauge-choice, all will give the same answer, and thus, regardless of the geodesic being spacelike or timelike, they will have the same functional expression, as we show below by combining \mathcal{L} in (B.2) with (B.4). This gives

$$\dot{r}^2 = (P^2 + f(r)) \mathcal{L}^2. \quad (\text{B.5})$$

Then, we can evaluate the geodesic length functional as

$$L = \int_{\xi_*}^{\xi_B} \mathcal{L} d\xi = \int_{r_*}^{r_B} \frac{dr}{\sqrt{P^2 + f(r)}} , \quad (\text{B.6})$$

where ξ_B is the parametrization of the boundary cutoff value where $r(\xi_B) = r_B$, and $r(\xi_*) = r_*$ represents the turning-point i.e. when $\dot{r} = 0$ in (B.5)

$$r_* = f^{-1}(-P^2) , \quad (\text{B.7})$$

where we are using that P is a conserved charge. Meanwhile, using the relation between t and v in (B.2), we have that $f(r)\dot{t}_{L/R} = -\mathcal{L}P$, i.e.

$$t = -2P \int_{\xi_*}^{\xi_B} \frac{dr}{f(r)\sqrt{P^2 + f(r)}} , \quad (\text{B.8})$$

where we are gauge-fixing $t_L = t_R \equiv t/2$.

We can now specialize in the cases of interest in the AdS_2 black hole (B.3), where (B.6) and (B.8) gives

$$L = 2\text{arccosh}\frac{r_B}{r_*} , \quad (\text{B.9a})$$

$$r_{\text{BH}}t = \arctan \frac{r_B\sqrt{r_*^2 - r_{\text{BH}}^2}}{r_{\text{BH}}\sqrt{r_B^2 - r_*^2}} . \quad (\text{B.9b})$$

Note that in the case of timelike geodesics ($r_* < r_B$) L (B.9a) becomes complex-valued, while t remains real-valued; while both L and t remain real-valued for spacelike geodesics, where $r_* > r_B$. One can simplify the above expressions by inverting $r_*(t)$ from (B.9a), plugging it back in (B.9b) and using hyperbolic trigonometric identities, which gives

$$L(t) = 2 \text{arcsinh}\left(\sqrt{\frac{r_B}{r_{\text{BH}}} - 1} \cosh(r_{\text{BH}}t)\right) . \quad (\text{B.10})$$

This indeed agrees with (3.50), where time includes the corresponding redshift factor. The geodesic length at finite cutoff has been previously noticed for the spacelike case in e.g. [37, 148].

C Sine Dilaton Gravity at Finite Cutoff

In this appendix, we explore the putative duality between the deformation of the DSSYK model and sine dilaton gravity at the disk topology level from finite cutoff holography. We are interested in the reality properties of the theory. Recent progress relating sine dilaton gravity and the DSSYK chord model can be found in [61, 66, 77, 85, 102, 106, 274] among others.

Sine dilaton gravity (in Euclidean-like signature) is described by (2.1) where the dilaton potential takes the form

$$U(\Phi) = 2 \sin \Phi . \quad (\text{C.1})$$

Since the metric and the dilaton in this model are complex-valued, the holographic dictionary implies that the deformation parameter in the deformed DSSYK model can be complex. Thus, we are particularly interested in the conditions for the energy spectrum of the deformed theory to be real, and its corresponding interpretation in the Lorentzian signature bulk spacetime. We also search for locations in the complex plane where the model has positive and near constant curvature, corresponding to first implementing the deformation and then taking the UV triple-scaling limit of the DSSYK model, which we applied in previous sections.

Reality Conditions One might be concerned that the Euclidean path integral of the theory might not converge when the energy spectrum is generically complex-valued. For instance, consider the partition

$$\int dE e^{S(E) - \beta E_y} , \quad (\text{C.2})$$

where $S(\theta) = S_0 - \frac{(\pi - 2\theta)^2}{\lambda}$ [183], S_0 is a constant; and $E(\theta)$ appears in (3.13). In principle, due to the complex spectrum (C.2) could diverge along the flow. After all, this is what happens for instance in JT gravity (and other set-ups) when the finite cutoff reaches the black hole horizon in the bulk, where instanton effects need to be taken into account [32]. However, the model that we study is UV finite, and (C.2) is well-defined even when the exponent of the integral is complex.³⁵

For the above reasons, we now analyze the constraints to recover a unitary energy spectrum (2.19) by considering that the radial bulk flow is described by the HJ equation (2.10). A diagram of the paths generating these flows is shown in Fig. 8,³⁶ where we choose as the final radial location for the boundary theories to be the black hole and cosmological stretched horizon in (C.10), and (C.11). To be more explicit about the trajectory, one can, for instance, use

$$\Phi_B = \pm \left(\frac{\pi}{2} + i \log(v + i \cos r_B) \right) , \quad (\text{C.3})$$

to connect $r = \frac{\pi}{2} + i\infty$ (the asymptotic boundary) with $r = r_B$. Meanwhile, the trajectory from the black hole horizon at $r = \theta$ and the boundary location $r = r_B$ can be expressed by

$$r = \theta\chi + (1 - \chi)r_B , \quad \chi \in [0, 1] . \quad (\text{C.4})$$

Here χ is a parametrization that allows us to interpolate between the location of the cos-

³⁵If the Hamiltonian has a complex-valued spectrum, one needs to include its left and right-eigenstates, in contrast to the past sections where we considered the eigenbasis for a Hermitian Hamiltonian.

³⁶As mentioned in Sec. 1, this is not the only possible way to place the seed theories; for instance, one could consider placing the boundaries in between the black hole region; or between several black hole and cosmological patches (similar to [158] in the extended SdS spacetime). Given that our focus is to probe the positive curvature region between the black hole and cosmological horizons, we leave these other possibilities for future directions (Sec. 7.1).

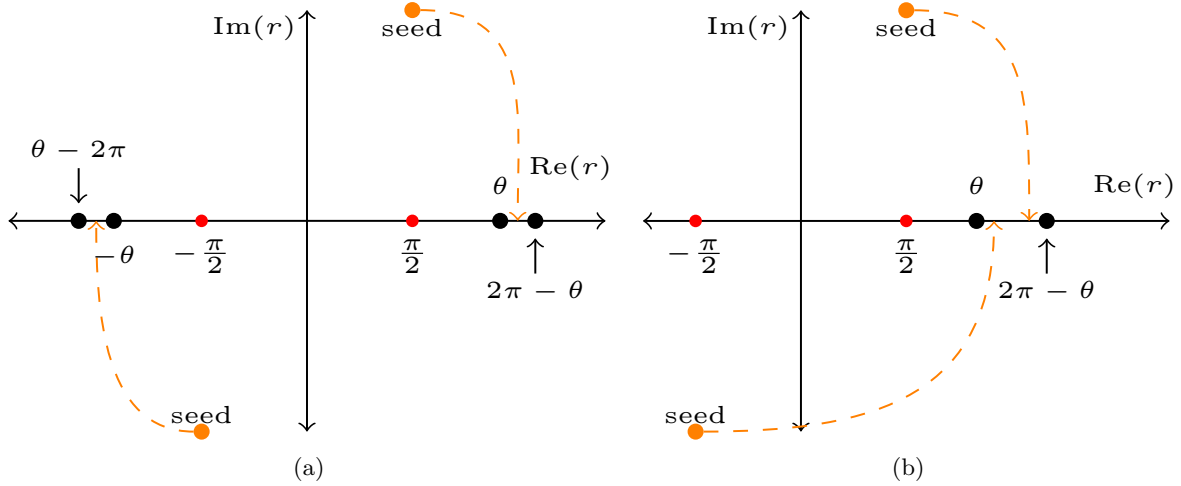


Figure 8. Moving the boundaries in the complex r -plane by T^2 deforming the DSSYK model according to the dictionary entry (2.16). The seed DSSYK model is initially located at $r \rightarrow \pm(\frac{\pi}{2} + i\infty)$, and it can be moved in the indicated contours (dashed orange lines) close to the horizons at (a) $r = \pm\theta$, and (b) $r = \theta, 2\pi - \theta$. Both ways can be used to probe the positive curvature regions between the black hole and cosmological horizons when $\theta \simeq \pi$ (see the respective Penrose diagrams in Fig. 10).

logical horizon (i.e. $\chi = 1$ in $r_B(\theta)$) and black hole horizon (i.e. $\chi = 0$ in $r_B(\theta)$)³⁷ in $r \in [-2\pi, 2\pi]$.

As we flow the boundary theory from $r_B \rightarrow \pm(\frac{\pi}{2} + i\infty)$ to a generic location $r_B \in \mathbb{C}$ in Fig. 8, the energy spectrum (2.20) becomes complex; however, one should notice that the metric (2.30) is also complex along this flow, and there is no Lorentzian interpretation where we could associate the complex energy spectrum, e.g. a dissipation process.³⁸ Once we reach the real line, we must study the locations where we can have a thermodynamic description of the system. First, notice that if we use the parametrization of the stretched horizon in (C.10) as the location of the boundary, we need to account for the functional dependence of $r_B(\theta)$. We can see that the blackening factor

$$F(r_B) = 2(\cos \theta - \cos(\theta + 2\chi(\pi - \theta))) , \quad (\text{C.5})$$

remains positive for $\chi \in [0, 1]$ and $\theta \in [0, \pi]$, as shown in Fig. 9.

In what follows, we search the reality constraints for unitary evolution in (2.19), meaning

³⁷ $\chi = 0$ implies $r_{B_1}^{(1)} = -\theta$, which is a 2π displacement (also referred to as a duplicate in [85]) of the cosmological horizon at $r = 2\pi - \theta$, so we will attribute it as a cosmological horizon as well.

³⁸In higher dimensions, a non-unitary energy spectrum with T^2 deformations has been studied in *Cauchy slice holography* [172, 173, 300]. The interpretation is that if one deforms a CFT living on the boundary of a Euclidean Cauchy slice, its energy spectrum is inherently complex. Once the deformation is large enough, the extrinsic curvature $K_{\alpha\beta}$ becomes timelike, resulting in a real energy spectrum, corresponding to a Lorentzian signature in the bulk.

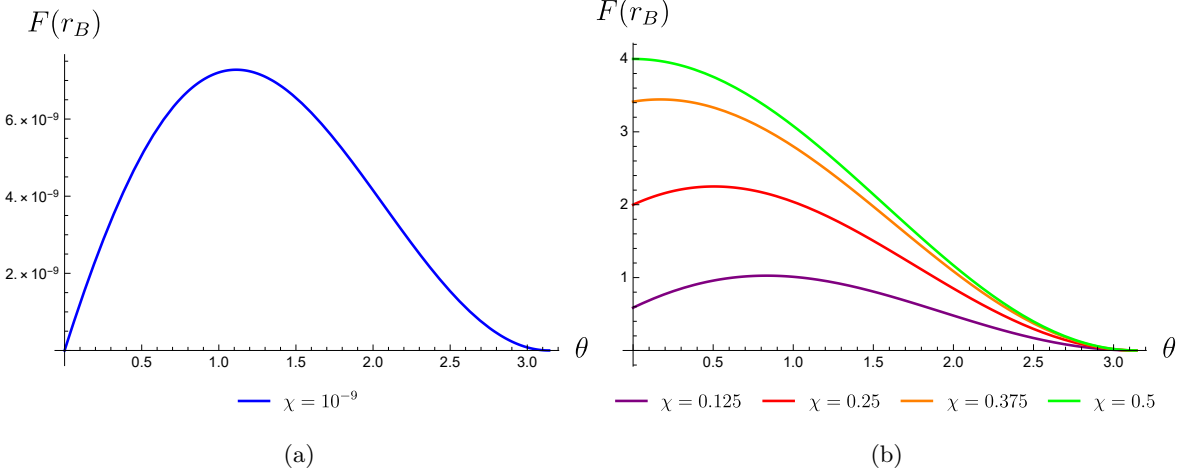


Figure 9. Evaluation of the blackening factor (C.5) at the stretched horizon defined in (C.10) in terms of the parameter χ (for the different values shown in the legend). It remains positive $\forall \theta \in [0, \pi]$.

that

$$1 \geq 2yE(\theta) . \quad (\text{C.6})$$

For concreteness, consider $\pi/2 \leq \theta \leq \pi$ so $E(\theta) \geq 0$. We identify different possibilities for the location r_B given the condition (C.6), as we list below.

- When $y > 0$,

$$\theta < r_B . \quad (\text{C.7})$$

However, in this case, the blackening factor in the metric (C.5) is $F(r_B) < 0$, so that r is a timelike coordinate and τ spacelike. Thus, the quantity (2.19) would be related to a conserved momentum instead of the energy spectrum of the system. One might attempt a double Wick rotation in $\tau \rightarrow it$ and $r \rightarrow i\tilde{r}$, but in that case, $F(r_B) \in \mathbb{C}$. For this reason, we will not consider this case. Notice that if we take $r_B = \pi + ir_0$ with $r_0 \in \mathbb{R}$, we will face a similar problem.

- When $y \leq 0$, there are no restrictions, and $F(r_B) > 0$. We can then perform the Wick rotation $\tau \rightarrow it$ in the metric (2.30) so that $E_y(\theta)$ in (2.19) along the real line indeed can be interpreted as conserved energy.

To draw the Penrose diagram, we consider the timelike Eddington–Finkelstein coordinates:

$$\begin{aligned} v &= t + r^*(r) , \quad u = t - r^*(r) , \\ r^*(r) &= \int_{r_0}^r \frac{dr'}{F(r')} = \frac{1}{2 \sin \theta} \log \left| \frac{\sin \frac{\theta-r}{2}}{\sin \frac{\theta+r}{2}} \right| , \end{aligned} \quad (\text{C.8})$$

where $r^*(r)$ is the tortoise coordinate, and we have chosen r_0 such that $r^*(r=0) = 0$. We then define Kruskal coordinates

$$U = e^u , \quad V = -e^{-v} , \quad (\text{C.9})$$

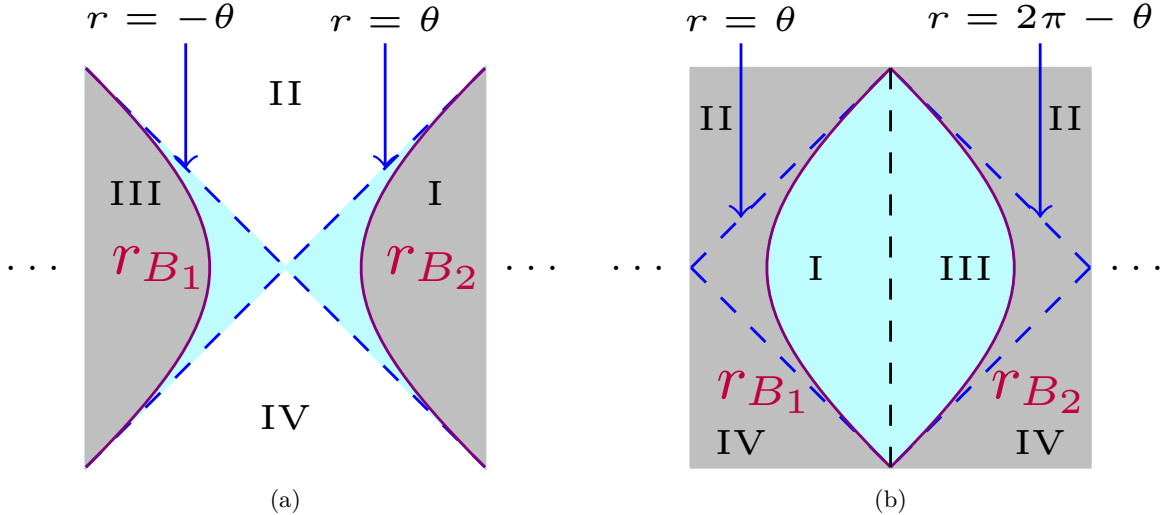


Figure 10. Penrose diagram in the \tilde{U}, \tilde{V} coordinates below (C.9) for all the quadrants (Roman numerals). The energy spectrum of the dual T^2 deformed dual DSSYK models (3.13) have a relative (a) $-$, and (b) $+$ sign. We have placed the Dirichlet boundaries (purple) in (a) (C.10), and (b) (C.11), corresponding to the respective bulk radial flow paths. The gray region represents the part of the bulk that has been cut out in the bulk interpretation of the T^2 deformation, and the light blue area between the stretched horizon and the black hole and cosmological horizons (dashed blue lines) represents the bulk positive curvature region (for $\theta \simeq \pi$). The dashed black line in (b) only serves to separate the respective quadrants, and the dots indicate the $2n\pi$ periodicity of the spacetime.

for the first quadrant of the Penrose diagram, Fig. 10, while $U = e^u, V = e^{-v}$ in the second; $U = -e^u, V = e^{-v}$ third; and $U = -e^u, V = -e^{-v}$ fourth. At last, we define compact coordinates $U = \tan \tilde{U}$ and $V = \tan \tilde{V}$ to generate the Penrose diagram. Notice that the location of the horizons is $UV = 0$, and the periodic nature of the diagram shares similarities with the (extended) full-reduction dS_2 spacetime (see e.g. [301–303]).

Probing the Bulk Interior We now probe the positive curvature region in Fig. 10 (and (8)) using two configurations for the *cosmological* and *black hole* stretched horizons where we move the boundaries into the locations:³⁹

$$r_{B_1}^{(1)} = r_B(-\theta), \quad r_{B_2}^{(1)} = r_B(\theta), \quad \text{where } r_B(\theta) = (1 - \chi)\theta + \chi(\theta - 2\pi), \quad (\text{C.10})$$

$$r_{B_1}^{(2)} = r_B(\theta), \quad r_{B_2}^{(2)} = r_B(2\pi - \theta). \quad (\text{C.11})$$

As seen from Fig. 10, by setting the boundary locations to be $r_B = r_{B_1}^{(1)}$, $r_B = r_{B_2}^{(1)}$ in (C.10), the deformed DSSYK model can be located at a very close distance with respect to the cosmological ($\chi \ll 1$) or black hole ($\chi \simeq 1$), where the bulk thermodynamics with respect

³⁹A similar definition as (C.10) was first proposed in [158] in the context of the extended Schwarzschild-de Sitter (SdS) black hole geometries. It allows us to generalize the notion of the stretched horizon in [1] for pure dS space to spacetimes with multiple horizons.

to the boundary locations can be associated with the respective black hole or cosmological horizon.

By taking $\theta \simeq \pi$, the region $r \in [-2\pi + \theta, -\theta] \cup [\theta, 2\pi - \theta]$ has a positive and near constant scalar curvature $\mathcal{R} \simeq 2$ [61]. This is equivalent to implementing the UV triple-scaling limit after performing the $T^2(+\Lambda_1)$ deformation in the DSSYK model, which we applied in previous sections, albeit without assuming the correspondence between sine dilaton gravity and the DSSYK model. The procedure in this section allows us to be more explicitly explore the structure of the finite cutoff holography with a concrete bulk dual for the range of its energy spectrum of the DSSYK model.

D Deformations with End-Of-The-World Branes and Wormholes

As emphasized in the main text, Hamiltonian deformations modifies the energy and microcanonical temperature of the chord auxiliary theory while keeping the thermodynamic entropy the same. There is a complementary situation where the thermodynamic entropy with respect to the seed theory is modified while keeping the same energy spectrum. This occurs when applying constraints in the chord Hilbert space of the DSSYK model [69], which lead to ETW brane Hamiltonians in sine dilaton gravity [87]. In this section, we implement Hamiltonian deformations in the DSSYK model with matter in constrained chord states, resulting in the ETW branes in the finite cutoff bulk theory,⁴⁰ and we develop its connection with the double trumpet geometry in the DSSYK model and sine dilaton gravity [55, 87, 106, 287, 289, 290, 305, 306].

Outline We begin App. D.1 with a brief review of the ETW brane Hamiltonian from implementing Hilbert space constraints used in Dirac quantization (see [307, 308] for reviews). In App. D.2 we investigate the semiclassical partition function based on the Al-Salam Chihara (ASC) polynomials and two-point correlation functions with the ETW branes in the DSSYK model. In App. D.3 we extend the results for trumpet geometries resulting from a Hilbert space trace.

D.1 Matter Chords as ETW Branes from Deformed DSSYK Model

We investigate Hamiltonian deformations in the ETW brane Hamiltonian for the DSSYK model, first studied by [309], and followed up by [55, 69, 87, 306], among others. The seed theory of interest is described by the ASC Hamiltonian [69, 87, 106],

$$\hat{H}_{\text{ASC}} = \frac{J}{\sqrt{\lambda(1-q)}} \left(e^{-i\hat{P}} + (X+Y)e^{-\hat{\ell}} + (1-XYe^{-\hat{\ell}})e^{i\hat{P}}(1-e^{-\hat{\ell}}) \right), \quad (\text{D.1})$$

which can be derived by imposing constraints in the chord Hilbert space (3.19) with one particle insertion [69], and X and Y are constant parameters which depend on the specific

⁴⁰There are higher dimensional analogs, such as in double holography [304] where both effects result in intricate dynamical observables.

symmetry sector under consideration. Details about the gauging procedure which fixes X and Y in (D.1) can be found in [69], which we briefly summarize below for completeness. We begin considering the one particle chord state

$$\mathcal{H}_1 = \text{span}\{|\Delta; n_L, n_R\rangle\} , \quad (\text{D.2})$$

and the corresponding one-particle chord Hamiltonian (3.23). We may study symmetry sectors in the one-particle chord space to recover the basis $|H_n\rangle$ (D.7) and the ASC Hamiltonian (D.1). By a symmetry we refer to a transformation, \hat{U}_i , that leaves a set of states $\{|\psi\rangle\}$ in the system invariant i.e.

$$\hat{U}_i : |\psi\rangle \rightarrow |\psi\rangle . \quad (\text{D.3})$$

One generates the physical Hilbert space $\mathcal{H}_{\text{phys}}$ from the set of states $\{|\psi\rangle\}$ that are annihilated by the generator of the corresponding transformation (D.3), which we refer to as constraints $\hat{\varphi}_i$:

$$\hat{\varphi}_i |\psi\rangle = 0 , \quad |\psi\rangle \in \mathcal{H}_{\text{phys}} , \quad (\text{D.4})$$

There are different constraints leading to a basis where the one-particle Hamiltonian adopts the ASC form (D.1), which we summarize below (based on [69]):

One-sided branes Let $\hat{\varphi}_A := \hat{P}_L - \delta \hat{\hat{P}}_L$, $\hat{\varphi}_B := \hat{\ell}_L - \hat{\hat{\ell}}_L/\delta$, where δ is a constant so that $[\hat{\ell}_L, \hat{P}_L] = [\hat{\hat{\ell}}_L, \hat{\hat{P}}_L]$ is invariant under the constraint, even under the limit $\delta \rightarrow 0$; and let $\hat{P}_R = \hat{P}$, $\hat{\ell}_R = \hat{\ell}$. By applying these constraints to build the physical Hilbert space, one of the chord Hamiltonians (3.23) takes the representation

$$\hat{H}_R \rightarrow \hat{H}_{\text{ASC}}^{(1s)} = \frac{J}{\sqrt{\lambda(1-q)}} \left(e^{-i\hat{P}} + e^{i\hat{P}} (1 - e^{-\hat{\ell}}) + q^\Delta e^{-\hat{\ell}} \right) , \quad (\text{D.5})$$

while \hat{H}_L becomes constant.

Two-sided branes We can take $\hat{\varphi}_A^{(L/R)} := \hat{P}_{L/R} - \hat{P}$, $\hat{\varphi}_B^{(L/R)} := \hat{\ell}_{L/R} - \hat{\ell}$, so that the total Hamiltonian can be represented as

$$\hat{H}_L + \hat{H}_R \rightarrow \hat{H}_{\text{ASC}}^{(2s)} = \frac{2J}{\sqrt{\lambda(1-q)}} \left(e^{-i\hat{P}} + (1 + q^{\Delta+1} e^{-\hat{\ell}}) e^{i\hat{P}} (1 - e^{-\hat{\ell}}) \right) . \quad (\text{D.6})$$

States in the Constrained Chord space Next, we summarize the general structure of the states $\{|H_n\rangle\}$ in the Hilbert space where the ASC Hamiltonian (D.1) acts. The operators in the Hamiltonian above can be represented by

$$e^{-i\hat{P}} |H_n\rangle = |H_{n+1}\rangle , \quad e^{i\hat{P}} |H_n\rangle = |H_{n-1}\rangle , \quad \hat{n} |H_n\rangle = n |H_n\rangle . \quad (\text{D.7})$$

We can also look for a basis that diagonalizes the Hamiltonian

$$\hat{H}_{\text{ASC}} |\theta\rangle = E(\theta) |\theta\rangle , \quad (\text{D.8})$$

where $\theta \in [0, \pi]$ is a parametrization of the energy. Next, by acting with the basis $\{|H_n\rangle\}$ and $|\theta\rangle$ in (D.1), we recover

$$2 \cos \theta |Q_n\rangle = Q_{n+1} + (X + Y)q^n Q_n + (1 - XYq^{n-1})(1 - q^n)Q_{n-1} , \quad (\text{D.9})$$

where

$$\langle \theta | H_n \rangle := Q_n(\cos \theta |X, Y; q) , \quad E(\theta) = \frac{2J}{\sqrt{\lambda(1-q)}} \cos \theta , \quad \theta \in [0, \pi] . \quad (\text{D.10})$$

By requiring $Q_0 = 1$ and $Q_{-1} = 0$, the recurrence relation is solved by the ASC polynomials [310], which are given by

$$Q_l(\cos \theta |X, Y; q) = \frac{(XY; q)_l}{X^l} \sum_{n=0}^{\infty} \frac{(q^{-l}, X e^{\pm i\theta}; q)_n}{(XY, q; q)_n} q^n . \quad (\text{D.11})$$

The ASC polynomials satisfy the relation

$$\int_0^\pi d\theta \tilde{\mu}(\theta) \frac{Q_{l_1}(\cos \theta, X, Y|q)}{\sqrt{(q, XY; q)_{l_1}}} \frac{Q_{l_2}(\cos \theta, X, Y|q)}{\sqrt{(q, XY; q)_{l_2}}} = \delta_{l_1, l_2} , \quad (\text{D.12})$$

where

$$\tilde{\mu}(\theta) = \mu(\theta) \frac{(XY; q)_\infty}{(X e^{\pm i\theta}; Y e^{\pm i\theta}; q)_\infty} , \quad \int_0^\pi d\theta \tilde{\mu}(\theta) |\theta\rangle \langle \theta| = \mathbb{1} . \quad (\text{D.13})$$

The integration measure can be expressed as

$$\tilde{\mu}(\theta) = \mu(\theta) \langle \Omega | B_{X,Y} \rangle , \quad (\text{D.14})$$

where $|B_{X,Y}\rangle$ refers to the ETW brane state, a generalized q-coherent state, which is defined to satisfy the relation:⁴¹

$$(\hat{a} + XY\hat{a}^\dagger) |B_{X,Y}\rangle \equiv \frac{X + Y}{\sqrt{1-q}} |B_{X,Y}\rangle , \quad (\text{D.15})$$

with \hat{a} , \hat{a}^\dagger being annihilation and creation operators in the zero-particle chord space in (3.11)

$$\hat{a} \equiv e^{i\hat{p}} \sqrt{[\hat{n}]}_q , \quad \hat{a}^\dagger \equiv \sqrt{[\hat{n}]}_q e^{-i\hat{p}} . \quad (\text{D.16})$$

D.2 Deformed ETW Brane theory

We consider deforming the Hamiltonian after gauging the corresponding symmetry sector in the chord Hilbert space⁴²

$$\begin{aligned} \text{Gauging: } & \hat{H}_{L/R} \rightarrow \hat{H}_{\text{ASC}} , \\ \text{Deforming: } & \hat{H}_{\text{ASC}} \rightarrow \hat{H}_{\text{ASC}}^y = f_y(\hat{H}_{\text{ASC}}) , \end{aligned} \quad (\text{D.18})$$

⁴¹See e.g. [306]; the dictionary relating our notation with theirs is $\beta_{\text{There}} = (1-q)/((1+X)(1+Y))$ and $\delta_{\text{There}} = -(1-q)XY/((1+X)(1+Y))$. The relation between X, Y to ETW brane parameters in sine dilaton gravity has been explored in [69].

⁴²Alternatively, one may deform the chord Hamiltonian with matter (4.1)

$$\hat{H}_{L/R} \rightarrow \hat{H}_{L/R, y} = f(\hat{H}_{L/R}) , \quad (\text{D.17})$$

and then gauge the corresponding symmetry $\hat{H}_{L/R, y} \rightarrow \hat{H}_{\text{ASC}}$.

with f_y being the Hamiltonian deformation function (4.13a).

Now, we evaluate the disk partition function with the ETW brane based on (D.18), which is

$$Z_{\text{ETW}}^{(y)}(\beta|X, Y) \equiv \langle H_0 | e^{-\beta \hat{H}_{\text{ASC}}^y} | H_0 \rangle = \int_0^\pi d\theta \frac{(XY, e^{\pm 2i\theta}; q)_\infty e^{-\beta E_y(\theta)}}{2\pi(X e^{\pm i\theta}, Y e^{\pm i\theta}; q)_\infty} \\ \stackrel{\lambda \rightarrow 0}{=} \int_0^\pi d\theta \sqrt{\frac{8\pi(1-XY) \sin^2 \theta}{\lambda(1+X^2-2X \cos \theta)(1+Y^2-2Y \cos \theta)}} e^{S_\Delta(\theta)-\beta E_y(\theta)}, \quad (\text{D.19})$$

where the thermodynamic entropy, and microcanonical temperature are respectively

$$S_{\text{ETW},y}(\theta) = S(\theta) + \frac{1}{\lambda} \left(\text{Li}_2(XY) + \frac{\pi^2}{6} + \sum_{\varepsilon=\pm} \left(\text{Li}_2(X e^{i\varepsilon\theta}) + \text{Li}_2(Y e^{i\varepsilon\theta}) \right) \right), \\ \frac{dS_{\text{ETW},y}}{dE_y} = \frac{dE}{dE_y} \left(\beta(\theta) + \frac{i}{2J \sin \theta} \log \frac{(1-X e^{i\theta})(1-Y e^{i\theta})}{(1-X e^{-i\theta})(1-Y e^{-i\theta})} \right). \quad (\text{D.20})$$

and $S(\theta)$, $\beta(\theta)$ appear in (2.24), (2.25).

Applying the constraints in the crossed four-point function (4.19), the corresponding two-point function in presence of an ETW brane contains redshift factor in (4.16) gives

$$G_2^{(\text{ETW})}(t, \theta) \equiv \frac{\langle H_0 | e^{-\left(\frac{\beta(\theta)}{2}-it\right) \hat{H}_{\text{ASC}}^y} q^{\Delta \hat{n}} e^{-\left(\frac{\beta(\theta)}{2}+it\right) \hat{H}_{\text{ASC}}^y} | H_0 \rangle}{\langle H_0 | e^{-\beta(\theta) \hat{H}_{\text{ASC}}^y} | H_0 \rangle} \\ \stackrel{\lambda \rightarrow 0}{=} \left(\frac{2 \sin^2 \theta}{1 + XY - (X + Y) \cos \theta + \cosh\left(\frac{2\pi t}{\beta_y(\theta)}\right) \prod_{X_i=X, Y} \sqrt{X_i^2 - 2X_i \cos \theta + 1}} \right)^\Delta, \quad (\text{D.21})$$

with $\tilde{\beta}_y$ in (4.19). We display the behavior of the two-point function in Fig. 11.

From the figure, it can be seen that, as expected in finite cutoff holography [18], once the deformation parameter approaches its critical value y_0 (3.77), it will experience an enhanced decay rate, while it leads to an enhanced rate of growth for crossed-four point functions (4.22). This is also expected since the growth of OTOCs is bounded by that of the two-point correlation functions [122]. We discussed its implications in the IR and UV regimes in Sec. 4.3 and 6.3 respectively.

D.3 Euclidean Wormholes from the DSSYK Model

Now, we proceed by studying the trumpet geometries from the deformed theory perspective.

The ASC Hamiltonian (D.1) can be used to evaluate partition functions and correlation functions for Euclidean wormhole geometries [69, 87]. In this subsection, we will study how the thermodynamics and correlation functions in the ETW brane and Euclidean wormhole theories are modified after implementing the deformations in the corresponding Hamiltonians.

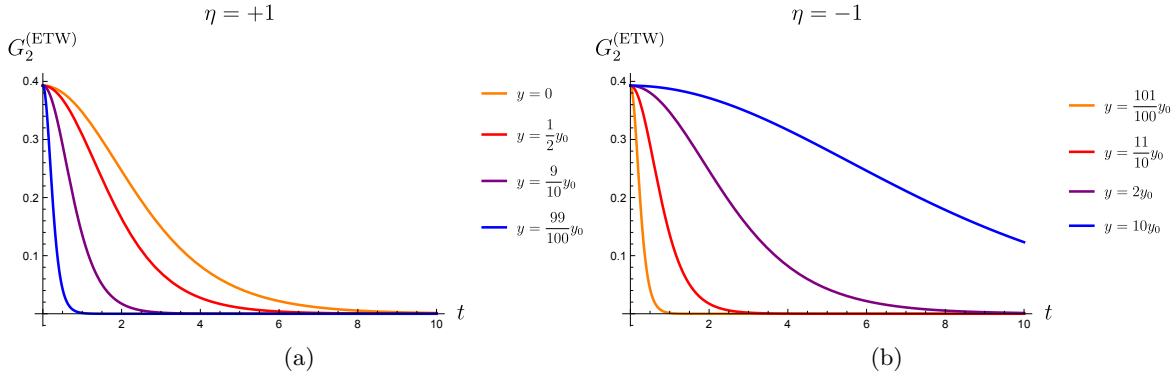


Figure 11. Two-point correlation function (D.21) resulting from (a) T^2 deformation ($\eta = +1$) and (b) $T^2 + \Lambda_1$ deformation ($\eta = -1$). We display the enhanced rate of decay of the two-point function as the deformation parameter approaches the critical value y_0 (3.77) due to the redshift factor in the fake temperature (4.19). The parameters in the plot are $\lambda = 10^{-4}$, $J = 1$, $\lambda\Delta_1 = 1$ $\Delta_2 = 1$ and $\theta = 3\pi/4$ for one-sided ETW brane ($X + Y = q^\Delta$ and $XY = 0$ in (D.21)). Similar results are recovered for two-sided ETW branes.

T^2 deformations in JT gravity with non-trivial topology have been recently considered in [32, 250]. This motivates us to look at the corresponding wormhole partition functions

$$\begin{aligned} Z_{X,Y}^{(y)}(\beta) &\equiv \text{Tr} \left[e^{-\beta \hat{H}_{\text{ASC}}^y} \right] \\ &= \sum_{n=0}^{\infty} \int_0^{\pi} d\theta \, \tilde{\mu}(\theta) e^{-\beta E_y(\theta)} \langle H_n | \theta \rangle \langle \theta | H_n \rangle = \int d\theta \, \delta(\theta - \theta) e^{-\beta E_y(\theta)}, \end{aligned} \quad (\text{D.22})$$

where we implemented $\mathbb{1} = \sum_{n=0}^{\infty} |H_n\rangle \langle H_n|$. This partition function can be visualized as cutting in half a partition function and gluing its ends, resulting in a trumpet geometry, as we illustrate in Fig. 12. While the above correlation function is singular, one can define a regularized version, which is the trumpet partition function

$$\begin{aligned} Z_b^{(y)}(\beta) &\equiv \frac{1}{2\pi i} \oint \frac{dY}{Y^{(b+1)}} Z_{X,Y}^{(y)}(\beta) \\ &= \frac{2}{(q;q)_\infty} \sum_{n=0}^{\infty} \int_0^{\pi} d\theta \, 2 \cos(b\theta) e^{-\beta E_y(\theta)} q^{nb}, \end{aligned} \quad (\text{D.23})$$

which we display in Fig. 13.

The above expression is not simple to evaluate; it would be interesting to use the techniques of resurgence, similar to the JT gravity analog [32], to complete the evaluation. One would be able to use the result to determine the double trumpet amplitude in the bulk

$$Z_b^{(y)}(\beta) := \frac{(q;q)_\infty (1 - q^b)}{2} \tilde{Z}_b^{(y)}(\beta), \quad (\text{D.24})$$

and construct a partition function for multiple-boundaries Euclidean wormhole [69]

$$Z_y(\beta_1, \beta_2, \dots, \beta_m) := \sum_{b=1}^{\infty} b Z_b^{(y)}(\beta_1) Z_b^{(y)}(\beta_2) \cdots Z_b^{(y)}(\beta_m), \quad (\text{D.25})$$

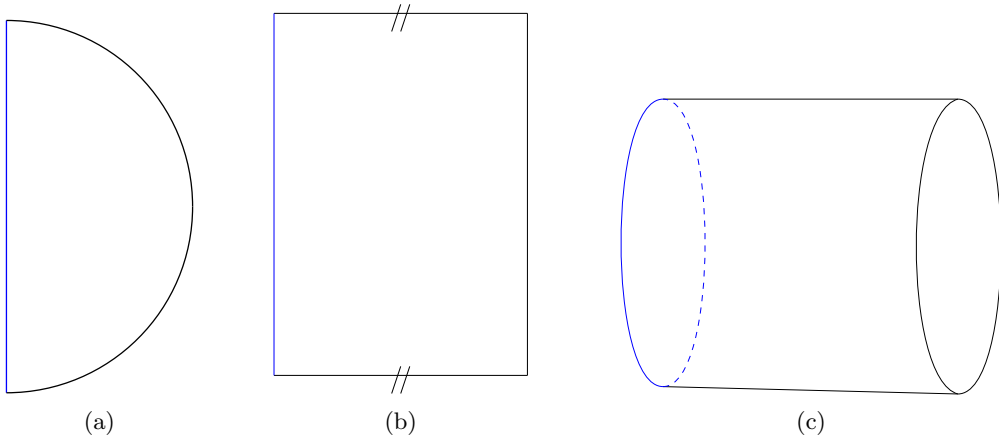


Figure 12. Construction of the cylinder partition function (D.22). (a) The disk topology with an ETW brane (blue solid line) is mapped to (b) a rectangle. The identification between two of its edges represents the Hilbert space trace $\sum \langle H_n | \cdots | H_n \rangle$, which is glued together to form (c) the cylinder, which leads to the divergence in (D.22).

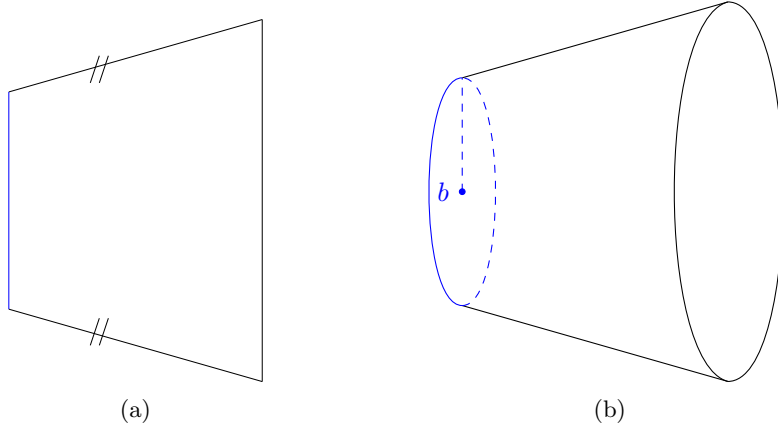


Figure 13. The regularization implemented in the trumpet partition function (D.23) can be seen as reducing the length of the ETW brane (solid blue line) in Fig. 12 to a finite size and gluing appropriately the edges of the plane.

which reduces to a double-trumpet partition function in the $m = 2$ case. Relevant evaluations for this quantity in finite cutoff holography have recently appeared in [37].

We move on to a unnormalized thermal two-point correlation function in the trumpet

configuration, given by gauging symmetries and implement the Hilbert space trace as

$$\begin{aligned}
G_{\text{cylinder}}^{(\Delta_w)} &= \text{Tr} \left(\hat{\mathcal{O}}_{\Delta_w} e^{-\beta_1 \hat{H}_{\text{ASC}}^y} \hat{\mathcal{O}}_{\Delta_w} e^{-\beta_2 \hat{H}_{\text{ASC}}^y} \right) \\
&= \sum_{n=0}^{\infty} \langle H_n | e^{-\beta_2 \hat{H}_{\text{ASC}}^y} q^{\Delta_w \hat{n}} e^{-\beta_1 \hat{H}_{\text{ASC}}^y} | H_n \rangle \\
&= \sum_{n=0}^{\infty} \left(\int_0^{\pi} \prod_{i=1}^2 d\theta_i \frac{(XY, e^{\pm 2i\theta_i}; q)_{\infty}}{(X e^{\pm i\theta_i}, Y e^{\pm i\theta_i}; q)_{\infty}} e^{-\beta_i E_y(\theta_i)} \right) \langle H_n | \theta_1 \rangle \langle \theta_1 | q^{\Delta_w \hat{n}} | \theta_2 \rangle \langle \theta_2 | H_n \rangle .
\end{aligned} \tag{D.26}$$

Using (D.12) and defining $\beta = \beta_1 + \beta_2$ one recovers

$$G_{\text{cylinder}}^{(\Delta_w)}(\beta) = \int_0^{\pi} d\theta \tilde{\mu}(\theta) \langle \theta | q^{\Delta_w \hat{n}} | \theta \rangle e^{-\beta E(\theta)}, \tag{D.27}$$

where $\tilde{\mu}(\theta) = \frac{(XY, e^{\pm 2i\theta}; q)_{\infty}}{(X e^{\pm i\theta}, Y e^{\pm i\theta}; q)_{\infty}}$. This can be further simplified by inserting the identity $\sum_n |K_n^y\rangle \langle K_n^y| = \mathbb{1}$ and $\hat{n}_y |K_n^y\rangle = n_y |K_n^y\rangle$, resulting into

$$G_{\text{cylinder}}^{(\Delta_w)}(\beta) = \sum_{n=0}^{\infty} q^{\Delta_w n} \int_0^{\pi} d\theta \tilde{\mu}(\theta) |\langle \theta | K_n \rangle|^2 e^{-\beta E_y(\theta)}. \tag{D.28}$$

It might be possible to simplify the result using saddle point method where the semiclassical solution takes the form

$$G_{\text{cylinder}}^{(\Delta_w)}(\beta) \underset{\lambda \rightarrow 0}{=} \sum_{n=0}^{\infty} q^{\Delta_w n} e^{-\beta E_y(\theta_{\text{s.p.}})} \int_0^{\pi} d\theta \tilde{\mu}(\theta) |\langle \theta | K_n \rangle|^2, \tag{D.29}$$

where $\theta_{\text{s.p.}}$ denotes the corresponding saddle-point solution. This would result from a one-loop quantum corrected two-point correlation function similar to [69]. However, the details of the evaluation are outside the scope of the current investigation, and we leave them for future directions.

E Almheiri-Goel-Hu Model

In this appendix, we explore the previous results on T^2 deformation for the model developed in [176], which is significantly simpler than the one in the main text. We are interested in its thermodynamic properties, correlation functions, and the evolution of the chord number.

Motivated by the high-temperature limit of the DSSYK model, [176] studied the limit where its ensemble averaged theory can be approximately described by

$$\hat{H} = \frac{1}{\sqrt{2}} (\hat{a} + \hat{a}^{\dagger}), \tag{E.1}$$

with \hat{a}^{\dagger} , \hat{a} being creation and annihilation operators of the harmonic oscillator.

By matching correlation functions with bulk geodesics, a (non-local like) dilaton gravity theory dual to the model was proposed by [176], which is described by (2.1) with a potential

$$U(\Phi) = \frac{96\pi^2}{\beta^4} (1 - \Phi)^{-1/3}, \tag{E.2}$$

where we have performed an overall rescaling in the dilaton field with respect to [176] to make it dimensionless as in the ansatz (2.30), where we now have

$$ds^2 = F(r)d\tau^2 + \frac{dr^2}{F(r)} , \quad F(r) = \frac{\beta^4}{4}(1 - (1 - r)^{2/3}) . \quad (\text{E.3})$$

We assume a counter term of the type (2.2) to keep the on-shell action finite at the asymptotic boundary, located at $\Phi_B = 1$.

Thermodynamics In the rest of the section, we investigate T^2 deformations of the AGH model (E.1). We can directly use the thermodynamic results in [176], where

$$\beta = -2E , \quad S = -E^2 , \quad (\text{E.4})$$

to derive the boundary inverse temperature of the T^2 deformed model in terms of energy spectrum (3.13) and thermodynamic entropy (2.24)

$$\beta_y = E_y(-2 + yE_y)(1 - 2yE_y) = -2\sqrt{|S|}\sqrt{1 - 2y\sqrt{|S|}} . \quad (\text{E.5})$$

where the interpretation of the negative thermodynamic entropy is similar to [176], namely a relative entropy with respect to the maximal mixed state of the model. Similarly the density of states (2.27b) and the heat capacity (2.28) can be calculated as:

$$\rho_y = e^S\sqrt{1 - 2y\sqrt{-S}} , \quad (\text{E.6})$$

$$C_y = \frac{(\beta_y)^2}{2 - 3yE_y(2 - yE_y)} . \quad (\text{E.7})$$

Moreover, using the dictionary entry (2.16), we can modify the boundary location from $r = 1$ to the stretched horizon (i.e. nearby $r = 0$). Note that since the potential (E.2) is obtained by matching geodesic lengths with two-point correlations, its boundary temperature will be modified $\beta \rightarrow \beta_y$, and the corresponding deformation parameter (2.16) is expressed as

$$y = \frac{2\kappa^2(\beta_y)^4}{144\pi^2(1 - r_B)^{2/3}} . \quad (\text{E.8})$$

Note that the boundary temperature dependence is consistent with the non-local nature of the theory proposed by [176], and the factor $2\kappa^2$ in (2.1) used to derive the flow equation (2.15) replaces $-\lambda$, which was required for the gravitational energy and entropy in (2.31) to match those of the DSSYK model (3.13, 2.24). For the same reason, given the normalization in (E.1), we will also set $2\kappa^2 = \sqrt{2}$.

The evaluation of (3.4) for different boundary locations $r_B \in (0, 1)$ (i.e. between the event horizon and the asymptotic boundary) used in (E.8) are shown in Fig. 14. We emphasize that, for the purposes of the analysis, we are allowing the boundary inverse temperature to have a finite range of values, even though the connection with the DSSYK model occurs at

high temperatures. As seen, for instance, in Fig. 14 the energy spectrum is real only under a finite range of boundary temperatures, which do not include strictly infinite boundary temperatures. Note also, there is a non-zero inverse boundary temperature where S and C_y will diverge, independent of the stretched horizon limit. Meanwhile, the fact that the model has a negative thermodynamic entropy (E.4, E.5) implies that the growth of the density of states is suppressed in the regime where S diverges. At last, is seen in Fig. 14 (d) that the system is manifestly thermodynamically stable for generic values of r_B . Further discussion of the results is provided at the end of this subsection.

Correlation functions We now proceed to evaluate the T^2 deformed thermal two-point correlation function of matter operators \hat{V} with conformal dimension Δ_V and the corresponding OTOCs (see Fig. 15), to compare with our previous findings in Sec. 4.2 for the sine dilaton gravity model. Note that while in Sec. 4.2 we evaluate the correlation functions through saddle point methods in the $\lambda \rightarrow 0$ regime, since we are viewing the (E.1) as a model by its own; which is not necessarily related to the DSSYK model at $\lambda \rightarrow 0$ regime, we will perform the evaluation without taking limits. In general, these evaluations become intricate due to the $E_y(E)$ factor (except in the $y = 0$ case). Fortunately for us, we notice that we can approach a stretched horizon regime for $y \ll 1$ in (E.8) when $\beta_y \rightarrow 0$, which is the high temperature regime where the AGH model is expected to describe the DSSYK model. For this reason, in this subsection, we will be mostly interested in a perturbative y expansion, in contrast to most of the work, which is at the non-perturbative order in y .

Similar to the identity (3.18), we can express the (Euclidean-signature) evolution of the oscillator number basis $\{|n\rangle\}$ (i.e. where $\hat{a}^\dagger \hat{a} |n\rangle = n |n\rangle$) of (E.1) in terms of a complete basis of energy eigenstates $|E\rangle$:

$$\left\langle \phi_n^{(y)}(\tau) \right\rangle \equiv e^{-\hat{H}_y \tau} |n\rangle = \int_{-\infty}^{\infty} dE \frac{e^{-E^2 - E_y(E)\tau} H_n(E)}{\sqrt{n! 2^n \pi}} |E\rangle , \quad (\text{E.9})$$

where $H_n(E) = \langle E | n \rangle$ is the n -th order Hermite polynomial. Note that

$$\left\langle \Omega \left| \phi_n^{(y=0)}(\tau) \right. \right\rangle = \frac{(-\tau)^n}{\sqrt{n! 2^n}} e^{\tau^2/4} . \quad (\text{E.10})$$

Two-point correlation functions We can then evaluate the correlation function in Fig. 15 (a) as:

$$\begin{aligned} \frac{1}{Z_y(\beta)} \langle \Omega | e^{-\tau_2 \hat{H}_y} \hat{V} e^{-\tau_1 \hat{H}_y} \hat{V} | \Omega \rangle &= \langle \Omega | e^{-\tau_2 \hat{H}_y} e^{-\Delta_V \hat{n}} e^{-\tau_1 \hat{H}_y} | \Omega \rangle \\ &= \sum_n \left\langle \phi_n^{(y)}(\tau_2) \right| \Omega \left\langle \Omega \left| \phi_n^{(y)}(\tau_1) \right. \right\rangle e^{-\Delta_V n} . \end{aligned} \quad (\text{E.11})$$

To perform the evaluation above, we will first consider a perturbative y expansion, where $E_y(E) = E + \frac{y}{2} E^2 + \mathcal{O}(y^2)$. In this case (E.11) with (E.10) can be expressed as

$$\begin{aligned} &\langle \Omega | e^{-\tau_2 \hat{H}_y} \hat{V} e^{-\tau_1 \hat{H}_y} \hat{V} | \Omega \rangle \\ &= \exp \left[\frac{1}{4} \sum_{i=1}^2 \tau_i^2 \left(1 - \frac{y}{2} \tau_i \right) + \frac{e^{-\Delta_V}}{2} \tau_1 \tau_2 \left(1 - \frac{y}{4} (\tau_1 + \tau_2) \right) + \mathcal{O}(y^2) \right] . \end{aligned} \quad (\text{E.12})$$

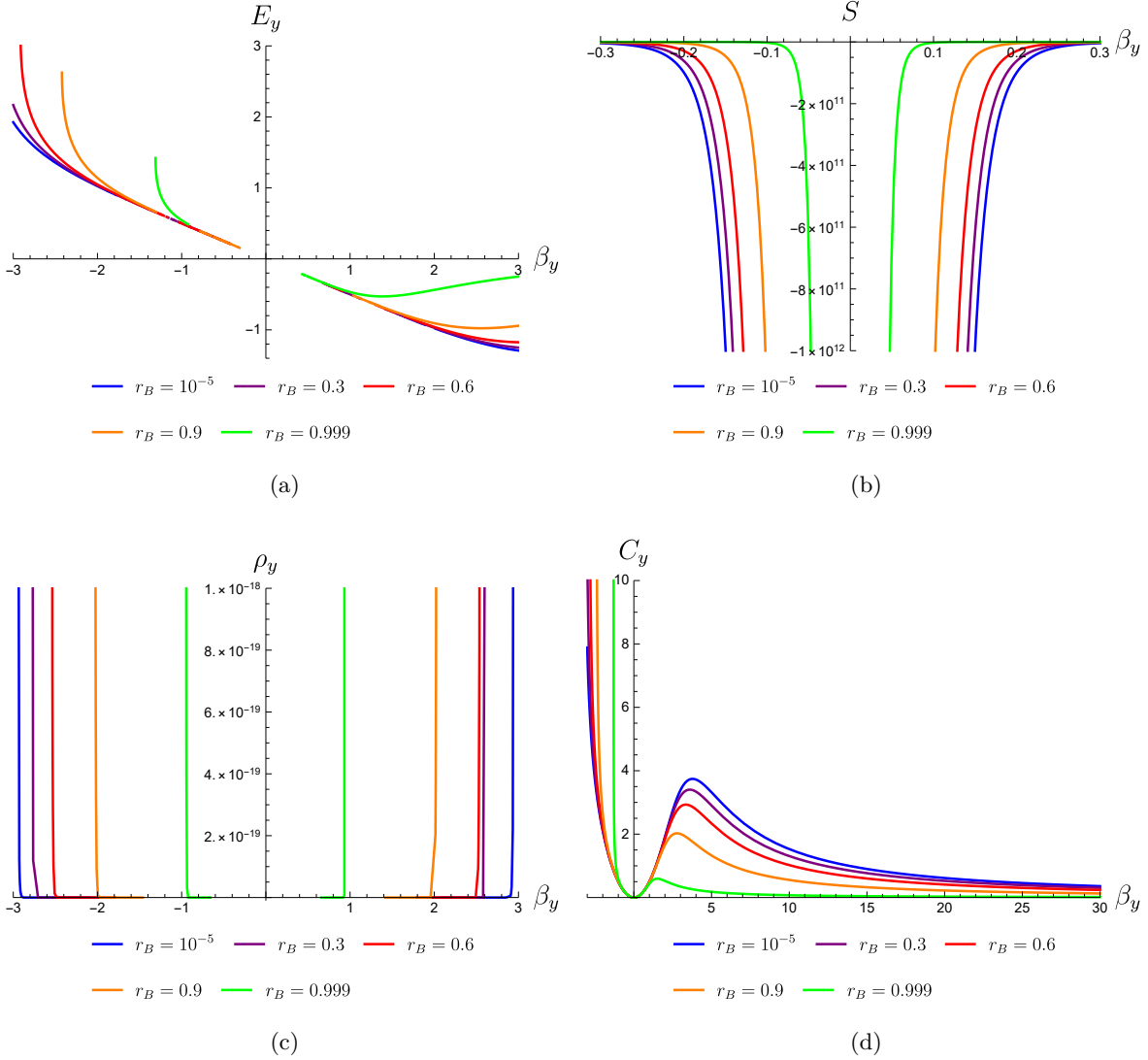


Figure 14. (a) T^2 deformed ($\eta = +1$ (2.16)) energy spectrum, (b) thermodynamic entropy, (c) density of states, and (d) heat capacity of the AGH model [176], using the map (E.8) for different values of the boundary location r_B .

We can then see the expansion $E_y(E) = E + \frac{y}{2}E^2 + \mathcal{O}(y^2)$ as the first order correction in y in the exponent of the correlation function.

To make the analytic continuation to Lorentzian signature, we take

$$\tau_1 = it + \frac{\beta}{2}, \quad \tau_2 = -it + \frac{\beta}{2}, \quad (\text{E.13})$$

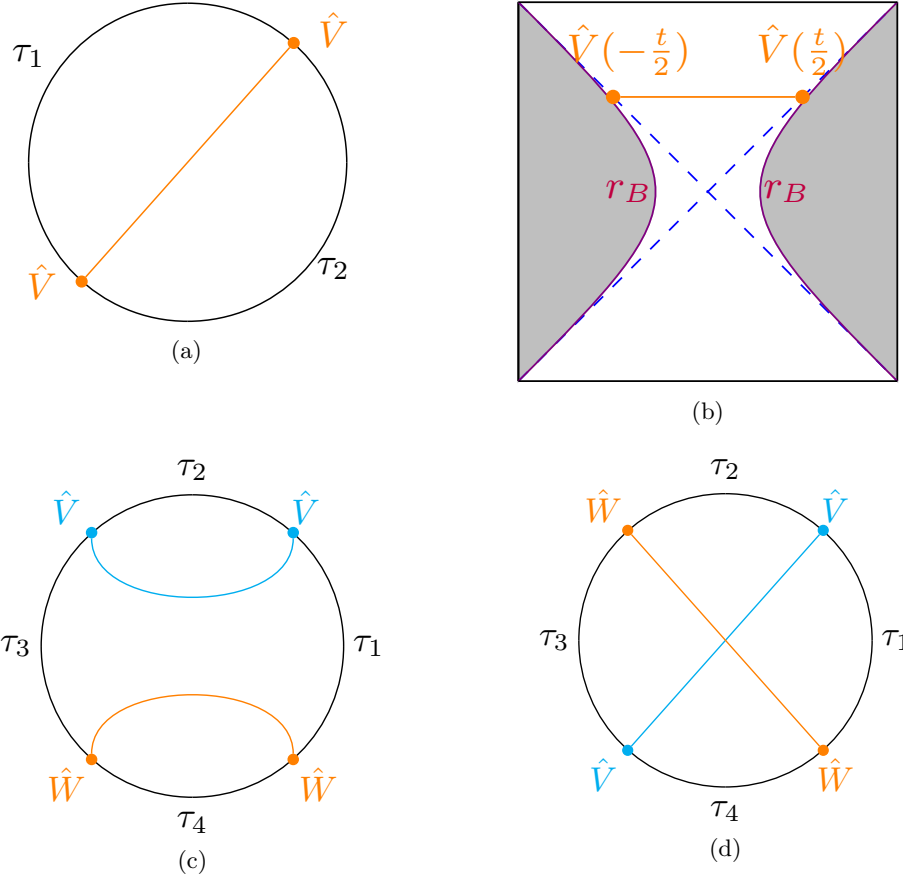


Figure 15. Correlation functions of matter field operators \hat{V} (cyan) and \hat{W} (orange) (with conformal dimension Δ_V and Δ_W respectively) in the AGH model: two-point correlation functions from the (a) boundary and (b) the Lorentzian-signature bulk perspectives (where $\hat{V}(t) = e^{i\hat{H}t}\hat{V}(0)e^{-i\hat{H}t}$); as well as the (c) uncrossed, and (d) crossed four-point correlation functions.

so that the normalized two-point correlation function becomes

$$\begin{aligned} \mathcal{G}(t) &\equiv \frac{\langle \Omega | e^{-(\beta/2-it)\hat{H}_y} \hat{V} e^{-(\beta/2+it)\hat{H}_y} \hat{V} | \Omega \rangle}{\langle \Omega | e^{-\frac{\beta}{2}\hat{H}_y} \hat{V} e^{-\frac{\beta}{2}\hat{H}_y} \hat{V} | \Omega \rangle} \\ &= \exp \left(-\frac{t^2}{2} \left((1 - e^{-\Delta_V}) + \frac{y\beta}{8} (1 - e^{-2\Delta_V}) + \mathcal{O}(y^2) \right) \right). \end{aligned} \quad (\text{E.14})$$

We can then see the time dependence of the function in (E.14) remains unaffected, at least at the first order perturbation in y . Moreover, it follows from (E.14) that the temperature, defined as the rate of decay of the thermal correlation functions, is a fixed value

$$\tilde{\beta}_y = 2\pi\alpha, \quad \text{where} \quad \alpha = \left(1 - e^{-\Delta_V} + \frac{y\beta}{8} (1 - e^{-2\Delta_V}) \right) + \mathcal{O}(y^2). \quad (\text{E.15})$$

where we notice that even without the perturbation, the system's temperature and decay of correlation functions are different in general, as in the DSSYK case [85].

Performing the calculation (E.11) at the non-perturbative level in the deformation parameter y is in general complicated; however, to get the answer at any order in perturbation theory, we can carry out the expansion

$$e^{-E_y(E)\tau} = e^{-E\tau} \sum_{m=0}^{\infty} \tilde{c}_m(\tau, y) E^m, \quad (\text{E.16})$$

where $\tilde{c}_m(\tau, y)$ is a polynomial function in τ and y , which can be explicitly evaluated for the 1D T^2 deformation (3.13). One can then use (E.10) to evaluate:

$$\int_{-\infty}^{\infty} dE E^m e^{-\tau E - E^2} H_n(E) = \left(-\frac{d}{d\tau} \right)^m \left[\frac{(-\tau)^n}{\sqrt{\pi}} e^{\tau^2/4} \right], \quad (\text{E.17})$$

and obtain (E.11) at any order in perturbation theory with respect to y . However, for the purpose of later computations, we find more convenient to evaluate the y -corrections in the exponent (E.14), instead of the correlation function itself. Lastly, to find the full, non-perturbative answer of (E.11), one might also attempt a numerical evaluation of the integral corresponding to $\langle \Omega | \phi_n(\tau) \rangle$ from (E.9) and performing the sum in n . However, we do not persuade this direction, since perturbation theory is a good approximation to study the stretched horizon regime analytically in the $\beta \rightarrow 0$ regime.

Squared correlators We would like to evaluate the Lorentzian-signature squared correlator defined by

$$\text{SC}_y(t) \equiv \frac{1}{Z_y(\beta)} \langle \Omega | e^{-\beta \hat{H}_y} \left[\hat{W}(0), e^{i\hat{H}_y t} \hat{V}(0) e^{-i\hat{H}_y t} \right]^2 | \Omega \rangle, \quad (\text{E.18})$$

for the operators \hat{V} and \hat{W} with conformal dimensions Δ_V and Δ_W respectively. The diagrammatic techniques for the calculation have been worked out in App. B of [176], so we state the results after incorporating the T^2 deformation at order $\mathcal{O}(y)$, which essentially amounts to the modification $\tau_i \rightarrow \tau_i(1 - \frac{y}{4}\tau_i)$ inside the overall exponent. This allows us to express the uncrossed four-point correlation function (Fig. 15 (c)):

$$\begin{aligned} & \log \left(\langle \Omega | e^{-\hat{H}_y \tau_4} V e^{-\hat{H}_y \tau_3} W e^{-\hat{H}_y \tau_2} W e^{-\hat{H}_y \tau_1} V | \Omega \rangle \right) \\ &= \sum_{i=1}^4 \tau_i^2 + (\tau_2 + \tau_4) \left(\frac{e^{-\Delta_V}}{2} \tau_3 + \frac{e^{-\Delta_W}}{2} \tau_1 \right) + \frac{e^{-\Delta_V - \Delta_W}}{2} \tau_2 \tau_4 + \frac{\tau_1 \tau_3}{2} \\ & \quad - \frac{y}{8} \left(e^{-\Delta_V} \tau_1 (\tau_2 (\tau_2 + \tau_3) + \tau_4 (\tau_1 + \tau_4)) + (\tau_1^3 + \tau_3^3 + (\tau_2 + \tau_4) (\tau_2^2 + \tau_4^2)) \right) \\ & \quad - \frac{y}{8} e^{-\Delta_V - \Delta_W} \tau_3 \left(\tau_1 (\tau_1 + \tau_3) + (\tau_2 (\tau_1 + \tau_2) + \tau_4 (\tau_3 + \tau_4)) e^{\Delta_V} \right) + \mathcal{O}(y^2), \end{aligned} \quad (\text{E.19})$$

as well as the crossed four-point correlation function (Fig. 15 (d)):

$$\begin{aligned}
& \langle \Omega | e^{-\hat{H}_y \tau_4} V e^{-\hat{H}_y \tau_3} W e^{-\hat{H}_y \tau_2} V e^{-\hat{H}_y \tau_1} W | \Omega \rangle \\
&= \sum_{i=1}^4 \tau_i^2 + \frac{e^{-\Delta_V}}{2} (\tau_1 \tau_2 + \tau_3 \tau_4) + \frac{e^{-\Delta_W}}{2} (\tau_2 \tau_3 + \tau_1 \tau_4) + \frac{e^{-\Delta_V - \Delta_W}}{2} (\tau_1 \tau_3 + \tau_2 \tau_4) - \Delta_V \Delta_W \\
&\quad - \frac{y}{8} \left((\tau_2 \tau_3 (\tau_2 + \tau_3) + \tau_1 \tau_4 (\tau_1 + \tau_4)) e^{-\Delta_W} + (\tau_1 \tau_2 (\tau_1 + \tau_2) + \tau_3 \tau_4 (\tau_3 + \tau_4)) e^{-\Delta_V} \right) \\
&\quad + \frac{y}{8} \left(\sum_{i=1}^4 \tau_i^3 - (\tau_1 \tau_3 (\tau_1 + \tau_3) + \tau_2 \tau_4 (\tau_2 + \tau_4)) e^{-\Delta_V - \Delta_W} \right) + \mathcal{O}(y^2) . \tag{E.20}
\end{aligned}$$

Combining (E.19) and (E.20), and choosing the corresponding value for τ_i , we can evaluate (E.18) at order $\mathcal{O}(y)$ as

$$\begin{aligned}
\text{SC}_y(t) &\equiv \frac{1}{Z_y(\beta)} \langle \Omega | e^{-\hat{H}_y \beta} [W(0), V(t)]^2 | \Omega \rangle \Big|_{\mathcal{O}(y)} \tag{E.21} \\
&= e^{\frac{1}{16}(-8t^2 - \beta t e^{-\Delta_V - \Delta_W} (e^{\Delta_V} (y(t(iy + \beta y - 4) - 2i\beta) + 8i) + 2i(\beta y - 4)) - \beta t e^{-\Delta_V} (y(t(iy + \beta y - 4) - 2i\beta) + 8i) - 2i\beta t (3\beta y - 4) - 2\beta^3 y)} \\
&\quad \left(e^{\frac{1}{32}t^2 e^{-\Delta_V - \Delta_W}} (e^{\Delta_V} (y(2t^2 y + \beta(\beta y - 12)) + 32) + e^{\Delta_W} (y(2t^2 y + \beta(\beta y - 12)) + 32) + y(2t^2 y + \beta(12 - \beta y)) + 4(3\beta y - 4) e^{\Delta_V + \Delta_W} - 32) \right. \\
&\quad \left(1 + e^{\frac{1}{8}i\beta t e^{-\Delta_V - \Delta_W}} (2e^{\Delta_W} (e^{\Delta_V} (3\beta y - 4) + \beta(-y) + 4) - 2(e^{\Delta_V} - 1)(\beta y - 4)) \right) - \left(e^{\frac{1}{16}\beta t^2 y e^{-\Delta_V}} (\beta y - 4) \right. \\
&\quad \left. + e^{\frac{1}{16}\beta t^2 y e^{-\Delta_W}} (\beta y - 4) \right) e^{\frac{1}{32}t e^{-\Delta_V}} (e^{\Delta_V} (16t + 4i\beta(3\beta y - 4)) - 4i\beta(e^{\Delta_V} - 1)e^{-\Delta_W} (\beta y - 4) - 4i\beta(\beta y - 4)) .
\end{aligned}$$

Note that the $y \rightarrow 0$ limit reproduces one of the results in [176]

$$\begin{aligned}
\text{SC}_{y \rightarrow 0}(t) &\equiv \frac{1}{Z(\beta)} \langle \Omega | e^{-\beta \hat{H}} [\hat{W}(0), \hat{V}(t)]^2 | \Omega \rangle \tag{E.22} \\
&= -2 + 2 \cos \left(\left(1 - e^{-\Delta_V} \right) \left(1 - e^{-\Delta_W} \right) \frac{\beta t}{2} \right) e^{-(1 - e^{-\Delta_V})(1 - e^{-\Delta_W})(1 + t^2)} .
\end{aligned}$$

A comparison between the evolution of (E.21) and (E.22) is shown in Fig. 16 in terms of a ratio

$$\tilde{r} \equiv \text{Re}((\text{SC}(t) - \text{SC}_{\text{AGH}}(t)) / \text{SC}_{\text{AGH}}(t)) \tag{E.23}$$

We notice that the increased rate of growth of the OTOC (E.21) is not significantly impacted in the stretched horizon limit $y \rightarrow \frac{2\sqrt{2}\beta^4}{144\pi^2}$. Moreover, one can evaluate the scrambling time in this model, defined as the time scale associated to the exponential decay in (E.21); one finds that it is not significantly different from the one corresponding to (E.22) $t_{\text{sc}} = \left((1 - e^{-\Delta_V})(1 - e^{-\Delta_W}) \right)^{-1/2}$, given that it is a $\mathcal{O}(1)$ value that remains below the time scale where SC and SC_{AGH} start differing substantially (see Fig. 16).

Chord number Meanwhile, the chord number, defined in (3.59), for the state $e^{-\hat{H}_y \tau} |\Omega\rangle$ can be evaluated directly from (E.11) by taking a derivative in Δ_V and taking the limit

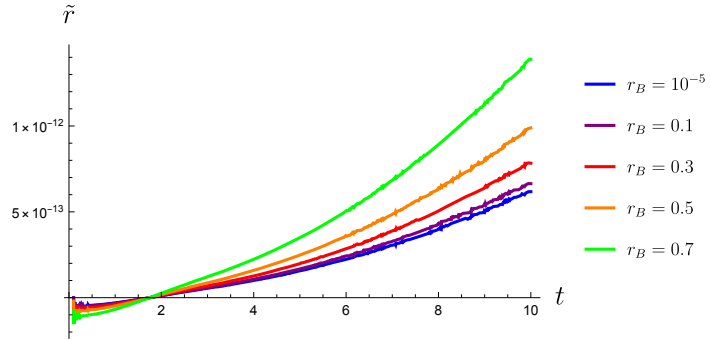


Figure 16. Real part of the relative difference between the out of time order correlator with the perturbative y correction (E.21) and the one in the seed theory (E.22), in terms of the ratio \tilde{r} (E.23), and the radial cutoff r_B related to the deformation parameter through (E.8) as it approaches the horizon located at $r = 0$. We have taken $\Delta_V = 1$, $\Delta_W = 2$, $\beta = 0.01$, and different values of r_B . The numerical noise is produced by the relative phases in (E.21)

$\Delta_V \rightarrow 0$ (see e.g. [66]). This results in:

$$\begin{aligned} \frac{1}{Z} \langle \Omega | e^{-\hat{H}_y \tau_2} \hat{n} e^{-\hat{H}_y \tau_1} | \Omega \rangle &= \sum_{n=0}^{\infty} n \langle \phi_n^{(y)}(\tau_2) | \Omega \rangle \langle \Omega | \phi_n^{(y)}(\tau_1) \rangle \\ &= \frac{\tau_1 \tau_2}{2} (1 + 2y(\tau_1 + \tau_2)) . \end{aligned} \quad (\text{E.24})$$

Its analytic continuation to Lorentzian signature (E.13) allows to evaluate the spread complexity as

$$\langle n \rangle_y(t) = \frac{\langle \Omega | e^{-\hat{H}_y \tau_2} \hat{n} e^{-\hat{H}_y \tau_1} | \Omega \rangle}{\langle \Omega | e^{-\hat{H}_y \beta y} | \Omega \rangle} = \frac{1}{2} t^2 (1 + 2y\beta) + \mathcal{O}(y^2) . \quad (\text{E.25})$$

Note that the rate of growth of $\langle n \rangle_y(t)$ is faster when $y \rightarrow \frac{\sqrt{2}\beta^4}{144\pi^2}$ (i.e. the stretched horizon limit), similar to our results in the main text. In contrast the thermodynamic properties in Fig. 14 do not display an enhancement in the same limit. Perhaps this is expected since [1] associates the enhanced growth of observables in time with a hyperfast scrambling of information, which would not be exhibited in generic integrable models, such as this one. It had been noticed in [85] that the model proposed in [176] displays quite different observables with respect to the $\lambda \rightarrow 0$ in the sine dilaton gravity model, which should still describe DSSYK model at high temperatures, without the Heisenberg algebra limit (E.1). Therefore, our findings in this section compared to Secs. 2.3, add more contrast between these two approaches, as different observables display rather different behaviors in the stretched horizon limit.

F First Law of Thermodynamics at Finite Cutoff

Motivated by recent developments on black hole thermodynamics in finite cutoff holography [311], we study the first law of thermodynamics in the deformed DSSYK model based on our

results in Sec. 2.

We specialize in $T^2(+\Lambda_1)$ deformations, where the relevant deformation parameter $\eta = \pm 1$ (2.16). Let us use the semiclassical entropy in (2.24) to express the energy spectrum in (2.20) ($\eta = +1$) for the T^2 deformation and (2.20) ($\eta = -1$) for the $T^2 + \Lambda_1$ deformation. This results in

$$E_y^\eta = \frac{1}{y} \left(1 - \eta \sqrt{\eta \left(1 - \frac{2y}{\pi V \sqrt{\lambda(1-q)}} \sin \sqrt{\frac{\lambda(S_0-S)}{2}} \right)} \right), \quad (\text{F.1})$$

where we have defined $V \equiv \frac{2\pi}{J}$. By taking variations with respect to each of the parameters in (F.1) we can write the extended first law for the deformed DSSYK model as

$$dE_y = P_y dV + (\beta_y)^{-1} dS + \tilde{\mu}_y d\lambda + \nu_y dy, \quad (\text{F.2})$$

$$P_y \equiv - \frac{\eta^2 \sin \left(\frac{\sqrt{\lambda(S_0-S)}}{\sqrt{2}} \right)}{\pi V^2 \sqrt{\lambda(1-q)} \sqrt{\eta - \frac{2\eta y \sin \left(\frac{\sqrt{\lambda(S_0-S)}}{\sqrt{2}} \right)}{\pi V \sqrt{\lambda(1-q)}}}}, \quad (\text{F.3})$$

$$\tilde{\mu}_y \equiv - \frac{\eta^2 q \left(\frac{2(\lambda q - q + 1) \sqrt{\lambda(S_0-S)} \sin \left(\frac{\sqrt{\lambda(S_0-S)}}{\sqrt{2}} \right)}{q} + \frac{\sqrt{2}\lambda(1-q)(S-S_0) \cos \left(\frac{\sqrt{\lambda(S_0-S)}}{\sqrt{2}} \right)}{q} \right)}{4\sqrt{\pi}\lambda(1-q)V\sqrt{\lambda(1-q)}\sqrt{\lambda(S_0-S)}\sqrt{\pi\eta - \frac{2\eta y \sin \left(\frac{\sqrt{\lambda(S_0-S)}}{\sqrt{2}} \right)}{V\sqrt{\lambda(1-q)}}}}, \quad (\text{F.4})$$

$$\nu_y \equiv \frac{\eta \sqrt{\eta - \frac{2\eta y \sin \left(\frac{\sqrt{\lambda(S_0-S)}}{\sqrt{2}} \right)}{\pi V \sqrt{\lambda(1-q)}} - 1}}{y^2} + \frac{\eta^2 \sin \left(\frac{\sqrt{\lambda(S_0-S)}}{\sqrt{2}} \right)}{\pi V y \sqrt{\lambda(1-q)} \sqrt{\eta - \frac{2\eta y \sin \left(\frac{\sqrt{\lambda(S_0-S)}}{\sqrt{2}} \right)}{\pi V \sqrt{\lambda(1-q)}}}}, \quad (\text{F.5})$$

while β_y appears in (2.25). One may interpret $\tilde{\mu}_y$ as a chemical potential associated with variations in the parameter λ (3.6) for a fixed deformation parameter y ; and similarly for ν_y , where y is allowed to vary instead. Note that the notation suggests that V and P_y are analogs to thermodynamic volumes and pressures in the bulk [311]; however, they are viewed only as definitions of different combinations of parameters from our analysis.

References

- [1] L. Susskind, *Entanglement and Chaos in De Sitter Space Holography: An SYK Example*, *JHAP* **1** (2021) 1 [[2109.14104](#)].
- [2] J.M. Maldacena, *The Large N limit of superconformal field theories and supergravity*, *Adv. Theor. Math. Phys.* **2** (1998) 231 [[hep-th/9711200](#)].

- [3] A.B. Zamolodchikov, *Expectation value of composite field T anti- T in two-dimensional quantum field theory*, [hep-th/0401146](#).
- [4] S. Dubovsky, R. Flauger and V. Gorbenko, *Solving the Simplest Theory of Quantum Gravity*, *JHEP* **09** (2012) 133 [[1205.6805](#)].
- [5] S. Dubovsky, V. Gorbenko and M. Mirbabayi, *Natural Tuning: Towards A Proof of Concept*, *JHEP* **09** (2013) 045 [[1305.6939](#)].
- [6] E. Tsolakidis, *Massive gravity generalization of $T\bar{T}$ deformations*, *JHEP* **09** (2024) 167 [[2405.07967](#)].
- [7] F.A. Smirnov and A.B. Zamolodchikov, *On space of integrable quantum field theories*, *Nucl. Phys. B* **915** (2017) 363 [[1608.05499](#)].
- [8] S. Dubovsky, V. Gorbenko and M. Mirbabayi, *Asymptotic fragility, near AdS_2 holography and $T\bar{T}$* , *JHEP* **09** (2017) 136 [[1706.06604](#)].
- [9] S. Dubovsky, V. Gorbenko and G. Hernández-Chifflet, *$T\bar{T}$ partition function from topological gravity*, *JHEP* **09** (2018) 158 [[1805.07386](#)].
- [10] J. Cardy, *The $T\bar{T}$ deformation of quantum field theory as random geometry*, *JHEP* **10** (2018) 186 [[1801.06895](#)].
- [11] O. Aharony, S. Datta, A. Giveon, Y. Jiang and D. Kutasov, *Modular invariance and uniqueness of $T\bar{T}$ deformed CFT*, *JHEP* **01** (2019) 086 [[1808.02492](#)].
- [12] A.J. Tolley, *$T\bar{T}$ deformations, massive gravity and non-critical strings*, *JHEP* **06** (2020) 050 [[1911.06142](#)].
- [13] Y. Jiang, *A pedagogical review on solvable irrelevant deformations of 2D quantum field theory*, *Commun. Theor. Phys.* **73** (2021) 057201 [[1904.13376](#)].
- [14] S. He, Y. Li, H. Ouyang and Y. Sun, *$T\bar{T}$ Deformation: Introduction and Some Recent Advances*, [2503.09997](#).
- [15] M. Guica, *From black holes to solvable irrelevant deformations and back*, [2512.23620](#).
- [16] A. Giveon, N. Itzhaki and D. Kutasov, *$T\bar{T}$ and LST*, *JHEP* **07** (2017) 122 [[1701.05576](#)].
- [17] L. Apolo, S. Detournay and W. Song, *TsT , $T\bar{T}$ and black strings*, *JHEP* **06** (2020) 109 [[1911.12359](#)].
- [18] L. McGough, M. Mezei and H. Verlinde, *Moving the CFT into the bulk with $T\bar{T}$* , *JHEP* **04** (2018) 010 [[1611.03470](#)].
- [19] L. Apolo, P.-X. Hao, W.-X. Lai and W. Song, *Extremal surfaces in glue-on $AdS/T\bar{T}$ holography*, *JHEP* **01** (2024) 054 [[2311.04883](#)].
- [20] L. Apolo, P.-X. Hao, W.-X. Lai and W. Song, *Glue-on AdS holography for $T\bar{T}$ -deformed CFTs*, *JHEP* **06** (2023) 117 [[2303.04836](#)].
- [21] M. Guica and R. Monten, *$T\bar{T}$ and the mirage of a bulk cutoff*, *SciPost Phys.* **10** (2021) 024 [[1906.11251](#)].
- [22] T. Hartman, J. Kruthoff, E. Shaghoulian and A. Tajdini, *Holography at finite cutoff with a T^2 deformation*, *JHEP* **03** (2019) 004 [[1807.11401](#)].
- [23] M. Taylor, *TT deformations in general dimensions*, [1805.10287](#).

[24] T. Morone, S. Negro and R. Tateo, *Gravity and $T\bar{T}$ flows in higher dimensions*, *Nucl. Phys. B* **1005** (2024) 116605 [[2401.16400](#)].

[25] G. Bonelli, N. Doroud and M. Zhu, *$T\bar{T}$ -deformations in closed form*, *JHEP* **06** (2018) 149 [[1804.10967](#)].

[26] C. Ferko, J. Hou, T. Morone, G. Tartaglino-Mazzucchelli and R. Tateo, *TT^- -like Flows of Yang-Mills Theories*, *Phys. Rev. Lett.* **134** (2025) 101603 [[2409.18740](#)].

[27] D.J. Gross, J. Kruthoff, A. Rolph and E. Shaghoulian, *$T\bar{T}$ in AdS_2 and Quantum Mechanics*, *Phys. Rev. D* **101** (2020) 026011 [[1907.04873](#)].

[28] D.J. Gross, J. Kruthoff, A. Rolph and E. Shaghoulian, *Hamiltonian deformations in quantum mechanics, $T\bar{T}$, and the SYK model*, *Phys. Rev. D* **102** (2020) 046019 [[1912.06132](#)].

[29] L.V. Iliesiu, J. Kruthoff, G.J. Turiaci and H. Verlinde, *JT gravity at finite cutoff*, *SciPost Phys.* **9** (2020) 023 [[2004.07242](#)].

[30] C.V. Johnson and F. Rosso, *Solving Puzzles in Deformed JT Gravity: Phase Transitions and Non-Perturbative Effects*, *JHEP* **04** (2021) 030 [[2011.06026](#)].

[31] F. Rosso, *$T\bar{T}$ deformation of random matrices*, *Phys. Rev. D* **103** (2021) 126017 [[2012.11714](#)].

[32] L. Griguolo, R. Panerai, J. Papalini and D. Seminara, *Nonperturbative effects and resurgence in Jackiw-Teitelboim gravity at finite cutoff*, *Phys. Rev. D* **105** (2022) 046015 [[2106.01375](#)].

[33] S.E. Aguilar-Gutierrez, A. Svesko and M.R. Visser, *$T\bar{T}$ deformations from AdS_2 to dS_2* , *JHEP* **01** (2025) 120 [[2410.18257](#)].

[34] S.E. Aguilar-Gutierrez, *T^2 deformations in the double-scaled SYK model: Stretched horizon thermodynamics*, [2410.18303](#).

[35] S. Ebert, C. Ferko, H.-Y. Sun and Z. Sun, *$T\bar{T}$ in JT Gravity and BF Gauge Theory*, *SciPost Phys.* **13** (2022) 096 [[2205.07817](#)].

[36] S. Ebert, C. Ferko, H.-Y. Sun and Z. Sun, *$T\bar{T}$ deformations of supersymmetric quantum mechanics*, *JHEP* **08** (2022) 121 [[2204.05897](#)].

[37] L. Griguolo, J. Papalini, L. Russo and D. Seminara, *A new perspective on dilaton gravity at finite cutoff*, [2512.21774](#).

[38] E. Witten, *Multitrace operators, boundary conditions, and AdS / CFT correspondence*, [hep-th/0112258](#).

[39] A. Parvizi, M.M. Sheikh-Jabbari and V. Taghiloo, *Freelance Holography, Part I: Setting Boundary Conditions Free in Gauge/Gravity Correspondence*, *SciPost Phys.* **19** (2025) 043 [[2503.09371](#)].

[40] A. Parvizi, M.M. Sheikh-Jabbari and V. Taghiloo, *Freelance Holography, Part II: Moving Boundary in Gauge/Gravity Correspondence*, [2503.09372](#).

[41] E. Coleman and V. Shyam, *Conformal boundary conditions from cutoff AdS_3* , *JHEP* **09** (2021) 079 [[2010.08504](#)].

[42] K. Allameh and E. Shaghoulian, *Timelike Liouville theory and AdS_3 gravity at finite cutoff*, [2508.03236](#).

[43] M.M. Sheikh-Jabbari and V. Taghiloo, *AdS₃ Freelance Holography, A Detailed Analysis*, [2510.10692](#).

[44] X.-Y. Ran, F. Hao and H. Ouyang, *Holography for stress-energy tensor flows*, [2508.12275](#).

[45] S. Sachdev and J. Ye, *Gapless spin-fluid ground state in a random quantum heisenberg magnet*, *Physical Review Letters* **70** (1993) 3339–3342.

[46] A. Kitaev, “Hidden Correlations in the Hawking Radiation and Thermal Noise.” <https://www.youtube.com/watch?v=0Q9qN8j7EZI>, November, 2015.

[47] A. Kitaev, “A simple model of quantum holography (part 1).” <http://online.kitp.ucsb.edu/online/entangled15/kitaev/>, April, 2015.

[48] A. Kitaev, “A simple model of quantum holography (part 2).” <http://online.kitp.ucsb.edu/online/entangled15/kitaev2/>, April, 2015.

[49] J.S. Cotler, G. Gur-Ari, M. Hanada, J. Polchinski, P. Saad, S.H. Shenker et al., *Black Holes and Random Matrices*, *JHEP* **05** (2017) 118 [[1611.04650](#)].

[50] L. Erdős and D. Schröder, *Phase Transition in the Density of States of Quantum Spin Glasses*, *Math. Phys. Anal. Geom.* **17** (2014) 441 [[1407.1552](#)].

[51] M. Berkooz, M. Isachenkov, V. Narovlansky and G. Torrents, *Towards a full solution of the large N double-scaled SYK model*, *JHEP* **03** (2019) 079 [[1811.02584](#)].

[52] M. Berkooz, P. Narayan and J. Simon, *Chord diagrams, exact correlators in spin glasses and black hole bulk reconstruction*, *JHEP* **08** (2018) 192 [[1806.04380](#)].

[53] H.W. Lin, *The bulk Hilbert space of double scaled SYK*, *JHEP* **11** (2022) 060 [[2208.07032](#)].

[54] J. Xu, *Von Neumann Algebras in Double-Scaled SYK*, [2403.09021](#).

[55] X. Cao and P. Gao, *Single-Sided Black Holes in Double-Scaled SYK Model and No Man’s Island*, [2511.01978](#).

[56] H.W. Lin and D. Stanford, *A symmetry algebra in double-scaled SYK*, *SciPost Phys.* **15** (2023) 234 [[2307.15725](#)].

[57] A. Almheiri and F.K. Popov, *Holography on the quantum disk*, *JHEP* **06** (2024) 070 [[2401.05575](#)].

[58] K. Schouten and M. Isachenkov, *The von Neumann algebraic quantum group $SU_q(1,1) \rtimes \mathbb{Z}_2$ and the DSSYK model*, [2512.10101](#).

[59] A. Belaey, T.G. Mertens and T. Tappeiner, *Quantum group origins of edge states in double-scaled SYK*, [2503.20691](#).

[60] M. Berkooz, M. Isachenkov, M. Isachenkov, P. Narayan and V. Narovlansky, *Quantum groups, non-commutative AdS_2 , and chords in the double-scaled SYK model*, *JHEP* **08** (2023) 076 [[2212.13668](#)].

[61] A. Blommaert, T.G. Mertens and S. Yao, *Dynamical actions and q-representation theory for double-scaled SYK*, *JHEP* **02** (2024) 067 [[2306.00941](#)].

[62] J. van der Heijden, E. Verlinde and J. Xu, *Quantum Symmetry and Geometry in Double-Scaled SYK*, [2511.08743](#).

- [63] E. Rabinovici, A. Sánchez-Garrido, R. Shir and J. Sonner, *A bulk manifestation of Krylov complexity*, *JHEP* **08** (2023) 213 [[2305.04355](#)].
- [64] M. Ambrosini, E. Rabinovici and J. Sonner, *Holography of K-complexity: Switchbacks and Shockwaves*, [2510.17975](#).
- [65] M. Ambrosini, E. Rabinovici, A. Sánchez-Garrido, R. Shir and J. Sonner, *Operator K-complexity in DSSYK: Krylov complexity equals bulk length*, [2412.15318](#).
- [66] M.P. Heller, J. Papalini and T. Schuhmann, *Krylov spread complexity as holographic complexity beyond JT gravity*, [2412.17785](#).
- [67] S.E. Aguilar-Gutierrez, *Building the holographic dictionary of the DSSYK from chords, complexity & wormholes with matter*, *JHEP* **10** (2025) 221 [[2505.22716](#)].
- [68] S.E. Aguilar-Gutierrez and J. Xu, *Geometry of Chord Intertwiner, Multiple Shocks and Switchback in Double-Scaled SYK*, [2506.19013](#).
- [69] S.E. Aguilar-Gutierrez, *Symmetry Sectors in Chord Space and Relational Holography in the DSSYK*, [2506.21447](#).
- [70] V. Balasubramanian, J.M. Magan, P. Nandi and Q. Wu, *Spread complexity and the saturation of wormhole size*, [2412.02038](#).
- [71] S. Forste, Y. Kruse and S. Natu, *Grand Canonical vs Canonical Krylov Complexity in Double-Scaled Complex SYK Model*, [2512.07715](#).
- [72] S.E. Aguilar-Gutierrez, *Evolution With(out) Time: Relational Holography & BPS Complexity Growth in $\mathcal{N} = 2$ Double-Scaled SYK*, [2510.11777](#).
- [73] B. Bhattacharjee, P. Nandy and T. Pathak, *Krylov complexity in large q and double-scaled SYK model*, *JHEP* **08** (2023) 099 [[2210.02474](#)].
- [74] P. Nandy, *Tridiagonal Hamiltonians modeling the density of states of the Double-Scaled SYK model*, [2410.07847](#).
- [75] T. Anegawa and R. Watanabe, *Krylov complexity of fermion chain in double-scaled SYK and power spectrum perspective*, [2407.13293](#).
- [76] S.E. Aguilar-Gutierrez, *Towards complexity in de Sitter space from the double-scaled Sachdev-Ye-Kitaev model*, *JHEP* **10** (2024) 107 [[2403.13186](#)].
- [77] M.P. Heller, F. Ori, J. Papalini, T. Schuhmann and M.-T. Wang, *De Sitter holographic complexity from Krylov complexity in DSSYK*, [2510.13986](#).
- [78] Y. Fu, H.-S. Jeong, K.-Y. Kim and J.F. Pedraza, *Toward Krylov-based holography in double-scaled SYK*, [2510.22658](#).
- [79] S.E. Aguilar-Gutierrez, R.N. Das, J. Erdmenger and Z.-Y. Xian, *Probing the Chaos to Integrability Transition in Double-Scaled SYK*, [2601.09801](#).
- [80] D.E. Parker, X. Cao, A. Avdoshkin, T. Scaffidi and E. Altman, *A Universal Operator Growth Hypothesis*, *Phys. Rev. X* **9** (2019) 041017 [[1812.08657](#)].
- [81] V. Balasubramanian, P. Caputa, J.M. Magan and Q. Wu, *Quantum chaos and the complexity of spread of states*, *Phys. Rev. D* **106** (2022) 046007 [[2202.06957](#)].

[82] S. Baiguera, V. Balasubramanian, P. Caputa, S. Chapman, J. Haferkamp, M.P. Heller et al., *Quantum complexity in gravity, quantum field theory, and quantum information science*, [2503.10753](#).

[83] E. Rabinovici, A. Sánchez-Garrido, R. Shir and J. Sonner, *Krylov Complexity*, [2507.06286](#).

[84] J. Boruch, H.W. Lin and C. Yan, *Exploring supersymmetric wormholes in $\mathcal{N} = 2$ SYK with chords*, *JHEP* **12** (2023) 151 [[2308.16283](#)].

[85] A. Blommaert, T.G. Mertens and J. Papalini, *The dilaton gravity hologram of double-scaled SYK*, *JHEP* **06** (2025) 050 [[2404.03535](#)].

[86] M. Berkooz, N. Brukner, S.F. Ross and M. Watanabe, *Going beyond ER=EPR in the SYK model*, *JHEP* **08** (2022) 051 [[2202.11381](#)].

[87] A. Blommaert, A. Levine, T.G. Mertens, J. Papalini and K. Parmentier, *Wormholes, branes and finite matrices in sine dilaton gravity*, *JHEP* **09** (2025) 123 [[2501.17091](#)].

[88] H. Verlinde, *Double-scaled SYK, chords and de Sitter gravity*, *JHEP* **03** (2025) 076 [[2402.00635](#)].

[89] H. Verlinde and M. Zhang, *SYK Correlators from 2D Liouville-de Sitter Gravity*, [2402.02584](#).

[90] L. Susskind, *Computational Complexity and Black Hole Horizons*, *Fortsch. Phys.* **64** (2016) 24 [[1403.5695](#)].

[91] H. Tang, *Entanglement entropy in type II₁ von Neumann algebra: examples in Double-Scaled SYK*, [2404.02449](#).

[92] S.E. Aguilar-Gutierrez, *Cosmological Entanglement Entropy from the von Neumann Algebra of Double-Scaled SYK & Its Connection with Krylov Complexity*, [2511.03779](#).

[93] S. Ryu and T. Takayanagi, *Holographic derivation of entanglement entropy from AdS/CFT*, *Phys. Rev. Lett.* **96** (2006) 181602 [[hep-th/0603001](#)].

[94] S. Ryu and T. Takayanagi, *Aspects of Holographic Entanglement Entropy*, *JHEP* **08** (2006) 045 [[hep-th/0605073](#)].

[95] T. Nishioka, S. Ryu and T. Takayanagi, *Holographic Entanglement Entropy: An Overview*, *J. Phys. A* **42** (2009) 504008 [[0905.0932](#)].

[96] M. Rangamani and T. Takayanagi, *Holographic Entanglement Entropy*, vol. 931, Springer (2017), [10.1007/978-3-319-52573-0](#), [[1609.01287](#)].

[97] B. Chen, *Holographic Entanglement Entropy: A Topical Review*, *Commun. Theor. Phys.* **71** (2019) 837.

[98] D. Harlow, *Jerusalem Lectures on Black Holes and Quantum Information*, *Rev. Mod. Phys.* **88** (2016) 015002 [[1409.1231](#)].

[99] V.E. Hubeny, M. Rangamani and T. Takayanagi, *A Covariant holographic entanglement entropy proposal*, *JHEP* **07** (2007) 062 [[0705.0016](#)].

[100] T. Faulkner, A. Lewkowycz and J. Maldacena, *Quantum corrections to holographic entanglement entropy*, *JHEP* **11** (2013) 074 [[1307.2892](#)].

[101] N. Engelhardt and A.C. Wall, *Quantum Extremal Surfaces: Holographic Entanglement Entropy beyond the Classical Regime*, *JHEP* **01** (2015) 073 [[1408.3203](#)].

- [102] A. Blommaert, A. Levine, T.G. Mertens, J. Papalini and K. Parmentier, *An entropic puzzle in periodic dilaton gravity and DSSYK*, *JHEP* **07** (2025) 093 [[2411.16922](#)].
- [103] A. Blommaert and A. Levine, *Sphere amplitudes and observing the universe's size*, [2505.24633](#).
- [104] L. Bossi, L. Griguolo, J. Papalini, L. Russo and D. Seminara, *Sine-dilaton gravity vs double-scaled SYK: exploring one-loop quantum corrections*, [2411.15957](#).
- [105] A. Blommaert, D. Tietto and H. Verlinde, *SYK collective field theory as complex Liouville gravity*, [2509.18462](#).
- [106] C. Cui and M. Rozali, *Splitting and gluing in sine-dilaton gravity: matter correlators and the wormhole Hilbert space*, [2509.01680](#).
- [107] M. Arundine, *The DSSYK Model: Charge and Holography*, other thesis, Università di Pisa, 12, 2025, [[2512.21366](#)].
- [108] V. Narovlansky and H. Verlinde, *Double-scaled SYK and de Sitter Holography*, [2310.16994](#).
- [109] V. Narovlansky, *Towards a microscopic description of de Sitter dynamics*, [2506.02109](#).
- [110] D. Tietto and H. Verlinde, *A microscopic model of de Sitter spacetime with an observer*, [2502.03869](#).
- [111] L. Susskind, *De Sitter Space, Double-Scaled SYK, and the Separation of Scales in the Semiclassical Limit*, [2209.09999](#).
- [112] L. Susskind, *De Sitter Space has no Chords. Almost Everything is Confined.*, *JHAP* **3** (2023) 1 [[2303.00792](#)].
- [113] H. Lin and L. Susskind, *Infinite Temperature's Not So Hot*, [2206.01083](#).
- [114] A.A. Rahman, *dS JT Gravity and Double-Scaled SYK*, [2209.09997](#).
- [115] A.A. Rahman and L. Susskind, *Comments on a Paper by Narovlansky and Verlinde*, [2312.04097](#).
- [116] A.A. Rahman and L. Susskind, *p-Chords, Wee-Chords, and de Sitter Space*, [2407.12988](#).
- [117] A.A. Rahman and L. Susskind, *Infinite Temperature is Not So Infinite: The Many Temperatures of de Sitter Space*, [2401.08555](#).
- [118] Y. Sekino and L. Susskind, *Double-Scaled SYK, QCD, and the Flat Space Limit of de Sitter Space*, [2501.09423](#).
- [119] S. Miyashita, Y. Sekino and L. Susskind, *DSSYK at Infinite Temperature: The Flat-Space Limit and the 't Hooft Model*, [2506.18054](#).
- [120] A. Herderschee and J. Kudler-Flam, *Stringy algebras, stretched horizons, and quantum-connected wormholes*, [2510.01556](#).
- [121] A. Milekhin and J. Xu, *Revisiting Brownian SYK and its possible relations to de Sitter*, *JHEP* **10** (2024) 151 [[2312.03623](#)].
- [122] A. Milekhin and J. Xu, *On scrambling, temperature and superdiffusion in de Sitter space*, *JHEP* **07** (2025) 272 [[2403.13915](#)].
- [123] K. Okuyama, *de Sitter JT gravity from double-scaled SYK*, *JHEP* **08** (2025) 181 [[2505.08116](#)].

[124] H. Yuan, X.-H. Ge and K.-Y. Kim, *Pole skipping in two-dimensional de Sitter spacetime and double-scaled SYK model*, *Phys. Rev. D* **112** (2025) 026022 [[2408.12330](#)].

[125] E. Gubankova, S. Sachdev and G. Tarnopolsky, *Scaling limits of complex Sachdev-Ye-Kitaev models and holographic geometry*, [2512.05294](#).

[126] Y. Ahn, S. Grozdanov, H.-S. Jeong and J.F. Pedraza, *Cosmological pole-skipping, shock waves and quantum chaotic dynamics of de Sitter horizons*, [2508.15589](#).

[127] S. Collier, L. Eberhardt, B. Mühlmann and V.A. Rodriguez, *Complex Liouville String*, *Phys. Rev. Lett.* **134** (2025) 251602 [[2409.17246](#)].

[128] S. Collier, L. Eberhardt, B. Mühlmann and V.A. Rodriguez, *The complex Liouville string: The worldsheet*, *SciPost Phys.* **19** (2025) 033 [[2409.18759](#)].

[129] S. Collier, L. Eberhardt, B. Mühlmann and V.A. Rodriguez, *The complex Liouville string: The matrix integral*, *SciPost Phys.* **18** (2025) 154 [[2410.07345](#)].

[130] S. Collier, L. Eberhardt, B. Mühlmann and V.A. Rodriguez, *The complex Liouville string: Worldsheet boundaries and non-perturbative effects*, *SciPost Phys.* **19** (2025) 034 [[2410.09179](#)].

[131] S. Collier, L. Eberhardt and B. Mühlmann, *A microscopic realization of dS_3* , *SciPost Phys.* **18** (2025) 131 [[2501.01486](#)].

[132] S. Collier, L. Eberhardt and B. Mühlmann, *The complex Liouville string: the gravitational path integral*, [2501.10265](#).

[133] D.A. Roberts, D. Stanford and A. Streicher, *Operator growth in the SYK model*, *JHEP* **06** (2018) 122 [[1802.02633](#)].

[134] R. Jackiw, *Lower dimensional gravity*, *Nuclear Physics B* **252** (1985) 343.

[135] C. Teitelboim, *Gravitation and hamiltonian structure in two spacetime dimensions*, *Physics Letters B* **126** (1983) 41.

[136] S. Ali Ahmad, A. Almheiri and S. Lin, *$T\bar{T}$ and the black hole interior*, [2503.19854](#).

[137] E. Silverstein and G. Torroba, *Timelike-bounded dS_4 holography from a solvable sector of the T^2 deformation*, [2409.08709](#).

[138] J.-C. Chang, Y. He, Y.-X. Liu and Y. Sun, *Toward a Unified de Sitter Holography: A Composite $T\bar{T}$ and $T\bar{T} + \Lambda_2$ Flow*, [2511.16098](#).

[139] V. Gorbenko, E. Silverstein and G. Torroba, *dS/dS and $T\bar{T}$* , *JHEP* **03** (2019) 085 [[1811.07965](#)].

[140] V. Shyam, *$T\bar{T} + \Lambda_2$ deformed CFT on the stretched dS_3 horizon*, *JHEP* **04** (2022) 052 [[2106.10227](#)].

[141] E. Coleman, E.A. Mazenc, V. Shyam, E. Silverstein, R.M. Soni, G. Torroba et al., *De Sitter microstates from $T\bar{T} + \Lambda_2$ and the Hawking-Page transition*, *JHEP* **07** (2022) 140 [[2110.14670](#)].

[142] E. Silverstein, *Black hole to cosmic horizon microstates in string/M theory: timelike boundaries and internal averaging*, [2212.00588](#).

[143] G. Batra, G.B. De Luca, E. Silverstein, G. Torroba and S. Yang, *Bulk-local dS_3 holography: the Matter with $T\bar{T} + \Lambda_2$* , [2403.01040](#).

[144] D. Anninos, D.A. Galante and C. Maneerat, *Cosmological observatories*, *Class. Quant. Grav.* **41** (2024) 165009 [[2402.04305](#)].

[145] R.C. Tolman, *On the extension of thermodynamics to general relativity*, *Proceedings of the National Academy of Sciences* **14** (1928) 268.

[146] R.C. Tolman, *Thermodynamics and relativity*, *Science* **77** (1933) 291.

[147] R. Tolman and P. Ehrenfest, *Temperature Equilibrium in a Static Gravitational Field*, *Phys. Rev.* **36** (1930) 1791.

[148] S. Chapman, D.A. Galante and E.D. Kramer, *Holographic complexity and de Sitter space*, *JHEP* **02** (2022) 198 [[2110.05522](#)].

[149] E. Jørstad, R.C. Myers and S.-M. Ruan, *Holographic complexity in dS_{d+1}* , *JHEP* **05** (2022) 119 [[2202.10684](#)].

[150] D. Galante, *Geodesics, complexity and holography in $(A)dS_2$* , *PoS CORFU2021* (2022) 359.

[151] R. Auzzi, G. Nardelli, G.P. Ungureanu and N. Zenoni, *Volume complexity of dS bubbles*, *Phys. Rev. D* **108** (2023) 026006 [[2302.03584](#)].

[152] T. Anegawa, N. Iizuka, S.K. Sake and N. Zenoni, *Is action complexity better for de Sitter space in Jackiw-Teitelboim gravity?*, *JHEP* **06** (2023) 213 [[2303.05025](#)].

[153] T. Anegawa and N. Iizuka, *Shock waves and delay of hyperfast growth in de Sitter complexity*, *JHEP* **08** (2023) 115 [[2304.14620](#)].

[154] S. Baiguera, R. Berman, S. Chapman and R.C. Myers, *The cosmological switchback effect*, *JHEP* **07** (2023) 162 [[2304.15008](#)].

[155] S.E. Aguilar-Gutierrez, M.P. Heller and S. Van der Schueren, *Complexity equals anything can grow forever in de Sitter space*, *Phys. Rev. D* **110** (2024) 066009 [[2305.11280](#)].

[156] S.E. Aguilar-Gutierrez, A.K. Patra and J.F. Pedraza, *Entangled universes in dS wedge holography*, *JHEP* **10** (2023) 156 [[2308.05666](#)].

[157] S.E. Aguilar-Gutierrez, *C=Anything and the switchback effect in Schwarzschild-de Sitter space*, *JHEP* **03** (2024) 062 [[2309.05848](#)].

[158] S.E. Aguilar-Gutierrez, S. Baiguera and N. Zenoni, *Holographic complexity of the extended Schwarzschild-de Sitter space*, [2402.01357](#).

[159] L. Susskind, *Black Holes Hint towards De Sitter Matrix Theory*, *Universe* **9** (2023) 368 [[2109.01322](#)].

[160] E. Shaghoulian, *The central dogma and cosmological horizons*, *JHEP* **01** (2022) 132 [[2110.13210](#)].

[161] E. Shaghoulian and L. Susskind, *Entanglement in De Sitter space*, *JHEP* **08** (2022) 198 [[2201.03603](#)].

[162] V. Franken, H. Partouche, F. Rondeau and N. Toumbas, *Bridging the static patches: de Sitter holography and entanglement*, *JHEP* **08** (2023) 074 [[2305.12861](#)].

[163] V. Franken, *de Sitter Connectivity from Holographic Entanglement*, in *23rd Hellenic School and Workshops on Elementary Particle Physics and Gravity*, 3, 2024 [[2403.14889](#)].

[164] D. Anninos and E. Harris, *Interpolating geometries and the stretched dS_2 horizon*, *JHEP* **11** (2022) 166 [[2209.06144](#)].

[165] R. Arnowitt and S. Deser, *Quantum Theory of Gravitation: General Formulation and Linearized Theory*, *Phys. Rev.* **113** (1959) 745.

[166] R.L. Arnowitt, S. Deser and C.W. Misner, *Canonical variables for general relativity*, *Phys. Rev.* **117** (1960) 1595.

[167] R.L. Arnowitt, S. Deser and C.W. Misner, *Gravitational-electromagnetic coupling and the classical self-energy problem*, *Phys. Rev.* **120** (1960) 313.

[168] R. Arnowitt, S. Deser and C.W. Misner, *Interior Schwarzschild solutions and interpretation of source terms*, *Phys. Rev.* **120** (1960) 321.

[169] R. Arnowitt, S. Deser and C.W. Misner, *Energy and the Criteria for Radiation in General Relativity*, *Phys. Rev.* **118** (1960) 1100.

[170] R.L. Arnowitt, S. Deser and C.W. Misner, *Coordinate invariance and energy expressions in general relativity*, *Phys. Rev.* **122** (1961) 997.

[171] R.L. Arnowitt, S. Deser and C.W. Misner, *Wave zone in general relativity*, *Phys. Rev.* **121** (1961) 1556.

[172] G. Araujo-Regado, R. Khan and A.C. Wall, *Cauchy slice holography: a new AdS/CFT dictionary*, *JHEP* **03** (2023) 026 [[2204.00591](#)].

[173] G. Araujo-Regado, *Holographic Cosmology on Closed Slices in 2+1 Dimensions*, [2212.03219](#).

[174] R.M. Soni and A.C. Wall, *A New Covariant Entropy Bound from Cauchy Slice Holography*, [2407.16769](#).

[175] G. Araujo-Regado, A. Thavaresan and A.C. Wall, *Holographic Cosmology at Finite Time*, [2511.04511](#).

[176] A. Almheiri, A. Goel and X.-Y. Hu, *Quantum gravity of the Heisenberg algebra*, *JHEP* **08** (2024) 098 [[2403.18333](#)].

[177] C. Zhang and W. Cai, *$T\bar{T}$ deformation on non-Hermitian two coupled SYK model*, [2312.03433](#).

[178] J.A. Wheeler, *SUPERSPACE AND THE NATURE OF QUANTUM GEOMETRODYNAMICS*, *Adv. Ser. Astrophys. Cosmol.* **3** (1987) 27.

[179] B.S. DeWitt, *Quantum Theory of Gravity. 1. The Canonical Theory*, *Phys. Rev.* **160** (1967) 1113.

[180] J.D. Brown and J.W. York, Jr., *Quasilocal energy and conserved charges derived from the gravitational action*, *Phys. Rev. D* **47** (1993) 1407 [[gr-qc/9209012](#)].

[181] D. Grumiller and R. McNees, *Thermodynamics of black holes in two (and higher) dimensions*, *JHEP* **04** (2007) 074 [[hep-th/0703230](#)].

[182] J. Kruthoff and O. Parrikar, *On the flow of states under $T\bar{T}$* , [2006.03054](#).

[183] A. Goel, V. Narovlansky and H. Verlinde, *Semiclassical geometry in double-scaled SYK*, *JHEP* **11** (2023) 093 [[2301.05732](#)].

[184] A. Svesko, E. Verheijden, E.P. Verlinde and M.R. Visser, *Quasi-local energy and microcanonical entropy in two-dimensional nearly de Sitter gravity*, *JHEP* **08** (2022) 075 [[2203.00700](#)].

[185] J.L.F. Barbon and E. Rabinovici, *Remarks on the thermodynamic stability of $T\bar{T}$ deformations*, *J. Phys. A* **53** (2020) 424001 [[2004.10138](#)].

[186] J. Maldacena and D. Stanford, *Remarks on the Sachdev-Ye-Kitaev model*, *Phys. Rev. D* **94** (2016) 106002 [[1604.07818](#)].

[187] G. Parisi, *D-dimensional arrays of josephson junctions, spin glasses and q -deformed harmonic oscillators*, *Journal of Physics A: Mathematical and General* **27** (1994) 7555–7568.

[188] M. Berkooz, N. Brukner, Y. Jia and O. Mamroud, *From Chaos to Integrability in Double Scaled SYK*, [2403.01950](#).

[189] M. Berkooz, N. Brukner, Y. Jia and O. Mamroud, *A Path Integral for Chord Diagrams and Chaotic-Integrable Transitions in Double Scaled SYK*, [2403.05980](#).

[190] P. Gao, H. Lin and C. Peng, *D-commuting SYK model: building quantum chaos from integrable blocks*, [2411.12806](#).

[191] M. Berkooz and O. Mamroud, *A cordial introduction to double scaled SYK*, *Rept. Prog. Phys.* **88** (2025) 036001 [[2407.09396](#)].

[192] J. Xu, *On Chord Dynamics and Complexity Growth in Double-Scaled SYK*, [2411.04251](#).

[193] J. Erdmenger, S.-K. Jian and Z.-Y. Xian, *Universal chaotic dynamics from Krylov space*, *JHEP* **08** (2023) 176 [[2303.12151](#)].

[194] P. Caputa, J.M. Magan, D. Patramanis and E. Tonni, *Krylov complexity of modular Hamiltonian evolution*, *Phys. Rev. D* **109** (2024) 086004 [[2306.14732](#)].

[195] P. Kraus, J. Liu and D. Marolf, *Cutoff AdS_3 versus the $T\bar{T}$ deformation*, *JHEP* **07** (2018) 027 [[1801.02714](#)].

[196] D. Basu, A. Chandra and Q. Wen, *Butterfly effect and $T\bar{T}$ -deformation*, [2505.14331](#).

[197] J. Maldacena, S.H. Shenker and D. Stanford, *A bound on chaos*, *JHEP* **08** (2016) 106 [[1503.01409](#)].

[198] S.H. Shenker and D. Stanford, *Multiple Shocks*, *JHEP* **12** (2014) 046 [[1312.3296](#)].

[199] E. Witten, *Gravity and the crossed product*, *JHEP* **10** (2022) 008 [[2112.12828](#)].

[200] V. Chandrasekaran, R. Longo, G. Penington and E. Witten, *An algebra of observables for de Sitter space*, *JHEP* **02** (2023) 082 [[2206.10780](#)].

[201] V. Chandrasekaran, G. Penington and E. Witten, *Large N algebras and generalized entropy*, *JHEP* **04** (2023) 009 [[2209.10454](#)].

[202] K. Jensen, J. Sorce and A.J. Speranza, *Generalized entropy for general subregions in quantum gravity*, *JHEP* **12** (2023) 020 [[2306.01837](#)].

[203] J. Kudler-Flam, S. Leutheusser and G. Satishchandran, *Generalized black hole entropy is von Neumann entropy*, *Phys. Rev. D* **111** (2025) 025013 [[2309.15897](#)].

[204] E. Witten, *APS Medal for Exceptional Achievement in Research: Invited article on entanglement properties of quantum field theory*, *Rev. Mod. Phys.* **90** (2018) 045003 [[1803.04993](#)].

[205] J. Sorce, *Notes on the type classification of von Neumann algebras*, *Rev. Math. Phys.* **36** (2024) 2430002 [[2302.01958](#)].

[206] H. Casini and M. Huerta, *Lectures on entanglement in quantum field theory*, *PoS TASI2021* (2023) 002 [[2201.13310](#)].

[207] H. Liu, *Lectures on entanglement, von Neumann algebras, and emergence of spacetime*, in *Theoretical Advanced Study Institute in Elementary Particle Physics 2023: Aspects of Symmetry*, 10, 2025 [[2510.07017](#)].

[208] I.E. Segal, *Irreducible representations of operator algebras*, *Bulletin of the American Mathematical Society* **53** (1947) 73.

[209] I. Gelfand and M. Neumark, *On the imbedding of normed rings into the ring of operators in hilbert space*, *Mathematical collection* **12** (1943) 197.

[210] G. Penington and E. Witten, *Algebras and States in JT Gravity*, [2301.07257](#).

[211] A. Goel, H.T. Lam, G.J. Turiaci and H. Verlinde, *Expanding the Black Hole Interior: Partially Entangled Thermal States in SYK*, *JHEP* **02** (2019) 156 [[1807.03916](#)].

[212] G. Wentzel, *Eine verallgemeinerung der quantenbedingungen für die zwecke der wellenmechanik*, *Zeitschrift für Physik* **38** (1926) 518.

[213] H.A. Kramers, *Wellenmechanik und halbzahlige quantisierung*, *Zeitschrift für Physik* **39** (1926) 828.

[214] L. Brillouin, *La mécanique ondulatoire de schrödinger; une méthode générale de résolution par approximations successives*, *CR Acad. Sci* **183** (1926) 24.

[215] A. Strominger, *The dS / CFT correspondence*, *JHEP* **10** (2001) 034 [[hep-th/0106113](#)].

[216] E. Witten, *Quantum gravity in de Sitter space*, in *Strings 2001: International Conference*, 6, 2001 [[hep-th/0106109](#)].

[217] M. Spradlin, A. Strominger and A. Volovich, *Les Houches lectures on de Sitter space*, in *Les Houches Summer School: Session 76: Euro Summer School on Unity of Fundamental Physics: Gravity, Gauge Theory and Strings*, pp. 423–453, 10, 2001 [[hep-th/0110007](#)].

[218] R. Bousso, A. Maloney and A. Strominger, *Conformal vacua and entropy in de Sitter space*, *Phys. Rev. D* **65** (2002) 104039 [[hep-th/0112218](#)].

[219] J.M. Maldacena, *Non-Gaussian features of primordial fluctuations in single field inflationary models*, *JHEP* **05** (2003) 013 [[astro-ph/0210603](#)].

[220] M.A. Vasiliev, *Higher spin gauge theories: Star product and AdS space*, [hep-th/9910096](#).

[221] M.A. Vasiliev, *Consistent equation for interacting gauge fields of all spins in (3+1)-dimensions*, *Phys. Lett. B* **243** (1990) 378.

[222] D. Anninos, T. Hartman and A. Strominger, *Higher Spin Realization of the dS/CFT Correspondence*, *Class. Quant. Grav.* **34** (2017) 015009 [[1108.5735](#)].

[223] G.S. Ng and A. Strominger, *State/Operator Correspondence in Higher-Spin dS/CFT*, *Class. Quant. Grav.* **30** (2013) 104002 [[1204.1057](#)].

[224] D. Anninos, F. Denef and D. Harlow, *Wave function of Vasiliev's universe: A few slices thereof*, *Phys. Rev. D* **88** (2013) 084049 [[1207.5517](#)].

[225] Y. Hikida, T. Nishioka, T. Takayanagi and Y. Taki, *Holography in de Sitter Space via Chern-Simons Gauge Theory*, *Phys. Rev. Lett.* **129** (2022) 041601 [[2110.03197](#)].

[226] Y. Hikida, T. Nishioka, T. Takayanagi and Y. Taki, *CFT duals of three-dimensional de Sitter gravity*, *JHEP* **05** (2022) 129 [[2203.02852](#)].

[227] H.-Y. Chen and Y. Hikida, *Three-Dimensional de Sitter Holography and Bulk Correlators at Late Time*, *Phys. Rev. Lett.* **129** (2022) 061601 [[2204.04871](#)].

[228] H.-Y. Chen, S. Chen and Y. Hikida, *Late-time correlation functions in dS_3/CFT_2 correspondence*, *JHEP* **02** (2023) 038 [[2210.01415](#)].

[229] J.B. Hartle, S.W. Hawking and T. Hertog, *Quantum Probabilities for Inflation from Holography*, *JCAP* **01** (2014) 015 [[1207.6653](#)].

[230] T. Hertog and J. Hartle, *Holographic No-Boundary Measure*, *JHEP* **05** (2012) 095 [[1111.6090](#)].

[231] N. Bobev, T. Hertog, J. Hong, J. Karlsson and V. Reys, *Microscopics of de Sitter Entropy from Precision Holography*, *Phys. Rev. X* **13** (2023) 041056 [[2211.05907](#)].

[232] D. Anninos and D.M. Hofman, *Infrared Realization of dS_2 in AdS_2* , *Class. Quant. Grav.* **35** (2018) 085003 [[1703.04622](#)].

[233] D. Anninos, D.A. Galante and D.M. Hofman, *De Sitter horizons & holographic liquids*, *JHEP* **07** (2019) 038 [[1811.08153](#)].

[234] D. Anninos and D.A. Galante, *Constructing AdS_2 flow geometries*, *JHEP* **02** (2021) 045 [[2011.01944](#)].

[235] D. Anninos, D.A. Galante and B. Mühlmann, *Finite features of quantum de Sitter space*, *Class. Quant. Grav.* **40** (2023) 025009 [[2206.14146](#)].

[236] S.E. Aguilar-Gutierrez, E. Bahiru and R. Espíndola, *The centaur-algebra of observables*, *JHEP* **03** (2024) 008 [[2307.04233](#)].

[237] D. Anninos, D.A. Galante and S.U. Sheorey, *Renormalisation group flows of deformed SYK models*, *JHEP* **11** (2023) 197 [[2212.04944](#)].

[238] S. Chapman, S. Demulder, D.A. Galante, S.U. Sheorey and O. Shoval, *Krylov complexity and chaos in deformed SYK models*, [2407.09604](#).

[239] D.A. Galante, *Modave lectures on de Sitter space & holography*, *PoS Modave2022* (2023) 003 [[2306.10141](#)].

[240] A. Strominger, *Inflation and the dS / CFT correspondence*, *JHEP* **11** (2001) 049 [[hep-th/0110087](#)].

[241] V. Balasubramanian, J. de Boer and D. Minic, *Mass, entropy and holography in asymptotically de Sitter spaces*, *Phys. Rev. D* **65** (2002) 123508 [[hep-th/0110108](#)].

[242] G.W. Gibbons and S.W. Hawking, *Action Integrals and Partition Functions in Quantum Gravity*, *Phys. Rev. D* **15** (1977) 2752.

[243] G.W. Gibbons and S.W. Hawking, *Cosmological Event Horizons, Thermodynamics, and Particle Creation*, *Phys. Rev. D* **15** (1977) 2738.

[244] M.M. Faruk, E. Morvan and J.P. van der Schaar, *Static sphere observers and geodesics in Schwarzschild-de Sitter spacetime*, *JCAP* **05** (2024) 118 [[2312.06878](#)].

[245] K. Doi, J. Harper, A. Mollabashi, T. Takayanagi and Y. Taki, *Pseudoentropy in dS/CFT and Timelike Entanglement Entropy*, *Phys. Rev. Lett.* **130** (2023) 031601 [[2210.09457](#)].

[246] S. Baiguera and R. Berman, *The Cosmological Switchback Effect II*, *JHEP* **08** (2024) 086 [[2406.04397](#)].

[247] A. Faraji Astaneh, *Quantum Complexity of $T\bar{T}$ -deformation and Its Implications*, [2408.06055](#).

[248] A. Chattopadhyay, V. Malvimat and A. Mitra, *Krylov complexity of deformed conformal field theories*, *JHEP* **08** (2024) 053 [[2405.03630](#)].

[249] P. Cooper, S. Dubovsky and A. Mohsen, *Ultraviolet complete Lorentz-invariant theory with superluminal signal propagation*, *Phys. Rev. D* **89** (2014) 084044 [[1312.2021](#)].

[250] A. Bhattacharyya, S. Ghosh, S. Pal and A. Vinod, *Wormholes in finite cutoff JT gravity: A study of baby universes and (Krylov) complexity*, [2502.13208](#).

[251] H. Adami, M.M. Sheikh-Jabbari and V. Taghiloo, *Gravity Is Induced By Renormalization Group Flow*, [2508.09633](#).

[252] Y.-Z. Li, Y. Xie and S. He, *Emergent classical gravity as stress-tensor deformed field theories*, [2508.15461](#).

[253] M.T. Anderson, *On boundary value problems for einstein metrics*, *Geometry & Topology* **12** (2008) 2009–2045.

[254] E. Witten, *A note on boundary conditions in Euclidean gravity*, *Rev. Math. Phys.* **33** (2021) 2140004 [[1805.11559](#)].

[255] Z. An and M.T. Anderson, *The initial boundary value problem and quasi-local Hamiltonians in General Relativity*, [2103.15673](#).

[256] D. Anninos, D.A. Galante and C. Maneerat, *Gravitational observatories*, *JHEP* **12** (2023) 024 [[2310.08648](#)].

[257] G. Batra, *Timelike boundaries in de Sitter JT gravity and the Gao-Wald theorem*, [2407.08913](#).

[258] B. Banihashemi, E. Shaghoulian and S. Shashi, *Flat space gravity at finite cutoff*, [2409.07643](#).

[259] D.A. Galante, C. Maneerat and A. Svesko, *Conformal boundaries near extremal black holes*, [2504.14003](#).

[260] B. Banihashemi, E. Shaghoulian and S. Shashi, *Thermal effective actions from conformal boundary conditions in gravity*, [2503.17471](#).

[261] D.A. Galante, R.C. Myers and T. Zikopoulos, *Conformal Boundary Conditions and Higher Curvature Gravity*, [2512.10930](#).

[262] D. Anninos, D.A. Galante, S. Georgescu, C. Maneerat and A. Svesko, *The Stretched Horizon Limit*, [2512.16738](#).

[263] X. Liu, J.E. Santos and T. Wiseman, *New Well-Posed boundary conditions for semi-classical Euclidean gravity*, *JHEP* **06** (2024) 044 [[2402.04308](#)].

[264] T. Ishii, S. Okumura, J.-I. Sakamoto and K. Yoshida, *Gravitational perturbations as $T\bar{T}$ -deformations in 2D dilaton gravity systems*, *Nucl. Phys. B* **951** (2020) 114901 [[1906.03865](#)].

[265] S. Okumura and K. Yoshida, *$T\bar{T}$ -deformation and Liouville gravity*, *Nucl. Phys. B* **957** (2020) 115083 [[2003.14148](#)].

[266] A. Lewkowycz and J. Maldacena, *Generalized gravitational entropy*, *JHEP* **08** (2013) 090 [[1304.4926](#)].

[267] J. Lin, *Entanglement entropy in Jackiw-Teitelboim Gravity*, [1807.06575](#).

[268] J. Lin, *Ryu-Takayanagi Area as an Entanglement Edge Term*, [1704.07763](#).

[269] A. Blommaert, T.G. Mertens and H. Verschelde, *Fine Structure of Jackiw-Teitelboim Quantum Gravity*, *JHEP* **09** (2019) 066 [[1812.00918](#)].

[270] J. Lin, *Entanglement entropy in Jackiw-Teitelboim gravity with matter*, [2107.11872](#).

[271] D.L. Jafferis and D.K. Kolchmeyer, *Entanglement Entropy in Jackiw-Teitelboim Gravity*, [1911.10663](#).

[272] T.G. Mertens, J. Simón and G. Wong, *A proposal for 3d quantum gravity and its bulk factorization*, *JHEP* **06** (2023) 134 [[2210.14196](#)].

[273] A. Belaey, T.G. Mertens and J. Papalini, *Probing the singularity at the holographic screen via q -holography*, [2507.13873](#).

[274] A. Blommaert, T.G. Mertens and S. Yao, *The q -Schwarzian and Liouville gravity*, [2312.00871](#).

[275] T.G. Mertens and G.J. Turiaci, *Liouville quantum gravity – holography, JT and matrices*, *JHEP* **01** (2021) 073 [[2006.07072](#)].

[276] Y. Fan and T.G. Mertens, *From quantum groups to Liouville and dilaton quantum gravity*, *JHEP* **05** (2022) 092 [[2109.07770](#)].

[277] H. Kyono, S. Okumura and K. Yoshida, *Comments on 2D dilaton gravity system with a hyperbolic dilaton potential*, *Nucl. Phys. B* **923** (2017) 126 [[1704.07410](#)].

[278] K. Suzuki and T. Takayanagi, *JT gravity limit of Liouville CFT and matrix model*, *JHEP* **11** (2021) 137 [[2108.12096](#)].

[279] A. Goel, L.V. Iliesiu, J. Kruthoff and Z. Yang, *Classifying boundary conditions in JT gravity: from energy-branes to α -branes*, *JHEP* **04** (2021) 069 [[2010.12592](#)].

[280] S. Collier, L. Eberhardt, B. Muehlmann and V.A. Rodriguez, *The Virasoro minimal string*, *SciPost Phys.* **16** (2024) 057 [[2309.10846](#)].

[281] J. De Vuyst, S. Eccles, P.A. Hoehn and J. Kirklin, *Gravitational entropy is observer-dependent*, [2405.00114](#).

[282] P.A. Hoehn, I. Kotecha and F.M. Mele, *Quantum Frame Relativity of Subsystems, Correlations and Thermodynamics*, [2308.09131](#).

[283] L. Susskind, *A Paradox and its Resolution Illustrate Principles of de Sitter Holography*, [2304.00589](#).

[284] D.N. Page and W.K. Wootters, *EVOLUTION WITHOUT EVOLUTION: DYNAMICS DESCRIBED BY STATIONARY OBSERVABLES*, *Phys. Rev. D* **27** (1983) 2885.

[285] W.K. Wootters, “*Time*” replaced by quantum correlations, *Int. J. Theor. Phys.* **23** (1984) 701.

[286] D.L. Jafferis, D.K. Kolchmeyer, B. Mukhametzhanov and J. Sonner, *Matrix Models for Eigenstate Thermalization*, *Phys. Rev. X* **13** (2023) 031033 [[2209.02130](#)].

[287] D.L. Jafferis, D.K. Kolchmeyer, B. Mukhametzhanov and J. Sonner, *Jackiw-Teitelboim gravity with matter, generalized eigenstate thermalization hypothesis, and random matrices*, *Phys. Rev. D* **108** (2023) 066015 [[2209.02131](#)].

[288] K. Okuyama, *Discrete analogue of the Weil-Petersson volume in double scaled SYK*, *JHEP* **09** (2023) 133 [[2306.15981](#)].

[289] K. Okuyama, *Matter correlators through a wormhole in double-scaled SYK*, *JHEP* **02** (2024) 147 [[2312.00880](#)].

[290] K. Okuyama, *Baby universe operators in double-scaled SYK*, [2408.03726](#).

[291] M. Guica, *An integrable Lorentz-breaking deformation of two-dimensional CFTs*, *SciPost Phys.* **5** (2018) 048 [[1710.08415](#)].

[292] S. Chakraborty and A. Mishra, *$T\bar{T}$ and $J\bar{T}$ deformations in quantum mechanics*, *JHEP* **11** (2020) 099 [[2008.01333](#)].

[293] M. Berkooz, V. Narovlansky and H. Raj, *Complex Sachdev-Ye-Kitaev model in the double scaling limit*, *JHEP* **02** (2021) 113 [[2006.13983](#)].

[294] R.A. Davison, W. Fu, A. Georges, Y. Gu, K. Jensen and S. Sachdev, *Thermoelectric transport in disordered metals without quasiparticles: The Sachdev-Ye-Kitaev models and holography*, *Phys. Rev. B* **95** (2017) 155131 [[1612.00849](#)].

[295] S. Sachdev, *Bekenstein-Hawking Entropy and Strange Metals*, *Phys. Rev. X* **5** (2015) 041025 [[1506.05111](#)].

[296] Y. Gu, A. Kitaev, S. Sachdev and G. Tarnopolsky, *Notes on the complex Sachdev-Ye-Kitaev model*, *JHEP* **02** (2020) 157 [[1910.14099](#)].

[297] M. Berkooz, N. Brukner, V. Narovlansky and A. Raz, *The double scaled limit of Super-Symmetric SYK models*, *JHEP* **12** (2020) 110 [[2003.04405](#)].

[298] H.W. Lin, J. Maldacena, L. Rozenberg and J. Shan, *Looking at supersymmetric black holes for a very long time*, *SciPost Phys.* **14** (2023) 128 [[2207.00408](#)].

[299] S. Chapman, D.A. Galante, E. Harris, S.U. Sheorey and D. Vegh, *Complex geodesics in de Sitter space*, *JHEP* **03** (2023) 006 [[2212.01398](#)].

[300] P. Caputa, J. Kruthoff and O. Parrikar, *Building Tensor Networks for Holographic States*, *JHEP* **05** (2021) 009 [[2012.05247](#)].

[301] V. Balasubramanian, A. Kar and T. Ugajin, *Islands in de Sitter space*, *JHEP* **02** (2021) 072 [[2008.05275](#)].

[302] A. Levine and E. Shaghoulian, *Encoding beyond cosmological horizons in de Sitter JT gravity*, *JHEP* **02** (2023) 179 [[2204.08503](#)].

- [303] S.E. Aguilar-Gutierrez, A. Chatwin-Davies, T. Hertog, N. Pinzani-Fokeeva and B. Robinson, *Islands in Multiverse Models*, *JHEP* **11** (2021) 212 [[2108.01278](#)].
- [304] F. Deng, Z. Wang and Y. Zhou, *End of the world brane meets $T\bar{T}$* , *JHEP* **07** (2024) 036 [[2310.15031](#)].
- [305] K. Okuyama and T. Suyama, *Solvable limit of ETH matrix model for double-scaled SYK*, *JHEP* **04** (2024) 094 [[2311.02846](#)].
- [306] M. Watanabe, *A JT/KPZ correspondence*, [2511.02529](#).
- [307] P.A. Dirac, *Lectures on quantum mechanics*, Courier Corporation (2013).
- [308] M. Henneaux and C. Teitelboim, *Quantization of Gauge Systems*, Princeton University Press (8, 1994).
- [309] K. Okuyama, *End of the world brane in double scaled SYK*, *JHEP* **08** (2023) 053 [[2305.12674](#)].
- [310] W. Al-Salam and T. Chihara, *Convolutions of orthonormal polynomials*, *SIAM Journal on Mathematical Analysis* **7** (1976) 16.
- [311] M. Zhang, W.-D. Tan, M. Lu, D. Bhattacharya, J. Yang and R.B. Mann, *Finite-cutoff Holographic Thermodynamics*, [2507.01010](#).